ENZYMATIC AND ELECTROCHEMICAL OXIDATION OF EMERGING CONTAMINANTS

by

SHANGTAO LIANG

(Under the Direction of Qingguo Huang)

ABSTRACT

Emerging contaminants, also known as chemicals of emerging concern (CoCs), have been widely detected in water systems, and are under intensive research because of their potential risks to human health and the environment. Developing cost-effective and environmentally friendly remediation technologies is in urgent demand to address the risks of CoCs.

Enzyme catalyzed oxidative humification reaction (ECOHR) is an enhanced natural process that is capable of degrading numerous recalcitrant organic compounds with the presence of oxidative enzyme and mediators. This study reported that the water extract of a natural matter, soybean meal, can be used as a cost-effective mediator solution, which facilitated the degradation of sulfadimethoxine in water via ECOHR, leading to over 95% removal in six hours. Several phenolic compounds were identified as the key mediators, and the transformation pathway of sulfadimethoxine as well as the toxicity of the treated solutions were studied. Other than being used as a standalone remediation technology, ECOHR can be coupled with other *in situ* adsorption technique to promote the degradation of contaminants on the sorbents. Our data showed that over 30% of a persistent CoC, perfluorooctanoic acid (PFOA), was removed in

batch reactor with granular activated carbon and enzyme added to induce ECOHR after 60 days of incubation.

This study also investigated the electrochemical oxidation of tetracycline using a novel ceramic electrode named Magnéli phase Ti_4O_7 electrode. The concentration of tetracycline spiked in solution was significantly reduced (>90%) in the electrolysis reactor after several hours, and its antibiotic activity also reduced as evidenced by antibiotic susceptibility test. In addition, electrochemical treatment was found to be a promising point of use water disinfection technology in an experiment that demonstrated the inactivation of *E Coli* spiked in water by 5 log using an electrochemical filtration device equipped with Magnéli phase Ti_4O_7 electrode.

The data collected in this study showed that certain environmentally friendly enzymatic or electrochemical oxidation processes can effectively degrade or inactivate COCs, including antibiotics, per- and polyfluoroalkyl substances, and pathogens, and thus hold promise in being used as novel schemes in remediation or treatment to address the risks posed by emerging contaminants.

INDEX WORDS: Emerging contaminants, Antibiotics, Per- and polyfluoroalkyl Substances, Pathogens, Remediation, Laccase, Electrochemical oxidation, Toxicity

ENZYMATIC AND ELECTROCHEMICAL OXIDATION OF EMERGING CONTAMINANTS

by

SHANGTAO LIANG

B.S., China Agricultural University, 2007

M.S., North Carolina State University, 2013

A Dissertation Submitted to the Graduate Faculty of The University of Georgia in Partial Fulfillment of the Requirements for the Degree

DOCTOR OF PHILOSOPHY

ATHENS, GEORGIA

2017

ENZYMATIC AND ELECTROCHEMICAL OXIDATION OF EMERGING CONTAMINANTS

by

SHANGTAO LIANG

Major Professor:	Qingguo Huang
Committee:	Jiasheng Wang
	Miguel Cabrera
	Mussie Habteselassie
	Sayed Hassan

Electronic Version Approved:

Suzanne Barbour
Dean of the Graduate School
The University of Georgia
December 2017

DEDICATION

To my parents

ACKNOWLEDGEMENTS

This work would never have been possible without the guidance of my committee members, help from colleagues, and the support from my family.

I would like to express my gratitude to my major advisor, Dr. Qingguo Huang, for his excellent guidance, patience, support, and providing me with a great atmosphere for conducting academic research. Each of the other members of my dissertation committee, Dr. Jiasheng Wang, Dr. Miguel Cabrera, Dr. Mussie Habteselassie, and Dr. Sayed Hassan, has also provided me extensive personal and professional guidance during my study. I would especially thank Dr. Zhengwei Pan, professor of Physics and Engineering, for guiding my research on electrode fabrication and material development.

I'm grateful to all of those with whom I have had the pleasure to work during my dissertation projects. Dr. Hui Lin generously shared his knowledge in electrochemical research with me and helped me with experiment design. Dr. Qi Luo provided extensive guidance in PFAS research, data analysis and scientific writing. I would like to especially thank Dr. Dora Chiang for providing me thoughtful advice and assistance on professional development and career advancement.

Finally, I would like to thank my family members, who were always supporting me and encouraging me with unending inspiration.

TABLE OF CONTENTS

Page

LIST OF TABLES

Page

LIST OF FIGURES

Page

CHARPTER 1

LITERATURE REVIEW

EMERGING CONTAMINANTS

Overview

Emerging contaminants, also known as chemicals of emerging concern (COCs), refer to chemicals that are commonly detected in water, but only recently recognized as significant water contaminants, and, in most cases, have not been regulated for various reasons. These chemicals can be of natural origin or synthetic, and are not commonly monitored, but have been found having known or suspected adverse effects to human and ecosystems. To date, over 200 compounds have been detected in the environments and recognized as emerging contaminants (Petrie, Barden, & Kasprzyk-Hordern, 2015), including pharmaceuticals, personal care products (PPCPs), pesticides, endocrine disrupting compounds (EDCs), perfluorinated compounds (PFCs), and some pathogens. These contaminants originate from various sources, typically in concentration ranging from ng L^{-1} to μg L^{-1} in ecosystems. The maximum detected concentration in river water was 6.5 mg L^{-1} for antibiotic ciprofloxacin (Hughes, Kay, & Brown, 2012). Acute toxicity studies (including algae and bacteria) conducted under controlled laboratory conditions revealed median effective concentrations to be <1 mg L^{-1} for several EDCs (DellaGreca et al., 2007; Giudice & Young, 2010). Natural attenuation and conventional treatment processes are not capable of removing most of those compounds from wastewater, surface water and drinking water, and many of them are reported to be bioaccumulative in human and animals. Therefore, the presence of emerging contaminants in the environment is posing a health threat to human and animal, given that they

usually exist in complex mixtures. Developing the treatment technologies for emerging contaminants in water is a priority that must be addressed in order to ensure the use of safe drinking water and manage the potential human and ecosystem health risks.

Antibiotics

Use of antimicrobials to enhance growth, livability and feed conversion efficiency in broiler production was introduced about 50 years ago. Antibiotics are permitted as additives to feed or water in the U.S., and it is estimated that nearly 80% of poultry units in the U.S. use antibiotics in feed (Cook, Netthisinghe, & Gilfillen, 2014). Antibiotics used in animal production system include bacitracin, bambermycin, chlortetracycline, dihydrostreptomycin, erythromycin, lincomycin, neomycin, oxytetracycline, penicillin, spectinomycin, streptomycin, tetracycline and tylosin (Bolan et al., 2010). Residues of these chemicals have been detected in manure at varying concentrations, depending on the amount, frequency, retention and stability of the chemicals, and composting status of the litter. About 30%-90% of the veterinary antibiotics used in animal food-producing industry were excreted as the parent compounds due to their poor absorption in the gut of animal (Alcock, Sweetman, & Jones, 1999; Elmund, Morrison, Grant, & Nevins, 1971). Although administered antibiotics may be converted to conjugated forms in animal body, microbes are able to rapidly transform the conjugated antibiotics back to its bio-active form after excretion (Renner, 2002). In general, as high as 95% of antibiotics administered can be excreted back into the environment in their active forms (BECONI‐BARKER, Hornish, Vidmar, Dame, & Brown, 1996).

Antibiotics can be released into the environment from human and agricultural sources through multiple pathways, including excretion, disposal of out-of-date medicines, medical wastes, and discharge from wastewater treatment plants. Similar to other organic compounds, the

transport of antibiotics in the environment is related to their chemical properties, soil moisture, weather conditions, etc.. The mobility of antibiotics in the environment varies among different categories. The occurrences of veterinary antibiotics have been assessed in various phases, including groundwater, sediments, soil, manure, and surface water, especially the streams, lakes or other aquatic water bodies adjacent to animal food-producing facilities (Petrie et al., 2015). It was reported that chlortetracycline, sulfamethazine, and lincomycin were the most frequently detected antibiotics in the surface water samples from six states in the United States (Meyer et al., 2000). The detection of veterinary antibiotics in groundwater has also been reported in agricultural areas with a large number of live stocks, and the concentration were in $\mu g\ L^{-1}$ level (Hirsch, Ternes, Haberer, & Kratz, 1999). Although the concentrations of antibiotics were found to be low in groundwater in general, the residual oxytetracycline concentration can reach 4000 µg/Kg in marine sediment in chemotherapy treated fish farms in the US (Capone, Weston, Miller, & Shoemaker, 1996).

There is a growing public concern over the contribution of agricultural antibiotic uses to the global rise of drug resistance in bacteria. Although the use of antibiotics as growth promoters in poultry feed has been reduced in the U.S., they are still being used therapeutically, and the potential environmental risks of proliferation and transport of antibiotic-resistant bacteria via land application of manure cannot be overlooked. Since antibiotics are designed to inactivate microorganisms in human and animals, they are potentially harmful to other non-pathogenic microbes in the environment. In general, the toxic doses of antibiotics for microorganisms are 2-3 orders of magnitude below the toxic levels of animals (Wollenberger, Halling-Sørensen, & Kusk, 2000). The presence of antibiotics in the aquatic environment was found to cause adverse effects on the early life stages of different aquatic organisms such as *Daphnia magna* (Kümpel, Alexy, &

Kümmerer, 2001). Besides its direct effects on microbial community, another concern associated with antibiotic contamination is the changes in natural microbiota population due to the evolution of antibiotic-resistant bacteria in the environment. A previous study revealed that the bacteria isolated from the gut of animals with exposure to antibiotics exhibited antibiotic resistance five times greater than corresponding antibiotic resistant bacteria strains (Witte, 1998). The occurrence of specific antibiotic resistance characteristics in the environment has been reported by several studies (Goñi-Urriza et al., 2000; McKeon, Calabrese, & Bissonnette, 1995).

Perfluorinated compounds

Perfluoroalkyl acids (PFAAs) are alkyl acids in which all hydrogens on carbon are replaced by fluorine atoms. Such unique molecular structures result in distinct physicochemical characteristics, including water and oil repellency, high surface activity, and extreme stability against chemical and thermal destructions (Paul, Jones, & Sweetman, 2008). Therefore, PFAAs have been used extensively in a wide range of industrial, medical and domestic applications, such as surfactants, surface treatment agents, semiconductor, metal coating, and fire retardants (De Witte, Piessens, & Dams, 1995; Fiedler, Pfister, & Schramm, 2010). For example, Poly- and Perfluoroalkyl Substances (PFASs) have been used as surfactants in aqueous film-forming foams (AFFFs) that have been widely used at DoD sites as extinguishing agents (Ahrens, 2011; Ahrens et al., 2010).

The widespread uses of PFAAs, in combination with their high environmental persistence, have resulted in their frequent detections in the environment (Davis, Aucoin, Larsen, Kaiser, & Hartten, 2007; Filipovic & Berger, 2015; Kannan et al., 2001). PFAAs can enter aquatic environments during manufacturing, transport, product use, and disposal (Davis et al., 2007). Historically, effluents from PFAA production and the points of use were neither impounded nor

pretreated prior to discharge, resulting in serious contamination in these areas including groundwater, sediment and soil (Pan et al., 2014). PFASs can be mobile and recalcitrant in the environment, and thus advance in groundwater plumes ahead of other co-contaminants. The groundwater at many sites where AFFFs were involved in firefighting practices has been found contaminated by PFAAs with concentrations detected from μg L^{-1} to several mg L^{-1} (Andersen et al., 2007; Borg, Lund, Lindquist, & Håkansson, 2013; Corsini et al., 2012).

These chemicals, in particular, perfluoroalkyl acids (PFAAs) are persistent in the environment and have been reported showing adverse effects to animals and humans (Houde et al., 2008), thus raising serious concerns. In particular, PFOA and PFOS are considered carcinogenic (Lau, Butenhoff, & Rogers, 2004). Currently, the United States Environmental Protection Agency (USEPA) has a lifetime health advisory level of 70 parts per trillion (ppt) for PFOS, PFOA and in combination. Some states have adopted 70 ppt for PFOS and PFOA as advisory or action criteria. Among PFASs, perfluoroalkyl acids (PFAAs) including perfluoroalkyl carboxylic acids (PFCAs) and perfluoroalkyl sulfonic acids (PFSAs) have chemical structures where all C-H bonds are replaced by the strongest covalent bond in nature, the C-F bond. Thus, they represent a class of chemicals that are extremely challenging to remediate. Unfortunately, there is not a technology available for effective treatment or remediation of PFAAs in water.

Pathogens

Worldwide, over 780 million people are lack of safe water source, and an estimate of 2.5 billion people do not have access to adequate clean water. Illnesses caused by waterborne pathogens are prevalent all over the world. Diarrheal diseases became the second leading cause of death among children under 5, killing more children than AIDS, malaria, and measles combined. In the United States, it was estimated that 4-33 million illnesses and 40,000 hospitalizations were

associated with exposure to contaminated municipal drinking water (Mead et al., 2000). Over 9.7 billion dollars losses can be accounted by just five waterborne disease (Bermúdez-Aguirre & Barbosa-Cánovas, 2013).

The consumption of fresh fruits and vegetables has been increasing significantly in recent years (Afari, Hung, & King, 2015), And those minimally processed fresh produce are often consumed raw. Therefore, fresh produce can be easily contaminated with pathogenic microorganisms and lead to foodborne diseases. The most common pathogenic bacteria found from drinking water and fresh produce include *Escherichia coli* O157:H7, *Salmonella spp*, *Listeria monocytogenes*, and *Staphylococcus aureus (Ruonan et al., 2015)*. They can survive in water, fresh and frozen produce for extended period of time and thus pose severe health hazards to consumers (Ruonan et al., 2015). Improper poultry litter disposal is considered another source of waterborne pathogens is the environment. A culture- and molecular-based work has shown that poultry litter is a reservoir for several zoonotic pathogens, including *Escherichia coli*, *Salmonella spp*., *Campylobacter jejuni*, *Listeria monocytogenes*, *Staphylococcus spp.*, and *Clostridium perfringens* (Bolan et al., 2010), with the two principle infectious bacteria being *Salmonella* and *Campylobacter* (Cook et al., 2014)*, Clostridium perfringens* is the causative agent of necrotic enteritis in chicken, which can form spores and is highly resistant to disinfection,, and therefore has a long survival time (M'Sadeq, Wu, Swick, & Choct, 2015). *Salmonella*, *E. coli*, *Clostridium perfringens*, and *Staphylococcus* spp. are well known to cause significant numbers of foodborne illnesses in people (Scallan et al., 2011).

Although *Escherichia coli* bacteria are usually part of the normal intestinal flora of animals and humans, some strains are capable of causing serious diarrheal infections in humans. The most prominent representative of pathogenic *E coli* is the *E coli O157:H7*, which was first recognized

as a human pathogen in 1982 (Riley et al., 1983). *E coli O157:H7* can cause acute bloody diarrhea and abdominal cramps with little or no fever, sometimes may cause nonbloody diarrhea or no symptoms. Children with age below 5 are most susceptible to *E coli* infection. A previous study reported that *E coli O157:H7* can grow in nutrient-limited, reconditioned wastewater over the temperature range of 4 to 46 ºC when the biological oxygen demand of this water is < 2 (Rajkowski & Thayer, 2000).

CURRENT TREATMENT TECHNOLOGIES

Antibiotics

The removal of micropollutants through conventional wastewater treatment plants (WWTPs) is usually insufficient, although the process is effective in eliminating particulates, nutrients and pathogens. The primary treatment process in WWTPs, which is designed to remove suspended solids, was demonstrated to be ineffective in removing micropollutants (Carballa, Omil, & Lema, 2005). For pharmaceuticals, the removal efficiency in primary treatment is very limited with the removal rate ranging from 13% to 43% (Stasinakis et al., 2013), which suggested limited adsorption of those compounds to sludge particles (Behera, Kim, Oh, & Park, 2011). In the secondary treatment, the major removal process for micropollutants are biodegradation and sorption during biological treatment. During biological degradation, antibiotics and other micropollutants are either partially degraded into organic byproducts or completed mineralized into water and carbon dioxide through multiple processes, including single substrate growth, mixed substrate growth, or co-metabolism. However, although most of the micropollutants showed degradation to various degrees ranging from 25% to 75%, antibiotics are generally reported to be not readily degradable during biological treatments (Salgado et al., 2012; Verlicchi, Al Aukidy, & Zambello, 2012). Sorption of micropollutants mainly occur through hydrophobic interactions

between the aliphatic and aromatic groups of compounds and the cell membrane or through the electrostatic interactions of the positively charged compounds and the negatively charged microbes. Unfortunately, the sorption of antibiotics onto sludge during the secondary process is also very limited (< 5%) (Verlicchi et al., 2012).

Coagulation is a process used to remove particulate matter, colloids and dissolved substances during water treatments. From literature review, the coagulation/flocculation processes were found having only limited effectiveness in removing many micropollutants in water with a removal efficiency ranged from 20% to 50% (Matamoros & Salvadó, 2013). Among different types of coagulants, $FeCl_3$ was found to achieve the optimal removal rates for most compounds (Suarez, Lema, & Omil, 2009). Several factors such as the composition of wastewater, and the operation conditions, including mixing conditions, pH and alkalinity, can govern the performance of coagulation process (Alexander, Hai, & Al-aboud, 2012).

Adsorption by activated carbon is another technique widely used in drinking water treatment to remove odor and taste as well as micropollutants. Both powdered activated carbon (PAC) and granular activated carbon (GAC) are effective adsorbents for antibiotics, and they can achieve a high removal rate than coagulation/flocculation process (Choi, Kim, & Kim, 2008). Using activated carbon adsorption technique is beneficial since it can be used seasonally or occasionally as emerging treatment response (Snyder et al., 2007). With PAC added into the wastewater, the reduction of a group of micropollutants including antibiotics reached 85% with a retention time of 2 days (Kovalova et al., 2013). Similar to PAC, a typical drinking water dose of GAC (< 10 mg L^{-1}) was suggested to be sufficient to guarantee a 2-log removal of xxx in a lake water (Rossner, Snyder, & Knappe, 2009). In general, the performance of PAC in removing antibiotics is governed by the carbon dose, contact time, contaminant properties, and the

composition of wastewater. Therefore, addition of activated carbon appears to be an attractive method for removing antibiotics from water, especially for upgrading WWTPs. However, adsorption on PAC and GAC is not a destructive method as the mass of antibiotics are not reduced. An effective destruction method is in need to provide a complete treatment solution.

Due to the persistent nature of some antibiotics, traditional physicochemical and biological processes are not able to achieve fast and complete degradation of micropollutants. Ozonation is a technology that can degrade contaminants directly or indirectly via the formation of strong oxidizing hydroxyl radicals. Most of the antibiotics are susceptible to ozone and hydroxyl radicals (Gerrity et al., 2011), and the generation of hydroxyl radical can be further promoted by adding H_2O_2 and Fenton reagent. With an ozone dose of 15 mg L^{-1}, antibiotics can be degraded by 79% in the biologically treated effluent (Hernández-Leal, Temmink, Zeeman, & Buisman, 2011). The specific degradation rate differed among chemicals, and it is found that micropollutants with electron-rich moieties (e.g., phenols, anilines, olefins and activated aromatic) exhibited the highest degradation rates (Gerrity et al., 2011). Other advanced oxidation processes (AOPs) such as UV and H_2O_2 Fenton were also demonstrated as effective technologies for eliminating pharmaceuticals. For example, UV irradiation alone was able to achieve 46% degradation of a wide range of antibiotics within 10 minutes, and a combined process of UV and H_2O_2 enhanced the performance to 80% total removal within the same duration (De la Cruz et al., 2012). Although being effective in degrading most contaminants, the major concern of applying advanced oxidation process in drinking water and wastewater treatment is the formation of oxidation by-products. The generation of harmful oxidation by-products needs to be minimized by post-treatment processes like biological filtration.

Perfluorinated compounds

Sorption is the predominant technology currently available to manage PFAAs-contaminated groundwater plumes by pump-and-treat processes. Granular activated carbon (GAC) adsorption of PFOS and PFOA is a prevailing technique that removes PFOA and PFOS from the contaminated water. However, GAC treatment is not as effective for shorter chain PFAAs, and its effectiveness for precursors is also uncertain. In addition, the spent GAC would need to be regenerated with off-site high temperature thermal destruction and the regenerated GAC will be recycled for reuse. Although GAC systems have been widely applied as an emergency response measure at industrial sites and public water systems, long term cost effective options for effective treatment of short and long chain PFCAs and PFSAs should be developed.

Ion exchange resin (IXR) has gained popularity in recent years as a sorbent alternative to GAC for PFAA treatment (Baciocchi & Chiavola, 2006; Merino et al., 2016; Senevirathna et al., 2010), for several advantages: 1) the sorption of PFAAs on IXR involves mainly electrostatic interactions, and thus its efficiency does not diminish appreciably for shorter chain PFAAs, unlike GAC that mainly involves relatively weak van der Waals forces; 2) the sorption of PFAAs on IXR tends to be less interfered by hydrophobic co-contaminants, because it involves mainly electrostatic interactions; 3) IXR can be readily regenerated on site using a mixture containing methanol and NaCl solution, while on-site regeneration is not possible for GAC. The IXR technology is particularly suitable for removing charged PFAAs present in low concentrations (e.g. groundwater contamination), in which the IXR column can last long time before being exhausted (Merino et al., 2016). The IXR regeneration procedure involves the use of a mixture of a small fraction of sodium chloride solution and a large fraction of methanol (Du et al., 2015; Senevirathna et al., 2010; Xiao, Davidsavor, Park, Nakayama, & Phillips, 2012). As part of the regeneration

process, the spent methanol is recovered by distillation for reuse. The methanol distillation process will reclaim methanol representing approximately 75% of the spent regenerant by volume. Although being effective in removing PFAS from groundwater, the GAC or IX-R treatment process does not destroy PFAAs and the off-site incineration option may soon become less available, as PFAS regulations evolve and public concern heightens.

The extreme chemical stability of PFAAs renders them highly resistant to conventional treatment technologies or advanced oxidation processes (AOPs). AOPs rely primarily on hydroxyl radicals (·OH) to destruct organic contaminants, but the relatively slow reaction rates between PFAAs and aqueous ·OH limit their applicability. Some technologies have shown limited success in degrading PFAAs in laboratory-scale studies. For example, some photolytic techniques have shown varying degrees of efficacy on high concentrations of PFAAs, including direct UV photolysis, photochemical oxidation with $K_2S_2O_8$, $H_3PW_{12}O_{40}$, KI and humic acid (HA), and photocatalysis in the presence of TiO_2 and In_2O_3 (Cheng, Vecitis, Park, Mader, & Hoffmann, 2008; Giri, Ozaki, Morigaki, Taniguchi, & Takanami, 2011; Yuan Wang & Zhang, 2011). Ultrasonic irradiation and plasma oxidation have shown effectiveness to degrade PFAAs (Horikoshi, Sato, Abe, & Serpone, 2011). Application of these technologies is however limited by their requirement on high energy input and/or special equipment. In summary, conventional destructive treatment technologies, including advanced oxidation processes (AOPs) and ozonation, were demonstrated inefficient in removing PFOA and PFOS from contaminated water. Other degradation methods require extreme conditions that are costly and impractical for remediation applications, such as high temperature and pressure.

Complete mineralization of PFAAs has been achieved by electrooxidation via direct electron transfer on “non-active” anodes, including boron-doped diamond (BDD), PbO_2, and

SnO_2, under room temperature and atmospheric pressure at fast rates (half-lives: 5.3-21.5 minutes) and relatively low energy consumption (Lin, Niu, Ding, & Zhang, 2012; Lin et al., 2013; Niu, Lin, Xu, Wu, & Li, 2012). In a report, electrooxidation was used to effectively degrade PFCAs (C_4~C_8) and PFSAs (C_4~C_8) and 6:2 fluorotelomer sulfonate in polluted groundwater in the presence of a high dissolved organic carbon (DOC) background (DOC/PFAAs ratio up to 50) (Zhuo et al., 2012). Another study reported degradation of PFAAs, including PFOA and PFOS, in AFFFs contaminated groundwater by electrooxidation at bench scale, and the main degradation products were F^- and CO_2 (Schaefer, Andaya, Urtiaga, McKenzie, & Higgins, 2015). These results suggest the promising potential of using electrooxidation for treatment of PFAAs in groundwater or industrial wastewater.

Pathogens

Chlorine, generally in the forms of sodium hypochlorite (NaClO), is the most widely used disinfectant chemical in the water treatment plants (Feliziani, Lichter, Smilanick, & Ippolito, 2016; Joshi, Mahendran, Alagusundaram, Norton, & Tiwari, 2013; Meireles, Giaouris, & Simoes, 2016) due to its cost effectiveness and high efficacy in microorganism inactivation. The efficacy of chlorine is mainly due to the concentration of free chlorine, which is the unreacted chlorine remained in solution and available for disinfection reactions (Feliziani et al., 2016). Generally, a free chlorine level of 5 to 200 mg L^{-1} with a maximum exposure time of 5 min can reach optimal disinfection effects for wastewater treatment, while further increase of exposure time would not result in increased disinfection efficacies (Meireles et al., 2016). The application of chlorine has however been reduced due to several limitations, including easy inactivation by organic matters, pH dependent efficacy, high corrosiveness to metals, and most importantly, the production of carcinogenic and toxic disinfection by-products (DBPs) with organic matters (Feliziani et al.,

2016; Joshi et al., 2013; Meireles et al., 2016). Toxic DBPs such as chloroform, trihalomethanes, chloramines, and haloacetic acids have been identified in water chlorination (Legay, Rodriguez, Serodes, & Levallois, 2010). As a result, the use of chlorine has been banned in several European countries, including Belgium, Denmark, Germany, and the Netherlands (Meireles et al., 2016).

There have been studies about the use of alternative and novel disinfectants for fresh produce, such as ozonated water, chlorine dioxide, electrolyzed oxidizing water, and peracetic acid. However, all these techniques have their limitations and drawbacks that prevent them from widespread application. Ozonated water has been approved as by FDA and it was proven to be highly effective in inactivating bacteria, fungi, viruses, protozoa, and microbial spores (Joshi et al., 2013). The disadvantages are however also obvious, as ozone is very unstable, and can decompose rapidly, especially when in contact with organic materials. Ozone can be very toxic in gaseous phase by causing irritations to eyes and respiratory systems (Artes, Gomez, Aguayo, Escalona, & Artes-Hernandez, 2009). More importantly, ozone can affect the physiochemical properties of produce (Foong-Cunningham, Verkaar, & Swanson, 2012). Chlorine dioxide was also studied and considered as a potential alternative, because it has stronger oxidizing potential, lower reactivity with organic matters, and capacity in enzymatic browning inhibition (Joshi et al., 2013). However, the maximum allowed concentration of chlorine dioxide is only 3 mg L^{-1} due to its explosive potential, and thus the disinfection efficacy will be limited. Electrolyzed oxidizing water is a relatively new technique and its efficacy in pathogen inactivation has been studied and reviewed by numerous literatures (Al-Haq, Sugiyama, & Isobe, 2005; Y. R. Huang, Hung, Hsu, Huang, & Hwang, 2008; Rahman, Imran, & Deog-Hwan, 2016). Its main advantages are the low corrosiveness compared with chlorine and the use of non-harmful chemicals (sodium chloride) for production. Free chlorine in electrolyzed oxidizing water is the primary compound for disinfection,

and therefore the concern of DBPs production still remains. In addition, peroxylacetic acid, a mixture composed of peroxyl compound, hydrogen peroxide, and acetic acid, was also recommended for produce disinfection (Joshi et al., 2013). Similar to ozone and chlorine dioxide, peroxylacetic acid was shown to be effective in inactivating pathogens like *E. coli* O157:H7 and *Salmonella (Joshi et al., 2013)*, but, same to chlorine dioxide, the maximum limit for peroxylacetic acid to be used on fresh produce is only 80 mg L^{-1}, which has limited efficacy for pathogen elimination. Therefore, new sanitizers that are equally or more effective in pathogen inactivation with less or no DBPs production and minimal impact on physiochemical properties of produce are needed.

ENZYME-CATALYZED OXIDATION

ECOHR refers to a class of reactions ubiquitous in natural soil/water/sediment systems that are facilitated by extracellular enzymes such as peroxidases and laccases. These enzymes effectively convert the phenolic and anilinic substrates into active intermediates, e.g. free radicals and quinones, which can subsequently bind covalently with each other, thus facilitating the genesis of humus during natural humification. It is intriguing that many bioactive micropollutants, including hormones and antimicrobials, contain either phenolic or anilinic structures as their bioactive moieties, and are thus the natural substrates of ECOHR enzymes. Numerous previous studies by us and other researchers have demonstrated that these bioactive micropollutants can be effectively transformed and detoxified during ECOHRs (Q. Huang & Weber, 2005; Liang, Luo, & Huang, 2017; Mao et al., 2010; Sun, Luo, Gao, & Huang, 2016). We have found that incubation in the presence of laccase can lead to near complete removal of 17β-estradiol (Sun, Liang, Kang, Gao, & Huang, 2016), the major estrogen contained in poultry litter, and sulfadimethoxine, a major

sulfonamide antimicrobial used in animal farming, from soil and poultry manure under unsaturated water content conditions as soon as 11 days (Singh, Sidhu, Zhang, & Huang, 2015).

ECOHRs can not only convert phenols and anilines as their direct substrates, but also other inert organic chemicals, because the free radicals and quinones formed during ECOHR can serve as mediators to activate the inert chemicals and thus incorporate them into humification reactions. Natural organic matter (NOM) contains abundant phenolic moieties that can interact with humification enzymes and serve as mediators to activate other none-substrate chemicals (Lu et al. 2009). It is therefore possible that a bioactive micropollutant that is not a direct substrate of humification enzymes can still be transformed indirectly during ECOHRs.

ECOHRs are indeed critically involved in the transformation of natural organic matter (NOM) in the nature. It is believed that three processes interact to effect NOM transformation as shown in Figure 1 (Senesi 1989). Biopolymers such as lipids, proteins and lignocelluloses are degraded to labile small molecules such as amino and fatty acids and monosaccharides that can be either mineralized to CO_2 or polymerized to humus via humification. ECOHRs are important reactions in humification to facilitate substrates polymerization via oxidative coupling of free radicals. In the meantime, ECOHRs also facilitate biopolymer degradation; for example, laccase mediates the degradation of lignin via a mediator-facilitated ECOHR mechanism (K. Li, Xu, & Eriksson, 1999).

ELECTROCHEMICAL OXIDATION

Electrochemical treatment is one approach that is nearly universally applicable, and thus may treat mixed contaminants all together without being interfered by the presence of multiple chemicals. Various mechanisms take effect in electrochemical treatment processes, dependent on applied voltage and conditions, including redox reactions by direct electron transfer or indirect

free radical reactions and sorption/retention by electric field. Electrooxidation is one most common electrochemical treatment process that oxidizes contaminants by either direct electron transfer or by hydroxyl radicals generated on anode, and has been proven effective for most organic contaminants. Electrochemical process is considered having a great potential in future wastewater treatment applications, because it can be applied to a wide spectrum of pollutants at ambient conditions without addition of chemicals, and can be readily automated and operated at decentralized locations.

EO is able to degrade CoCs and disinfect pathogens mainly via oxidation by direct electron transfer on the anode and/or by the hydroxyl free radicals generated on the anode surface via water electrolysis. Numerous studies have demonstrated effective degradation of PFAAs via electrochemical oxidation (EO) on various electrodes at fast rates and relatively low energy consumption (Lin et al., 2012; Lin et al., 2013; Niu et al., 2012; Schaefer, Andaya, Urtiaga, et al., 2015; Zhuo et al., 2012). Unlike traditional AOPs that involve only hydroxyl free radicals, EO can promote direct electron transfer of PFAAs on the anode surfaces to convert them into free radicals, which can then be attacked by hydroxyl free radicals that are also generated on the anode surfaces during the EO process (Lin et al., 2013). A recent study demonstrated the degradation of PFOA and PFOS in AFFF impacted groundwater using a commercial Ti/RuO_2 anode, reaching the defluorination rates of 58% and 98%, respectively (Schaefer, Andaya, Urtiaga, et al., 2015). In another study, EO was applied to effectively degrade PFOA, PFOS and shorter-chain PFAAs in groundwater on boron doped diamond (BDD) anode with half-lives less than one hour (Zhuo et al., 2012).

Previous research on the electrooxidation of PFAAs has focused on “non-active” anode materials that have high oxygen overvoltage, including SnO_2, PbO_2 and BDD. However, BDD

electrode is costly and difficult to produce in large size for scaled up applications. SnO_2-based hybrid electrodes, such as Ti/SnO_2-Sb, are inexpensive and easy to prepare, but their service lives are relatively short (Lin et al., 2012). PbO_2 electrodes have a long history of industrial applications because of their cost-effectiveness, ease of preparation, long service life, and good conductivity (Niu et al., 2012). Possible release of toxic Pb ions is the main drawback for environmental applications of PbO_2 electrodes. Thus, application of electrochemical processes in environmental remediation is limited unless an effective, low-cost, durable, and environmentally benign electrode material is available.

Ti_4O_7 is one of the Magnéli phase titanium sub-oxides that have recently been explored as promising candidates for electrochemical applications because of their high conductivity, chemical inertness, and low cost of production (Walsh & Wills, 2010). These materials comprise a series of distinct compounds having the generic formula Ti_nO_{2n-1} ($3< n <10$), while Ti_4O_7 has the greatest electric conductivity, comparable to graphite (Bunce & Bejan, 2014). Ti_4O_7 is robust in aggressive solution media, such as highly acidic and basic solutions, and has been widely used in cathodic protection, fuel cell, and as supporting materials for coating various materials including noble metals and carbon (Bunce & Bejan, 2014; Yao, Li, Li, & Xia, 2012). Ti_4O_7 can serve as an ideal electrode in electrochemical wastewater treatment, being stable with respect to water decomposition under anodic (> 2.0 V vs SCE) and cathodic (~ -1.4 V vs SCE) polarizations (Bunce & Bejan, 2014). Studies have shown that Ti_4O_7 behaves as typical "non-active" electrodes and thus produces physisorbed ·OH via water oxidation, and is also active for direct electron transfer reactions (Bunce & Bejan, 2014; Zaky & Chaplin, 2013).

Despite the many advantages of EO technology and Magnéli phase Ti_4O_7 anode material, EO is yet feasible to directly treat large volumes of groundwater containing low concentrations of

PFAAs. This is because that the mass transfer of the target chemical from bulk solution to the anode surfaces is limited when its concentration is low, thus limiting the overall EO efficiency. It has been noted that the energy consumption of PFAAs degradation is dependent on their concentrations; for instance, the energy required to degrade one mole of PFOA increased by about an order of magnitude when PFOA concentration was lowered by 2 orders of magnitude (Zhuo et al., 2012). . One way to overcome the rate limiting by interfacial mass transfer is to operate the electrode as a membrane in filtration mode, also known as reactive electrochemical membrane (REM) operation, which significantly improves interfacial mass transfer via convection-enhanced dispersion. In order to address the mass transfer limitation, three-dimensional porous electrodes have been developed and operated in a filtration mode, i.e. cross-flow or dead-end. Not only such electrodes offer much greater surface areas as a result of the porous structure, but also the filtration mode supports advection-enhanced mass transfer, which is significantly faster than the flow-by or batch operation. These factors in combination greatly enhance the electrooxidation efficiency by overcoming the mass-transfer limit. In the meantime, the electrooxidation can mitigate the membrane fouling by degrading organic foulants. Therefore, the process involves both membrane filtration and electrooxidation in a synergistic manner, which offers a potentially transformative technology that may address a wide range of challenges in wastewater treatment and recycling.

LITERATURE CITED

Afari, G. K., Hung, Y.-C., & King, C. H. (2015). Efficacy of Neutral pH Electrolyzed Water in Reducing Escherichia coli O157:H7 and Salmonella Typhimurium DT 104 on Fresh Produce Items using an Automated Washer at Simulated Food Service Conditions. *Journal of Food Science, 80*(8), M1815-M1822. doi: 10.1111/1750-3841.12936

Ahrens, L. (2011). Polyfluoroalkyl compounds in the aquatic environment: a review of their occurrence and fate. *Journal of Environmental Monitoring, 13*(1), 20-31.

Ahrens, L., Taniyasu, S., Yeung, L. W., Yamashita, N., Lam, P. K., & Ebinghaus, R. (2010). Distribution of polyfluoroalkyl compounds in water, suspended particulate matter and sediment from Tokyo Bay, Japan. *Chemosphere, 79*(3), 266-272.

Al-Haq, M. I., Sugiyama, J., & Isobe, S. (2005). Applications of Electrolyzed Water in Agriculture & Food Industries. [Applications of Electrolyzed Water in Agriculture & Food Industries]. *Food Science and Technology Research, 11*(2), 135-150. doi: 10.3136/fstr.11.135

Alcock, R. E., Sweetman, A., & Jones, K. C. (1999). Assessment of organic contanhnant fate in waste water treatment plants I: Selected compounds and physicochemical properties. *Chemosphere, 38*(10), 2247-2262.

Alexander, J. T., Hai, F. I., & Al-aboud, T. M. (2012). Chemical coagulation-based processes for trace organic contaminant removal: Current state and future potential. *Journal of environmental management, 111*, 195-207.

Andersen, M. E., Butenhoff, J. L., Chang, S.-C., Farrar, D. G., Kennedy Jr, G. L., Lau, C., . . . Wallace, K. B. (2007). Perfluoroalkyl acids and related chemistries—toxicokinetics and modes of action. *Toxicological Sciences, 102*(1), 3-14.

Artes, F., Gomez, P., Aguayo, E., Escalona, V., & Artes-Hernandez, F. (2009). Sustainable

sanitation techniques for keeping quality and safety of fresh-cut plant commodities (Vol. 51, pp. 287-296): Postharvest and Refrigeration Group, Department of Food Engineering and Institute of Plant Biotechnology, Technical University of Cartagena, Paseo Alfonso XIII, 48. 30203 Cartagena, Murcia, Spain. Tel. +34 968 325510. Fax +34 968 325433. E-mail fr.artes@upct.es.

Baciocchi, R., & Chiavola, A. (2006). Ion exchange process in the presence of high sulphate concentration: resin regeneration and spent brine reuse. *Water Science and Technology: Water Supply, 6*(3), 35-41.

BECONI-BARKER, M., Hornish, R., Vidmar, T., Dame, K., & Brown, S. (1996). Ceftiofur hydrochloride: plasma and tissue distribution in swine following intramuscular administration at various doses. *Journal of veterinary pharmacology and therapeutics, 19*(3), 192-199.

Behera, S. K., Kim, H. W., Oh, J.-E., & Park, H.-S. (2011). Occurrence and removal of antibiotics, hormones and several other pharmaceuticals in wastewater treatment plants of the largest industrial city of Korea. *Science of the Total Environment, 409*(20), 4351-4360.

Bermúdez-Aguirre, D., & Barbosa-Cánovas, G. V. (2013). Disinfection of selected vegetables under nonthermal treatments: chlorine, acid citric, ultraviolet light and ozone. *Food Control, 29*(1), 82-90.

Bolan, N. S., Szogi, A., Chuasavathi, T., Seshadri, B., Rothrock, M. J., & Panneerselvam, P. (2010). Uses and management of poultry litter. *World's Poultry Science Journal, 66*(4), 673-698.

Borg, D., Lund, B.-O., Lindquist, N.-G., & Håkansson, H. (2013). Cumulative health risk assessment of 17 perfluoroalkylated and polyfluoroalkylated substances (PFASs) in the Swedish population. *Environment international, 59*, 112-123.

Bunce, N. J., & Bejan, D. (2014). Pollutants in Water-Electrochemical Remediation Using Ebonex Electrodes *Encyclopedia of Applied Electrochemistry* (pp. 1629-1633): Springer.

Capone, D. G., Weston, D. P., Miller, V., & Shoemaker, C. (1996). Antibacterial residues in marine sediments and invertebrates following chemotherapy in aquaculture. *Aquaculture, 145*(1), 55-75.

Carballa, M., Omil, F., & Lema, J. M. (2005). Removal of cosmetic ingredients and pharmaceuticals in sewage primary treatment. *Water Research, 39*(19), 4790-4796.

Cheng, J., Vecitis, C. D., Park, H., Mader, B. T., & Hoffmann, M. R. (2008). Sonochemical degradation of perfluorooctane sulfonate (PFOS) and perfluorooctanoate (PFOA) in landfill groundwater: environmental matrix effects. *Environmental Science and Technology, 42*(21), 8057-8063.

Choi, K.-J., Kim, S.-G., & Kim, S.-H. (2008). Removal of antibiotics by coagulation and granular activated carbon filtration. *Journal of Hazardous Materials, 151*(1), 38-43.

Cook, K., Netthisinghe, A., & Gilfillen, R. (2014). Detection of pathogens, indicators, and antibiotic resistance genes after land application of poultry litter. *Journal of Environmental Quality, 43*(5), 1546-1558.

Corsini, E., Sangiovanni, E., Avogadro, A., Galbiati, V., Viviani, B., Marinovich, M., . . . Germolec, D. R. (2012). In vitro characterization of the immunotoxic potential of several perfluorinated compounds (PFCs). *Toxicology and Applied Pharmacology, 258*(2), 248-255.

Davis, K. L., Aucoin, M. D., Larsen, B. S., Kaiser, M. A., & Hartten, A. S. (2007). Transport of ammonium perfluorooctanoate in environmental media near a fluoropolymer manufacturing facility. *Chemosphere, 67*(10), 2011-2019.

De la Cruz, N., Giménez, J., Esplugas, S., Grandjean, D., De Alencastro, L., & Pulgarin, C. (2012). Degradation of 32 emergent contaminants by UV and neutral photo-fenton in domestic wastewater effluent previously treated by activated sludge. *Water Research, 46*(6), 1947-1957.

De Witte, J., Piessens, G., & Dams, R. (1995). Fluorochemical intermediates, surfactants and their use in coatings. *Surface Coatings International, 78*(2), 58-64.

DellaGreca, M., Iesce, M. R., Isidori, M., Nardelli, A., Previtera, L., & Rubino, M. (2007). Phototransformation products of tamoxifen by sunlight in water. Toxicity of the drug and its derivatives on aquatic organisms. *Chemosphere, 67*(10), 1933-1939.

Du, Z., Deng, S., Chen, Y., Wang, B., Huang, J., Wang, Y., & Yu, G. (2015). Removal of perfluorinated carboxylates from washing wastewater of perfluorooctanesulfonyl fluoride using activated carbons and resins. *Journal of Hazardous Materials, 286*, 136-143.

Duran, N., & Esposito, E. (2000). Potential applications of oxidative enzymes and phenoloxidase-like compounds in wastewater and soil treatment: a review. *Applied catalysis B: environmental, 28*(2), 83-99.

Elmund, G. K., Morrison, S., Grant, D., & Nevins, M. (1971). Role of excreted chlortetracycline in modifying the decomposition process in feedlot waste. *Bulletin of Environmental Contamination and Toxicology, 6*(2), 129-132.

Feliziani, E., Lichter, A., Smilanick, J. L., & Ippolito, A. (2016). Disinfecting agents for controlling fruit and vegetable diseases after harvest (Vol. 122, pp. 53-69): Correspondence address, A. Ippolito, Department of Agricultural, Food and Environmental Sciences, Marche Polytechnic University, Via Brecce Bianche, 60131, Ancona, Italy. E-mail antonio.ippolito@uniba.it.

Fiedler, S., Pfister, G., & Schramm, K.-W. (2010). Poly-and perfluorinated compounds in household consumer products. *Toxicological and Environ Chemistry, 92*(10), 1801-1811.

Filipovic, M., & Berger, U. (2015). Are perfluoroalkyl acids in waste water treatment plant effluents the result of primary emissions from the technosphere or of environmental recirculation? *Chemosphere, 129*, 74-80.

Foong-Cunningham, S., Verkaar, E. L. C., & Swanson, K. (2012). Microbial decontamination of fresh produce. In A. Dermirci & M. O. Ngadi (Eds.), *Microbial decontamination in the food industry: novel methods and applications*. Cambridge; UK: Woodhead Publishing Ltd.

Gerrity, D., Gamage, S., Holady, J. C., Mawhinney, D. B., Quiñones, O., Trenholm, R. A., & Snyder, S. A. (2011). Pilot-scale evaluation of ozone and biological activated carbon for trace organic contaminant mitigation and disinfection. *Water Research, 45*(5), 2155-2165.

Giri, R., Ozaki, H., Morigaki, T., Taniguchi, S., & Takanami, R. (2011). UV photolysis of perfluorooctanoic acid (PFOA) in dilute aqueous solution. *Water Science and Technology, 63*(2), 276-282.

Giudice, B. D., & Young, T. M. (2010). The antimicrobial triclocarban stimulates embryo production in the freshwater mudsnail Potamopyrgus antipodarum. *Environmental Toxicology and Chemistry, 29*(4), 966-970.

Goñi-Urriza, M., Capdepuy, M., Arpin, C., Raymond, N., Caumette, P., & Quentin, C. (2000). Impact of an Urban Effluent on Antibiotic Resistance of Riverine Enterobacteriaceae andAeromonas spp. *Applied and Environmental Microbiology, 66*(1), 125-132.

Hernández-Leal, L., Temmink, H., Zeeman, G., & Buisman, C. (2011). Removal of micropollutants from aerobically treated grey water via ozone and activated carbon. *Water Research, 45*(9), 2887-2896.

Hirsch, R., Ternes, T., Haberer, K., & Kratz, K.-L. (1999). Occurrence of antibiotics in the aquatic environment. *Science of the Total Environment, 225*(1), 109-118.

Horikoshi, S., Sato, S., Abe, M., & Serpone, N. (2011). A novel liquid plasma AOP device integrating microwaves and ultrasounds and its evaluation in defluorinating perfluorooctanoic acid in aqueous media. *Ultrasonics Sonochemistry, 18*(5), 938-942.

Houde, M., Czub, G., Small, J. M., Backus, S., Wang, X., Alaee, M., & Muir, D. C. (2008). Fractionation and bioaccumulation of perfluorooctane sulfonate (PFOS) isomers in a Lake Ontario food web. *Environmental Science and Technology, 42*(24), 9397-9403.

Huang, Y. R., Hung, Y. C., Hsu, S. Y., Huang, Y. W., & Hwang, D. F. (2008). Application of electrolyzed water in the food industry. *Food Control, 19*(4), 329-345.

Hughes, S. R., Kay, P., & Brown, L. E. (2012). Global synthesis and critical evaluation of pharmaceutical data sets collected from river systems. *Environmental Science and Technology, 47*(2), 661-677.

Joshi, K., Mahendran, R., Alagusundaram, K., Norton, T., & Tiwari, B. K. (2013). Review: Novel disinfectants for fresh produce. *Trends in Food Science & Technology, 34*, 54-61. doi: 10.1016/j.tifs.2013.08.008

Kannan, K., Hansen, S., Franson, C., Bowerman, W., Hansen, K., Jones, P., & Giesy, J. (2001). Perfluorochemical surfactants in the environment. *Environmental Science and Technology, 35*, 3065-3070.

Kovalova, L., Siegrist, H., Von Gunten, U., Eugster, J., Hagenbuch, M., Wittmer, A., . . . McArdell, C. S. (2013). Elimination of micropollutants during post-treatment of hospital wastewater with powdered activated carbon, ozone, and UV. *Environmental Science and Technology, 47*(14), 7899-7908.

Kümpel, T., Alexy, R., & Kümmerer, K. (2001). What Do We Know about Antibiotics in the Environment? *Pharmaceuticals in the Environment* (pp. 67-76): Springer.

Lau, C., Butenhoff, J. L., & Rogers, J. M. (2004). The developmental toxicity of perfluoroalkyl acids and their derivatives. *Toxicology and Applied Pharmacology, 198*(2), 231-241.

Legay, C., Rodriguez, M. J., Serodes, J. B., & Levallois, P. (2010). Estimation of chlorination by-products presence in drinking water in epidemiological studies on adverse reproductive outcomes: a review (Vol. 408, pp. 456-472): Correspondence address, M. J. Rodriguez, Ecole superieure d'amenagement du territoire de l'Universite Laval, Pavillon Antoine Savard, Universite Laval, Quebec City, Que. G1K 7P4, Canada. Tel. +1 418 656 2131x8933. Fax +1 418 626 2018. E-mail manuel.rodriguez@esad.ulaval.ca.

Li, K., Xu, F., & Eriksson, K.-E. L. (1999). Comparison of fungal laccases and redox mediators in oxidation of a nonphenolic lignin model compound. *Applied and Environmental Microbiology, 65*(6), 2654-2660.

Lin, H., Niu, J., Ding, S., & Zhang, L. (2012). Electrochemical degradation of perfluorooctanoic acid (PFOA) by Ti/SnO 2–Sb, Ti/SnO 2–Sb/PbO 2 and Ti/SnO 2–Sb/MnO 2 anodes. *Water Research, 46*(7), 2281-2289.

Lin, H., Niu, J., Xu, J., Huang, H., Li, D., Yue, Z., & Feng, C. (2013). Highly efficient and mild electrochemical mineralization of long-chain perfluorocarboxylic acids (C9–C10) by Ti/SnO2–Sb–Ce, Ti/SnO2–Sb/Ce–PbO2, and Ti/BDD electrodes. *Environmental Science and Technology, 47*(22), 13039-13046.

M'Sadeq, S. A., Wu, S., Swick, R. A., & Choct, M. (2015). Towards the control of necrotic enteritis in broiler chickens with in-feed antibiotics phasing-out worldwide. *Animal Nutrition, 1*(1), 1-11.

Matamoros, V., & Salvadó, V. (2013). Evaluation of a coagulation/flocculation-lamellar clarifier and filtration-UV-chlorination reactor for removing emerging contaminants at full-scale wastewater treatment plants in Spain. *Journal of environmental management, 117*, 96-102.

McKeon, D. M., Calabrese, J. P., & Bissonnette, G. K. (1995). Antibiotic resistant gram-negative bacteria in rural groundwater supplies. *Water Research, 29*(8), 1902-1908.

Mead, P. S., Slutsker, L., Dietz, V., McCaig, L. F., Bresee, J. S., Shapiro, C., . . . Tauxe, R. V. (2000). Food-Related Illness and Death in the United States. *Journal of Environmental Health, 62*(7), 9.

Meireles, A., Giaouris, E., & Simoes, M. (2016). Alternative disinfection methods to chlorine for use in the fresh-cut industry (Vol. 82, pp. 71-85): Correspondence address, M. Simoes, LEPABE, Department of Chemical Engineering, Faculty of Engineering, University of Porto, Rua Dr. Roberto Frias, s/n, 4200-465 Porto, Portugal. E-mail mvs@fe.up.pt.

Merino, N., Qu, Y., Deeb, R. A., Hawley, E. L., Hoffmann, M. R., & Mahendra, S. (2016). Degradation and removal methods for perfluoroalkyl and polyfluoroalkyl substances in water. *Environmental Engineering Science, 33*(9), 615-649.

Meyer, M., Bumgarner, J., Varns, J. L., Daughtridge, J., Thurman, E., & Hostetler, K. A. (2000). Use of radioimmunoassay as a screen for antibiotics in confined animal feeding operations and confirmation by liquid chromatography/mass spectrometry. *Science of the Total Environment, 248*(2), 181-187.

Niu, J., Lin, H., Xu, J., Wu, H., & Li, Y. (2012). Electrochemical mineralization of perfluorocarboxylic acids (PFCAs) by Ce-doped modified porous nanocrystalline PbO2 film electrode. *Environmental Science and Technology, 46*(18), 10191-10198.

Pan, C.-G., Zhao, J.-L., Liu, Y.-S., Zhang, Q.-Q., Chen, Z.-F., Lai, H.-J., . . . Ying, G.-G. (2014).

Bioaccumulation and risk assessment of per-and polyfluoroalkyl substances in wild freshwater fish from rivers in the Pearl River Delta region, South China. *Ecotoxicology and Environmental Safety, 107*, 192-199.

Paul, A. G., Jones, K. C., & Sweetman, A. J. (2008). A first global production, emission, and environmental inventory for perfluorooctane sulfonate. *Environmental Science and Technology, 43*(2), 386-392.

Rahman, S. M. E., Imran, K., & Deog-Hwan, O. (2016). Electrolyzed water as a novel sanitizer in the food industry: current trends and future perspectives (Vol. 15, pp. 471-490): Correspondence address, Deog-Hwan Oh, Dept. of Food Science and Biotechnology, School of Bio-convergence Science and Technology, Kangwon Natl. Univ, Chuncheon, South Korea. E-mail deoghwa@kangwon.ac.kr.

Rajkowski, K. T., & Thayer, D. W. (2000). Reduction of Salmonella spp. and strains of Escherichia coli O157: H7 by gamma radiation of inoculated sprouts. *Journal of Food Protection, 63*(7), 871-875.

Renner, R. (2002). Do cattle growth hormones pose an environmental risk? : ACS Publications.

Rice, E. W., Clark, R. M., & Johnson, C. H. (1999). Chlorine inactivation of Escherichia coli O157: H7. *Emerging infectious diseases, 5*(3), 461.

Riley, L. W., Remis, R. S., Helgerson, S. D., McGee, H. B., Wells, J. G., Davis, B. R., . . . Hargrett, N. T. (1983). Hemorrhagic colitis associated with a rare Escherichia coli serotype. *New England Journal of Medicine, 308*(12), 681-685.

Rossner, A., Snyder, S. A., & Knappe, D. R. (2009). Removal of emerging contaminants of concern by alternative adsorbents. *Water Research, 43*(15), 3787-3796.

Ruonan, M., Guomin, W., Ying, T., Kaile, W., Jue, Z., & Jing, F. (2015). Non-thermal plasma-

activated water inactivation of food-borne pathogen on fresh produce. *Journal of Hazardous Materials, 300*, 643-651.

Salgado, R., Marques, R., Noronha, J., Carvalho, G., Oehmen, A., & Reis, M. (2012). Assessing the removal of pharmaceuticals and personal care products in a full-scale activated sludge plant. *Environmental Science and Pollution Research, 19*(5), 1818-1827.

Scallan, E., Hoekstra, R. M., Angulo, F. J., Tauxe, R. V., Widdowson, M.-A., Roy, S. L., . . . Griffin, P. M. (2011). Foodborne illness acquired in the United States—major pathogens. *Emerging infectious diseases, 17*(1), 7.

Schaefer, C. E., Andaya, C., Urtiaga, A., McKenzie, E. R., & Higgins, C. P. (2015). Electrochemical treatment of perfluorooctanoic acid (PFOA) and perfluorooctane sulfonic acid (PFOS) in groundwater impacted by aqueous film forming foams (AFFFs). *Journal of Hazardous Materials, 295*, 170-175.

Senevirathna, S., Tanaka, S., Fujii, S., Kunacheva, C., Harada, H., Shivakoti, B., & Okamoto, R. (2010). A comparative study of adsorption of perfluorooctane sulfonate (PFOS) onto granular activated carbon, ion-exchange polymers and non-ion-exchange polymers. *Chemosphere, 80*(6), 647-651.

Snyder, S. A., Adham, S., Redding, A. M., Cannon, F. S., DeCarolis, J., Oppenheimer, J., . . . Yoon, Y. (2007). Role of membranes and activated carbon in the removal of endocrine disruptors and pharmaceuticals. *Desalination, 202*(1-3), 156-181.

Stasinakis, A. S., Thomaidis, N. S., Arvaniti, O. S., Asimakopoulos, A. G., Samaras, V. G., Ajibola, A., . . . Lekkas, T. D. (2013). Contribution of primary and secondary treatment on the removal of benzothiazoles, benzotriazoles, endocrine disruptors, pharmaceuticals and perfluorinated compounds in a sewage treatment plant. *Science of the Total Environment,*

463, 1067-1075.

Suarez, S., Lema, J. M., & Omil, F. (2009). Pre-treatment of hospital wastewater by coagulation–flocculation and flotation. *Bioresource Technology, 100*(7), 2138-2146.

Verlicchi, P., Al Aukidy, M., & Zambello, E. (2012). Occurrence of pharmaceutical compounds in urban wastewater: removal, mass load and environmental risk after a secondary treatment—a review. *Science of the Total Environment, 429*, 123-155.

Walsh, F., & Wills, R. (2010). The continuing development of Magnéli phase titanium sub-oxides and Ebonex® electrodes. *Electrochimica Acta, 55*(22), 6342-6351.

Wang, Y., & Zhang, P. (2011). Photocatalytic decomposition of perfluorooctanoic acid (PFOA) by TiO 2 in the presence of oxalic acid. *Journal of Hazardous Materials, 192*(3), 1869-1875.

Witte, W. (1998). Medical consequences of antibiotic use in agriculture. *Science, 279*(5353), 996-997.

Wollenberger, L., Halling-Sørensen, B., & Kusk, K. O. (2000). Acute and chronic toxicity of veterinary antibiotics to Daphnia magna. *Chemosphere, 40*(7), 723-730.

Xiao, F., Davidsavor, K. J., Park, S., Nakayama, M., & Phillips, B. R. (2012). Batch and column study: sorption of perfluorinated surfactants from water and cosolvent systems by Amberlite XAD resins. *Journal of Colloid and Interface Science, 368*(1), 505-511.

Yao, C., Li, F., Li, X., & Xia, D. (2012). Fiber-like nanostructured Ti4O7 used as durable fuel cell catalyst support in oxygen reduction catalysis. *Journal of Materials Chemistry, 22*(32), 16560-16565. doi: 10.1039/C2JM

Zaky, A. M., & Chaplin, B. P. (2013). Porous Substoichiometric TiO2 Anodes as Reactive Electrochemical Membranes for Water Treatment. *Environmental Science & Technology, 47*(12), 6554-6563. doi: 10.1021/es401287e

Zhuo, Q., Deng, S., Yang, B., Huang, J., Wang, B., Zhang, T., & Yu, G. (2012). Degradation of perfluorinated compounds on a boron-doped diamond electrode. *Electrochimica Acta, 77*, 17-22.

CHARPTER 2

DEGRADATION OF SULFADIMETHOXINE CATALYZED BY LACCASE WITH SOYBEAN MEAL EXTRACT AS NATURAL MEDIATOR: MECHANISM AND REACTION PATHWAY[1]

[1]Liang, S., Luo, Q., & Huang, Q. Accepted by *Chemosphere*. Reprinted here with permission of publisher, November 1, 2017.

ABSTRACT

Natural laccase-mediator systems have been well recognized as an eco-friendly and energy-saving approach in environmental remediation, whose further application is however limited by the high cost of natural mediators and relatively long treatment time span. This study evaluated the water extract of soybean meal, a low-cost compound system, in mediating the laccase catalyzed degradation of a model contaminant of emerging concern, sulfadimethoxine (SDM), and demonstrated it as a promising alternative mediator for soil and water remediation. Removal of 73.3% and 65.6% was achieved in 9 hrs using soybean meal extract (SBE) as the mediating system for laccase-catalyzed degradation of sulfadimethoxine at the concentration of 1 mg L^{-1} and 10 mg L^{-1}, respectively. Further degradation of sulfadimethoxine was observed with multiple SBE additions. Using SBE as mediator increased the 9-h removal of SDM at 1 mg L^{-1} initial concentration by 52.9%, 49.4%, and 36.3% in comparison to the system mediated by 1-Hydroxybenzotriazole (HBT), *p*-Coumaric acid (COU) and 2,2′-azinobis(3-ethylbenzthiazoline-6-sulfonate) (ABTS), respectively. With the detection of stable coupling products formed with radical scavenger (5,5-Dimethyl-1-pyrroline N-oxide, DMPO), three phenolic compounds (vanillin, apocynin, and daidzein) in SBE were confirmed to serve as mediators for *Trametes versicolor* laccase. Reaction pathways were proposed based on the results of High Resolution Mass Spectrometry. SO_2 excursion happened during SDM transformation, leading to elimination of antimicrobial activity. Therefore, as a natural, phenol rich, and affordable compound system, the future application of SBE in wastewater and soil remediation is worth exploring.

Keywords: Soybean meal; Laccase; Mediator; Sulfadimethoxine; Remediation

INTRODUCTION

Sulfadimethoxine (SDM), a sulfonamide antibiotic, is commonly used to treat infections in livestock and poultry production, and it is approved in some countries to treat human disease. In fresh water fishery industry, sulfadimethoxine is often used in combination with ormetoprim to prevent spread of disease (Guerard et al., 2009). Antimicrobials and their biologically active degradation products may be introduced into terrestrial system through manure application, or in the case of aquafarming, discharged directly into surface waters, thus endangering the aquatic ecology. In environmental systems, sulfonamides were detected at concentrations ranging from 2 mg/kg to 20 mg/kg in liquid manure samples (Haller et al., 2002; Jacobsen and Halling-Sørensen, 2006) and from 0.06 to 15 $\mu g\ L^{-1}$ in surface water samples (Lindsey et al., 2001). The half-lives of sulfadimethoxine range from 3 – 11 d in manure samples (Wang et al., 2006b), from 10.5 – 49.8 d in natural water samples (Zhang et al., 2012), from 42.0 – 58.2 d in lake water sediments (Zhang et al., 2012), and from 1.36 to 10.2 d in manure amended soils (Wang et al., 2006a).

Widespread use of antibiotics and release of their metabolites into the environment has promoted the evolution of antibiotic resistance genes and impacted microcosm functionality. The prevalence of sulfonamide resistance bacteria and significant enrichment of antibiotic resistance genes (ARGS) was observed in pig slurry samples, river water, sediments, and soils adjacent to livestock production facilities worldwide (Byrne-Bailey et al., 2009; Hsu et al., 2014; Pei et al., 2006; Zhu et al., 2013). In a previous study, the quantity of *sul(I)* and *sul(II)*, two predominant sulfonamide-resistant genes, increased by more than 40% in agricultural soil with periodic additions of manure than in the untreated land (Heuer et al., 2011).

Laccase, a blue multicopper oxidase, is capable of transferring four electrons from four reducing substrate molecules to one molecule oxygen with no requirement of cofactors, producing

water as the only byproduct. In this process, substrates become radicals, and then may undergo cross-coupling reactions, decarboxylations, demethylations and/or dehalogenations. The unique characteristic of laccase to degrade phenolic aromatic compounds, which are normally toxic or recalcitrant in environmental matrices, has raised considerable interest as an eco-friendly bioremediation approach for contaminated wastewater and soil. Previous studies have demonstrated successful application of laccase in treating a broad range of substrates, including phenols, methoxy phenols, aromatic amines, polyphenols, and polyamines (Cañas et al., 2007; d'Acunzo et al., 2002).

However, the application of laccase is limited because of its incapability to oxidize pollutants with high redox potentials. Redox mediators are low-molecular-weight phenols that were found to produce active free radicals that can further react with inert chemicals, thus expanding the substrate spectrum. Synthetic mediators, such as 2, 2'-azine-bis (3-ethylbenzothiazoline-6-sulfonic acid (ABTS), 2,2,6,6-tetramethyl-1-piperidinyloxyl (TMPO), and 1-Hydroxybenzotriazole (HBT), have been reported to promote laccase-catalyzed oxidation of numerous toxic compounds, including antibiotics (Cañas and Camarero, 2010; Morozova et al., 2007; Weng et al., 2012; Weng et al., 2013). Plant-, especially legume-derived natural phenolic compounds (vanillin, *p*-coumaric acid, sinapic acid, acetovanillone, ferulic acid, salicylic acid, syringaldehyde) can also act as mediators, but are less efficient than synthetic mediators (Camarero et al., 2005; Cañas and Camarero, 2010; Johannes and Majcherczyk, 2000). A recent study compared the effects of both synthetic and natural mediators on sulfadimethoxine degradation and indicated that ABTS-mediated treatment achieved the highest removal rate of 90% at 20 ºC (Weng et al., 2013). Similar result was found by another study, suggesting ABTS can lead to faster degradation of sulfadimethoxine than other tested mediators (Weng et al., 2012). Although the

laccase-mediator system (LMS) has great potential as an environmentally benign remediation technology, its feasibility is hindered because of the high cost and the potential toxic effects of mediators.

Soybean meal is produced as the residue of oil extraction process. Its superior amino-acid profile, high digestibility, and low cost make it an ideal vegetable-protein meal for animal production. Soybean meal is also commonly used as soil amendment in organic farming to provide nitrogen source for crops. The heating process during soybean meal production can transform aromatic amino acids in soybean into phenolic compounds (Kato et al., 1971), in addition to the phenolic contents (up to 1.13 mg gallic acid equivalent (GAE)/g) originally in soybean (Lee et al., 2011). Its high phenolic content makes soybean meal a potential cheaper and nontoxic alternative mediator for laccase oxidation reaction. The objective of this study is to investigate the feasibility of using the water extract of soybean meal to mediate laccase-catalyzed degradation of sulfadimethoxine. The reaction products were identified using high resolution mass spectrometry, based on which the reaction mechanism is elucidated. The phenolic compounds in SBE acting as mediators were studied, and their reactions with laccase to form radicals were verified via a radical scavenging probe.

MATERIALS AND METHODS

Chemicals and Materials

Sulfadimethoxine (SDM), 2,2'-azino-bis(3-ethylbenzothiazoline-6-sulfonic acid) diammonium salt (ABTS), 1-hydroxybenzotriazole (HBT), *p*-coumaric acid (COU), gallic acid (GA), vanillin (VA), apocynin (AP), daidzein (DA), 5,5-dimethyl-1-pyrroline-N-oxide (DMPO), Folin-Ciocalteu's phenol reagent, sodium carbonate and laccase from *Trametes versicolor* were obtained from Sigma-Aldrich (St. Louis, MO). Soybean meal (organic soil amendment) was

purchased from Eureka Springs Organics (Eureka Springs, AR). Aqueous solutions used in this work were prepared from Barnstead Nanopure system with a resistivity of $\geqslant$18 MΩ cm^{-1}. HPLC grade acetonitrile and formic acid were provided by Sigma-Aldrich (St. Louis, MO).

Soybean meal extract (SBE) was prepared by shaking 10g of soybean meal on shaker with 300 mL HPLC water at 150 rpm for 5 days. The extract was then passed through 0.45 μm cellulose acetate membrane and stored at 4 ºC for subsequent use.

Degradation experiments

The experiments were conducted in 20 mL polyethylene vials containing 1 mg L^{-1} of sulfadimethoxine, 0.5 U mL^{-1} laccase (one unit of laccase was previously defined (Luo et al., 2015)), and 1 mg L^{-1} mediators (ABTS, HBT, COU, VA, AP, and DA) or various doses of soybean meal extract in a total reaction volume of 10 mL. For reactors containing 10 mg L^{-1} of sulfadimethoxine, the concentrations of laccase and mediators were 5 U mL^{-1} and 10 mg L^{-1} respectively. Reactors were covered by Parafilm to allow passive aeration, and continuously shaken at 150 rpm in dark under room temperature. At each pre-determined sampling point, 100 μl of reaction mixture was taken from the reactor, and the reaction was stopped immediately by adding 900 μl acetonitrile to the sample. All samples were tested in triplicate.

Folin-Ciocalteu assay for total phenolic content

The total phenolic content of soybean meal extract was examined colorimetrically as modified by Singleton et al., 1999. Briefly, 0.5 mL of soybean meal extract or gallic acid standard solution was mixed with 2.5 mL of 10-fold diluted Folin-Ciocalteu phenol reagent and 2 mL of 7.5% (w/v) sodium carbonate. The absorbance was measured at 765 nm after 15 min incubation at 45ºC in dark using a Beckman Coulter DU 800 spectrophotometer (Brea, CA). Quantification

was done on the basis of a standard curve of gallic acid, and the total phenolic content was expressed as gallic acid equivalent (GAE, mg L^{-1}).

Radical scavenging assessment

DMPO was used as a spin trap agent in this study, because it can form stable DMPO adducts with phenoxyl radicals. The reaction sample was prepared by mixing 1 mL of SBE, 50 µl of 100 mg mL^{-1} freshly made DMPO solution, and 50 µl of 120 U mL^{-1} laccase solution in a tube and incubated for 5 hrs in dark. The final reaction solution was analyzed with an Orbitrap Elite high-resolution mass spectrometer (Thermo Scientific, San Jose, CA) to detect the coupling product formed between DMPO and phenoxyl radicals. Control samples containing SBE but not DMPO was also processed and measured along with the reaction samples.

UV-Vis absorption spectrum study

The absorption spectra of the soybean meal extract, the initial reaction solution and the reaction solution after 24h treatment was scanned at 1200 nm/min from 200 nm to 500 nm using a Beckman Coulter DU 800 spectrophotometer (Brea, CA).

Quantification of sulfadimethoxine

Aqueous samples were passed through 0.22 µm cellulose membrane, and 100 µL of sample was reconstituted in 900 µL of acetonitrile/water (50/50, v/v) mixture before further analysis. Sulfadimethoxine was quantified by a Waters ACQUITY UPLC I-class system coupled with a Xevo TQD tandem mass spectrometer (UPLC-MS/MS) (Milford, MA) with a mobile phase consisting of acetonitrile (solvent A) and 0.1% formic acid in water (solvent B) at a flow rate of 0.3 mL/min for a total retention time of 6 mins. The spectrometer was operated in electrospray positive (ESI+) mode with the following parameters: capillary voltage 2.60 kV, cone voltage 38.34 V, desolvation temperature 500 ºC, cone gas flow 50 L/Hr, and desolvation gas flow 500 L/Hr.

Multiple reaction monitoring (MRM) mode was employed to detect and quantify sulfadimethoxine based on the precursor ion (m/z 311.00)/daughter ion (m/z 156.10) spectra.

Identification of products

The sample for product identification was prepared by degradation treatment solution at 1 mg L^{-1} initial SDT concentration, 0.5 unit/mL laccase, and 1 mg L^{-1} mediator, which yielded around 50% SDM removal. A positive control that contained only SDM in water, and a negative control that did not contain SDM but SBE were also incubated and processed along with the treatment sample. MS full scan (m/z 50 – 1000, resolution R = 120000) analyses were performed on the treatment and control samples using an Orbitrap Elite high-resolution tandem mass spectrometer (Thermo Scientific, Waltham, MA) operated in electrospray positive mode. Possible products were identified by screening the m/z peaks present in the treatment samples but not in the controls using the mass filtration function in Xcalibur 2.1 software (Thermo Scientific, Waltham, MA). Molecular formulas of the possible products were assigned using Formula Finder with 5 mg L^{-1} mass error allowed. Tandem MS (MS/MS) was further performed on the possible products (resolution R = 30000), based on which the molecular structure of each product was deduced by general MS fragmentation rules.

RESULTS AND DISCUSSION

SDM degradation in LMS

As shown in **Figure 2.1A** and 2.**1B**, the residual SDM relative to the initial concentration decreased along the degradation duration. After reacting for 9 hrs in the systems with SDM initial concentration at 1 mg L^{-1}, the removal rates were 73.3%, 37.1%, 23.9%, and 20.4% in reactors containing SBE, ABTS, HBT, and COU respectively. The same trend was observed in the systems with SDM initial concentration at 10 mg L^{-1}: the 9-h removal of SDM in SBE mediated system

was 65.6%, which was much higher than those of the systems mediated by ABTS (54.9%), HBT (46.5%) and COU (38.8%), respectively. In previous studies, ABTS-mediated system was found to achieve the fastest removal rate in laccase-catalyzed sulfadimethoxine oxidations at room temperature (Weng et al., 2012; Weng et al., 2013). Moreover, as the most intensively studied mediators, ABTS, HBT and COU were also reported to be effective in mediating laccase degradation of several other sulfonamide antibiotics (e.g., sulfathiazole, sulfamethoxazole, sulfadiazine, and sulfamethazine) (Rahmani et al., 2015; Shi et al., 2014). The extraordinary performance of soybean meal extract may be attributed to its high contents of nitrogen, phenolic compounds and divalent cations, which will be elucidated in more detail later in this report. Additionally, the concentration of SDM reduced dramatically during the first hour of SBE-mediated degradation in the experiments with 1 mg L^{-1} initial concentration **(Figure 2.1A)**, with 89.3% of the total SDM removal over the 9-h reaction achieved within the first hour. This is consistent with the previous finding that the rate-limiting step in LMS is the process of producing free radicals from mediators, which is governed by the laccase-mediator redox status (Li et al., 1999; Xu et al., 2000). The large redox potential difference between phenolic compounds in SBE and *Trametes versicolor* laccase may lead to fast production of phenolic radicals, and thus accelerate the radical-initiated degradation of SDM, especially when the concentration of the substrate is relatively low. Moreover, when the free radical of laccase mediator is present at high concentration, laccase will be inactivated due to the feedback mechanism (Li et al., 1999), which well explains the low enzyme activity observed in SBE mediated systems (**Table S2.1**).

In the SBE-mediated reaction systems with initial SDM concentrations at both 1 mg L^{-1} and 10 mg L^{-1}, a plateau phase was observed in the last stage of degradation (**Figure 2.1**). Also, slightly decreased degradation rate was found in the systems with10-mg L^{-1} initial concentrations

(65.6%) compared to those with 1-mg L^{-1} initial concentration (73.3%). Both evidences suggested the depletion of mediators in SBE as the reaction went on, especially in systems with high SDM concentrations. An experiment with multiple mediator additions (2 ml each time) was conducted to test this hypothesis and the result is shown in **Figure S2.1**. Further removal of SDM was achieved after each SBE addition.

Identification of laccase mediators in soybean meal extract

Although a great majority of the natural laccase mediators reported so far are of soybean origin phenolic compounds, not all phenolic compounds are laccase substrates and can play the role of mediators. In order to identify those in SBE that can potentially serve as laccase mediators, DMPO was employed as a scavenger to probe the free radicals formed under laccase catalysis. DMPO is ideal for this purpose because it is inactive towards redox reactions, while form relatively stable radical adducts with oxygen-centered free radicals (Guo et al., 2003). Three DMPO adducts (**Figure 2.2**) were identified using high resolution mass spectrometry and their structures were confirmed based on high resolution MS data (**Table 2.1**) and MS/MS spectra (**Figure S2.2**). Vanillin and apocynin (acetovanillone) are known laccase mediators extracted from a variety of plant sources (Martens, 2002; Stuppner et al., 1995; Walton et al., 2003). They significantly promoted the removal of various recalcitrant chemicals (dyes, pentachlorophenol, and polycycline aromatic hydrocarbons (PAH)) by laccase in previous studies (Camarero et al., 2005; Cañas et al., 2007; Jeon et al., 2008). Daidzein is one of the major isoflavones contained in soybean meal with a concentration as high as 706 μg/g wet weight (Reinli and Block, 1996). To our best knowledge, this is the first report on daidzein as a natural mediator of laccase.

The degradation of sulfadimethoxine in laccase oxidation system mediated by vanillin, apocynin, and daidzein were determined separately. The results (**Figure 2.3**) confirmed that the

addition of each of these three chemicals enhanced the removal of sulfadimethoxine. However, the 20-h removal rate (14.7% for DA, 28.2% for VA, 31.9% for AP) was not as high as that achieved by soybean meal extract in 9 h (65.6%). The particularly effective laccase mediation effect of soybean meal extract may arise from: 1) soybean meal is a protein-based organic fertilizer rich in nitrogen content that can decay into nitroso compound (Hedler et al., 1979), while it is known that nitroso compound, such as 1-hydroxybenzotriazole (HBT), N-hydroxyphthalimide (HPI) and violuric acid (VLA), are major classes of laccase mediators that has been reported having the best efficiency for laccase oxidation of recalcitrant compounds (Cañas and Camarero, 2010; Morozova et al., 2007); 2) the total phenolic content of SBE was determined to be 91.0 mg L^{-1} gallic acid equivalent (GAE), which is much greater than those of the other mediators tested in present study (**Table S2.2**). The total phenolic content may be positively correlated to oxidation efficiency as most of the natural mediators are phenolic compounds; 3) soybean meal extract is especially high in total organic carbon, magnesium, and calcium content (**Table S2.3**), while it has been found in previous studies that transition metal ions (e.g. Mn^{2+}) and metallic complexes can act as mediators when they were oxidized by enzyme (Höfer and Schlosser, 1999; Schlosser and Höfer, 2002), and the organic content in SBE may provide natural chelating agents to complex with metals, thus facilitating its oxidation by enzyme (Schlosser and Höfer, 2002); and 4) co-existence of multiple mediators may lead to synergic effect in laccase-mediator systems. Enhanced reaction rate was observed in previous laccase oxidation study when ABTS and natural mediators were present in combination (Jeon et al., 2008). This is because not only the primary radical species but also the secondary species generated through chain reactions among primary radicals can attack the organic pollutants, leading to more efficient oxidation.

The degradation of SDM was also studied in a series of SBE water diluents at various total phenolic contents (**Figure 2.4**). The result revealed a positive relationship between the degradation rate of SDM and the dilution rate of SBE. The treatments achieved 64.2% and 43.4% of SDM removal when SBE (originally ~90 mg GAE L^{-1}) was diluted to 50 and 25 mg GAE L^{-1}, allowing remediation application by dosing SBE into contaminated water at a specific dilution rate. Further reduction of the amount of SBE addition is achievable as the total phenolic content in SBE can be increased by raising the soybean meal to water ratio during extraction or extending the extraction time. Besides, considering that soybean meal is commonly amended to soil as a nutrient booster, its application in soil remediation is especially promising. The feasibility of applying soybean meal extract in soil remediation is being examined in our ongoing projects.

Reaction Pathways

Possible reaction products were identified by screening the peaks present in HRMS spectra of the treatment samples while not in those of the controls. The high mass accuracy (5 mg L^{-1} at m/z 400) allows for an unambiguous assignment of the elemental composition of a possible product, as indicated in **Table 2.2**. The molecular structure was then deduced based on the daughter ions detected in MS/MS analysis according to common fragmentation rules (McLafferty and František, 1993), as depicted in **Figure S2.3**. Based on the product identification, reaction pathways were proposed for SDM degradation as illustrated in **Figure 2.5**. The product (m/z 232.1080) assigned with the elemental composition of $C_{12}H_{13}O_2N_3$ (Table 2) corresponds to the loss of SO_2 and an amino group accompanied by rearrangement of a hydrogen. The relative MS peak intensity of this molecule to SDM was 55.59%. A similar pathway was reported in a study on the reaction of several sulfonamides catalyzed by *Trametes versicolor* laccase, including sulfadimethoxine (García-Galán et al., 2011; Schwarz et al., 2010). Moreover, loss of sulfonate

group, also known as SO_2 excursion, is a common transformation pathway found in enzymatic degradation, microbial metabolism, anodic Fenton treatment, and chlorinolysis of sulfonamides (Gao et al., 2012; García-Galán et al., 2011; Mohatt et al., 2011; Neafsey et al., 2010; Schwarz et al., 2010). This process is critical in detoxification treatments because it destroys sulfonyl and amide functional groups, which are responsible for the antimicrobial activity of sulfonamide antibiotics (Henry, 1943). In the UV-Vis spectrum shown in **Figure 2.6**, the featured peak of sulfadimethoxine at 265 nm diminished significantly after 24 h enzymatic treatment, providing strong evidence to the removal of sulfonamide group from the parent chemical. Subsequent loss of $-OCH_2$ or $-CH_2$ group led to the formation of $C_{11}H_{11}ON_3$ (m/z 202.0996) or $C_{11}H_{11}O_2N_3$ (m/z 218.0948), respectively, as shown in **Figure 2.5**. This is the first report on the detection of these two intermediates in enzymatic oxidation of sulfodimethoxine. These two products may further convert to aniline C_6H_7N (m/z 94.0647), through hydrolysis. Aniline was also detected in a previous study as a metabolite of SDM by fungal laccase (Schwarz et al., 2010). Alternatively, SO_2 and aniline can be eliminated directly from SDM to form a pyrimidine product at m/z 156.0763 ($C_6H_9O_2N_3$). In the presence of ligninolytic enzyme and its mediators, aniline and other intermediates may undergo further degradation/mineralization to form smaller molecules, CO_2, and water (Mahendra et al., 2007; Xu, 1996; Yang et al., 2016).

CONCLUSIONS

The addition of soybean meal extract with laccase effectively transformed sulfadimethoxine at environmentally relevant condition, while the degradation rates were faster than those tested using HBT, ABTS and *p*-Coumaric acid as mediators. Loss of sulfonate group was the major transformation pathway detected, which resulted in the removal of antimicrobial activity. This study is the first to report the degradation process, mediator identification and

reaction pathways in LMS system mediated by the extract of naturally origin soybean meal. It is worthwhile in future studies to understand the relative contributions of phenolic compounds, metal ions, and the interactions between these chemicals and organic pollutants.

SUPPORTING INFORMATION AVAILABLE

Results of multi-dosing SBE test; Enzyme activity; HRMS data and MS/MS spectrum of DMPO and mediator coupling products; HRMS data and MS/MS spectrum of SDM degradation products; Total phenolic content, total organic carbon and metal ion contents of soybean meal extract and other mediator solutions.

ACKNOWLEDGEMENTS

The study was supported in part by U.S. Department of Defense SERDP ER-2127, W912HQ-11-C-0022. We thank the Proteomics and Mass Spectrometry Core Facility at the University of Georgia for performing the high resolution mass spectrometry analysis for our samples.

LITERATURE CITED

Byrne-Bailey, K.G., Gaze, W.H., Kay, P., Boxall, A.B.A., Hawkey, P.M., Wellington, E.M.H., 2009. Prevalence of sulfonamide resistance genes in bacterial isolates from manured agricultural soils and pig slurry in the United Kingdom. Antimicrob. Agents Chemother. 53, 696-702.

Camarero, S., Ibarra, D., Martínez, M.J., Martínez, Á.T., 2005. Lignin-derived compounds as efficient laccase mediators for decolorization of different types of recalcitrant dyes. Appl. Environ. Microbiol. 71, 1775-1784.

Cañas, A.I., Alcalde, M., Plou, F., Martínez, M.J., Martínez, Á.T., Camarero, S., 2007. Transformation of polycyclic aromatic hydrocarbons by laccase is strongly enhanced by phenolic compounds present in soil. Environ. Sci. Technol. 41, 2964-2971.

Cañas, A.I., Camarero, S., 2010. Laccases and their natural mediators: Biotechnological tools for sustainable eco-friendly processes. Biotechnol. Adv. 28, 694-705.

d'Acunzo, F., Galli, C., Masci, B., 2002. Oxidation of phenols by laccase and laccase-mediator systems. Eur. J. Biochem. 269, 5330-5335.

Gao, J., Hedman, C., Liu, C., Guo, T., Pedersen, J.A., 2012. Transformation of sulfamethazine by manganese oxide in aqueous solution. Environ. Sci. Technol. 46, 2642-2651.

García-Galán, M.J., Rodríguez-Rodríguez, C.E., Vicent, T., Caminal, G., Díaz-Cruz, M.S., Barceló, D., 2011. Biodegradation of sulfamethazine by *Trametes versicolor*: Removal from sewage sludge and identification of intermediate products by UPLC–QqTOF-MS. Sci. Total Environ. 409, 5505-5512.

Guerard, J.J., Chin, Y.-P., Mash, H., Hadad, C.M., 2009. Photochemical fate of sulfadimethoxine in aquaculture waters. Environ. Sci. Technol. 43, 8587-8592.

Guo, Q., Qian, S.Y., Mason, R.P., 2003. Separation and identification of DMPO adducts of oxygen-

centered radicals formed from organic hydroperoxides by HPLC-ESR, ESI-MS and MS/MS. J. Am. Soc. Mass. Spectrom. 14, 862-871.

Haller, M.Y., Müller, S.R., McArdell, C.S., Alder, A.C., Suter, M.J.F., 2002. Quantification of veterinary antibiotics (sulfonamides and trimethoprim) in animal manure by liquid chromatography–mass spectrometry. J. Chromatogr. A 952, 111-120.

Hedler, L., Schurr, C., Marquardt, P., 1979. Determination of volatile N-nitroso compounds in various samples of edible vegetable oils and margarine (commercially available products). J. Am. Oil Chem. Soc. 56, 681-684.

Henry, R.J., 1943. The mode of action of sulfonamides. Bacteriol. Rev. 7, 175-262.

Heuer, H., Solehati, Q., Zimmerling, U., Kleineidam, K., Schloter, M., Müller, T., Focks, A., Thiele-Bruhn, S., Smalla, K., 2011. Accumulation of sulfonamide resistance genes in arable soils due to repeated application of manure containing sulfadiazine. Appl. Environ. Microbiol. 77, 2527-2530.

Höfer, C., Schlosser, D., 1999. Novel enzymatic oxidation of Mn_2^+ to Mn_3^+ catalyzed by a fungal laccase. FEBS Lett. 451, 186-190.

Hsu, J.-T., Chen, C.-Y., Young, C.-W., Chao, W.-L., Li, M.-H., Liu, Y.-H., Lin, C.-M., Ying, C., 2014. Prevalence of sulfonamide-resistant bacteria, resistance genes and integron-associated horizontal gene transfer in natural water bodies and soils adjacent to a swine feedlot in northern Taiwan. J. Hazard. Mater. 277, 34-43.

Jacobsen, A.M., Halling-Sørensen, B., 2006. Multi-component analysis of tetracyclines, sulfonamides and tylosin in swine manure by liquid chromatography–tandem mass spectrometry. Anal. Bioanal. Chem. 384, 1164-1174.

Jeon, J.-R., Murugesan, K., Kim, Y.-M., Kim, E.-J., Chang, Y.-S., 2008. Synergistic effect of

laccase mediators on pentachlorophenol removal by *Ganoderma lucidum* laccase. Appl. Microbiol. Biotechnol.81, 783-790.

Johannes, C., Majcherczyk, A., 2000. Natural mediators in the oxidation of polycyclic aromatic hydrocarbons by laccase mediator systems. Appl. Environ. Microbiol. 66, 524-528.

Kato, S., Kurata, T., Fujimaki, M., 1971. Thermal degradation of aromatic amino acids. Agric. Biol. Chem. 35, 2106-2112.

Lee, J.H., Jeon, J.K., Kim, S.G., Kim, S.H., Chun, T., Imm, J.-Y., 2011. Comparative analyses of total phenols, flavonoids, saponins and antioxidant activity in yellow soy beans and mung beans. Int. J. Food Sci. Technol. 46, 2513-2519.

Li, K., Xu, F., Eriksson, K.-E.L., 1999. Comparison of fungal laccases and redox mediators in oxidation of a nonphenolic lignin model compound. Appl. Environ. Microbiol. 65, 2654-2660.

Lindsey, M.E., Meyer, M., Thurman, E.M., 2001. Analysis of trace levels of sulfonamide and tetracycline antimicrobials in groundwater and surface water using solid-phase extraction and liquid chromatography/mass spectrometry. Anal. Chem. 73, 4640-4646.

Luo, Q., Lu, J., Zhang, H., Wang, Z., Feng, M., Chiang, S.-Y.D., Woodward, D., Huang, Q., 2015. Laccase-catalyzed degradation of perfluorooctanoic acid. Environ. Sci. Technol. Lett. 2, 198-203.

Mahendra, S., Petzold, C. J., Baidoo, E. E., Keasling, J. D., Alvarez-Cohen, L., 2007. Identification of the intermediates of in vivo oxidation of 1, 4-dioxane by monooxygenase-containing bacteria. Environ. Sci. Technol. 41, 7330-7336.

Martens, D.A., 2002. Identification of phenolic acid composition of alkali-extracted plants and soils. Soil Sci. Am. J. 66, 1240-1248.

McLafferty, F.W., František T., 1993. Interpretation of mass spectra, fourth ed. University science books, Sausalito

Mohatt, J.L., Hu, L., Finneran, K.T., Strathmann, T.J., 2011. Microbially mediated abiotic transformation of the antimicrobial agent sulfamethoxazole under iron-reducing soil conditions. Environ. Sci. Technol. 45, 4793-4801.

Morozova, O.V., Shumakovich, G.P., Shleev, S.V., Yaropolov, Y.I., 2007. Laccase-mediator systems and their applications: a review. Appl. Biochem. Microbiol. 43, 523-535.

Neafsey, K., Zeng, X., Lemley, A.T., 2010. Degradation of sulfonamides in aqueous solution by membrane anodic fenton treatment. J. Agric. Food Chem. 58, 1068-1076.

Pei, R., Kim, S.-C., Carlson, K.H., Pruden, A., 2006. Effect of river landscape on the sediment concentrations of antibiotics and corresponding antibiotic resistance genes (ARG). Water Res. 40, 2427-2435.

Rahmani, K., Faramarzi, M.A., Mahvi, A.H., Gholami, M., Esrafili, A., Forootanfar, H., Farzadkia, M., 2015. Elimination and detoxification of sulfathiazole and sulfamethoxazole assisted by laccase immobilized on porous silica beads. Int. Biodeter. Biodegr. 97, 107-114.

Reinli, K., Block, G., 1996. Phytoestrogen content of foods—a compendium of literature values. Nutr. Cancer. 26, 123-148.

Schlosser, D., Höfer, C., 2002. Laccase-catalyzed oxidation of Mn_2^+ in the presence of natural Mn_3^+ chelators as a novel source of extracellular H_2O_2 production and its impact on manganese peroxidase. Appl. Environ. Microbiol. 68, 3514-3521.

Schwarz, J., Aust, M.-O., Thiele-Bruhn, S., 2010. Metabolites from fungal laccase-catalysed transformation of sulfonamides. Chemosphere 81, 1469-1476.

Shi, L., Ma, F., Han, Y., Zhang, X., Yu, H., 2014. Removal of sulfonamide antibiotics by oriented

immobilized laccase on Fe_3O_4 nanoparticles with natural mediators. J. Hazard. Mater. 279, 203-211.

Singleton, V.L., Orthofer, R., Lamuela-Raventós, R.M., 1999. Analysis of total phenols and other oxidation substrates and antioxidants by means of folin-ciocalteu reagent. Methods Enzymol. 299, 152-178.

Stuppner, H., Reinisch, O., Wiedermann, C.J., Wagner, H., 1995. Acetophenones — compounds from plant origin with inhibitory effects on neutrophil in vitro respiration burst activity. Phytomedicine 1, 283-286.

Walton, N.J., Mayer, M.J., Narbad, A., 2003. Vanillin. Phytochemistry 63, 505-515.

Wang, Q., Guo, M., Yates, S.R., 2006a. Degradation kinetics of manure-derived sulfadimethoxine in amended soil. J. Agric. Food Chem. 54, 157-163.

Wang, Q.Q., Bradford, S.A., Zheng, W., Yates, S.R., 2006b. Sulfadimethoxine degradation kinetics in manure as affected by initial concentration, moisture, and temperature. J. Environ. Qual. 35, 2162-2169.

Weng, S.-S., Ku, K.-L., Lai, H.-T., 2012. The implication of mediators for enhancement of laccase oxidation of sulfonamide antibiotics. Bioresour. Technol. 113, 259-264.

Weng, S.-S., Liu, S.-M., Lai, H.-T., 2013. Application parameters of laccase–mediator systems for treatment of sulfonamide antibiotics. Bioresour. Technol. 141, 152-159.

Xu, F., 1996. Oxidation of phenols, anilines, and benzenethiols by fungal laccases: Correlation between activity and redox potentials as well as halide inhibition. Biochemistry. 35, 7608-7614.

Xu, F., Kulys, J.J., Duke, K., Li, K., Krikstopaitis, K., Deussen, H.-J.W., Abbate, E., Galinyte, V., Schneider, P., 2000. Redox chemistry in laccase-catalyzed oxidation of N-hydroxy

compounds. Appl. Environ. Microbiol. 66, 2052-2056.

Yang, C.-W., Hsiao, W.-C., Chang, B.-V., 2016. Biodegradation of sulfonamide antibiotics in sludge. Chemosphere 150, 559-565.

Zhang, Y., Xu, J., Zhong, Z., Guo, C., Li, L., He, Y., Fan, W., Chen, Y., 2012. Degradation of sulfonamides antibiotics in lake water and sediment. Environ. Sci. Pollut. Res. 20, 2372-2380.

Zhu, Y.-G., Johnson, T.A., Su, J.-Q., Qiao, M., Guo, G.-X., Stedtfeld, R.D., Hashsham, S.A., Tiedje, J.M., 2013. Diverse and abundant antibiotic resistance genes in Chinese swine farms. Proc. Natl. Acad. Sci. U.S.A. 110, 3435-3440.

Table 2.1. High resolution mass spectrometry data of DMPO-mediator coupling products.

Notation	Elemental Composition	$[M+H]^+$		Error ($mg\ L^{-1}$)
		Measured Mass	Theoretical Mass	
DMPO + Vanillin	$C_{14}H_{18}O_4N$	265.1304	265.1309	-1.73
DMPO + Apocynin	$C_{15}H_{20}O_5N$	295.1410	295.1414	-1.59
DMPO + Daidzein	$C_{21}H_{21}O_5N$	368.1496	368.1492	0.91

Table 2.2. High resolution mass spectrometry data of SDM degradation products.

Notation	Elemental Composition	$[M+H]^+$		Error (mg L^{-1})	Relative Intensity (%)
		Measured Mass	Theoretical Mass		
Aniline	C_6H_7N	94.0647	94.0651	-4.53	1.33
SDM-SO_2-Aniline	$C_6H_9O_2N_3$	156.0763	156.0768	-2.75	0.27
SDM-SO_2-NH-OCH_2	$C_{11}H_{11}ON_3$	202.0975	202.0975	-0.07	11.08
SDM-SO_2-NH-CH_2	$C_{11}H_{11}O_2N_3$	218.0923	218.0924	-0.53	9.61
SDM-SO_2-NH	$C_{12}H_{13}O_2N_3$	232.1080	232.1081	-0.41	55.59
SDM	$C_{12}H_{14}O_4N_4S$	311.0802	311.0809	-2.14	100.00

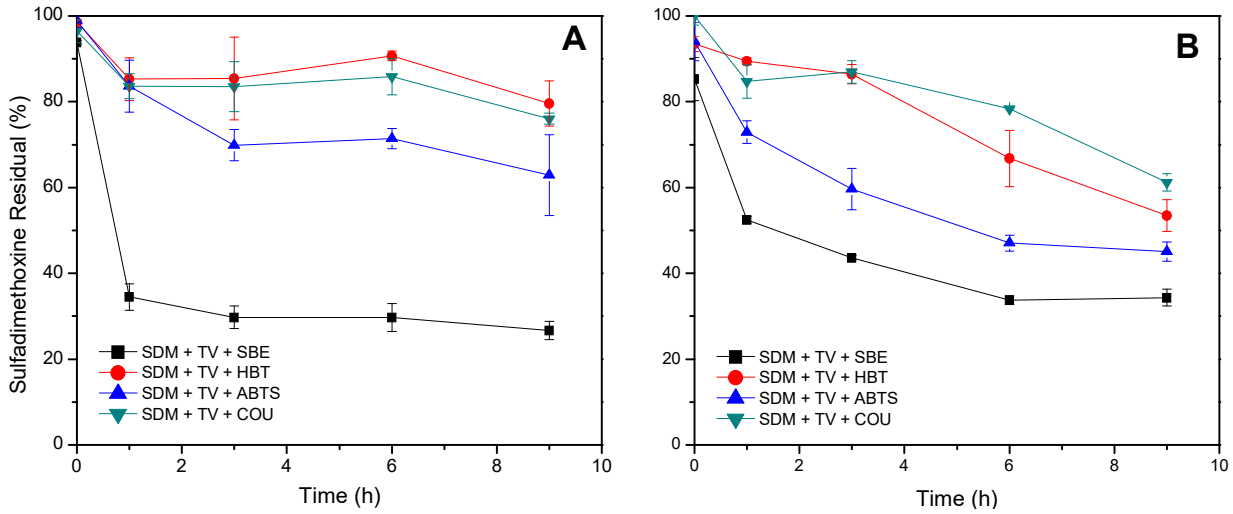

Figure 2.1. Degradation of sulfadimethoxine (SDM) in laccase-mediator systems at 25 ºC. (A) 1 mg L^{-1} initial SDM, 0.5 unit mL^{-1} enzyme activity, 1 mg L^{-1} initial mediator concentration; (B) 10 mg L^{-1} initial SDM, 5 unit mL^{-1} enzyme activity, 10 mg L^{-1} initial mediator concentration; TV, *trametes versicolor* laccase; SBE, soybean meal extract; HBT, 1-Hydroxybenzotriazole; ABTS, 2,2'-azino-bis(3-ethylbenzothiazoline-6-sulphonic acid); COU, *p*-coumaric acid.

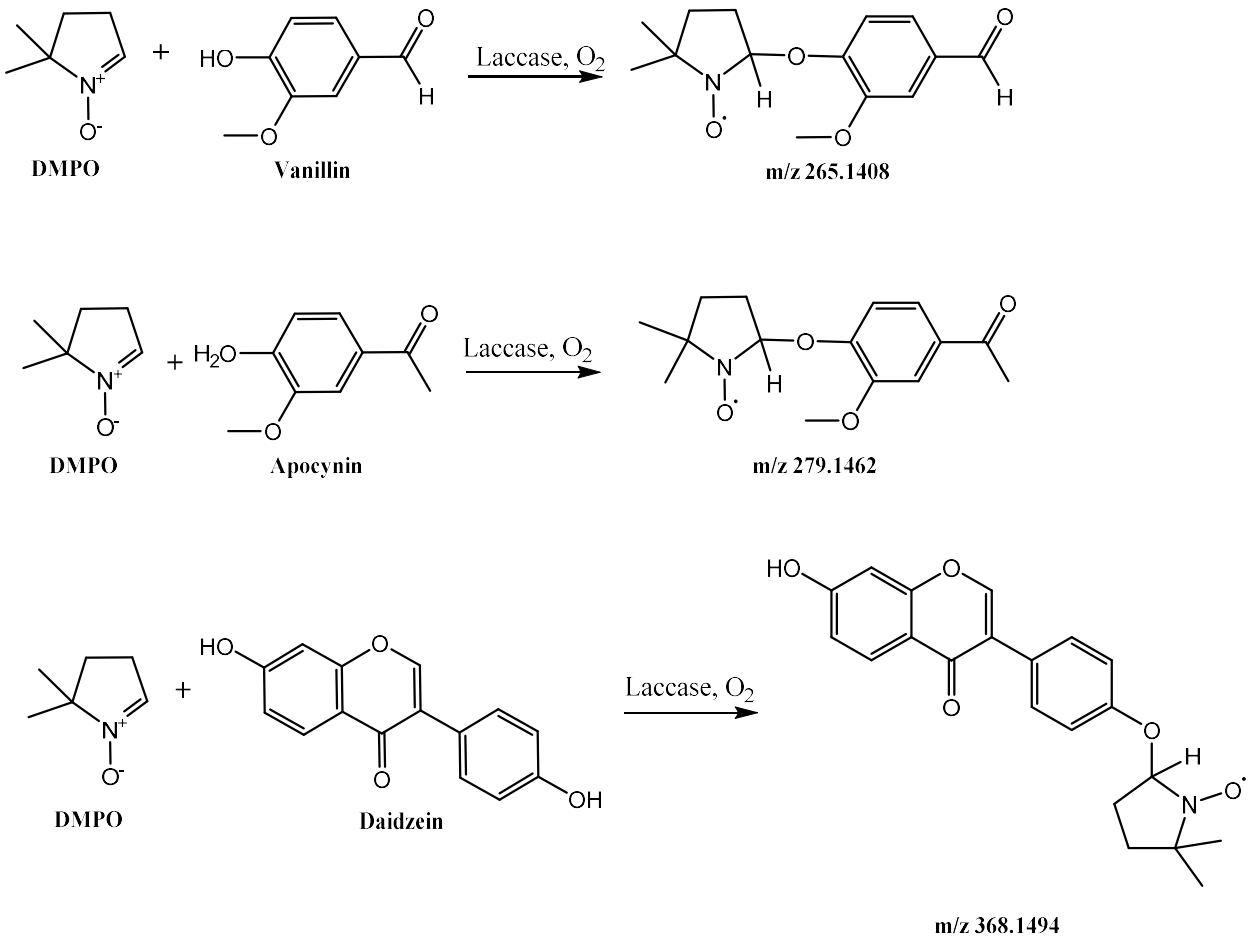

Figure 2.2. Proposed coupling reactions between 5, 5-Dimethyl-1-Pyrroline-N-Oxide (DMPO) and phenolic mediators.

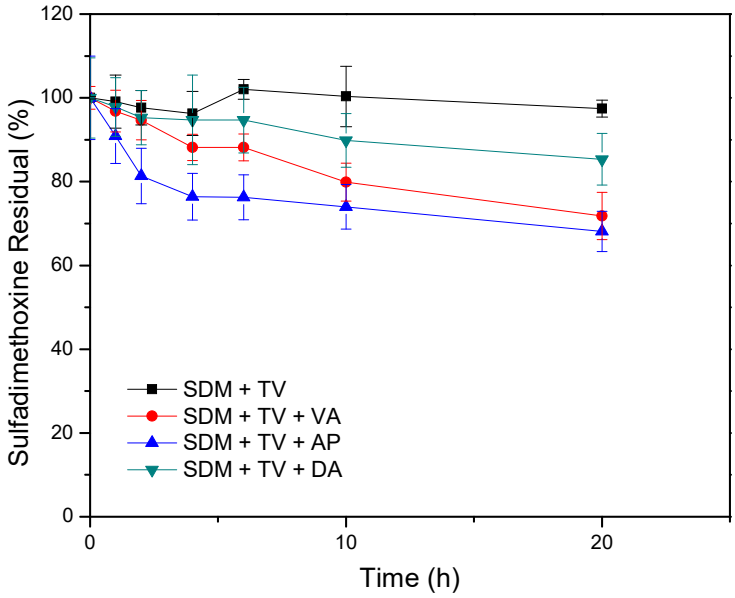

Figure 2.3. Degradation of sulfadimethoxine (SDM) in laccase-mediator systems at 25 ºC. TV, *trametes versicolor* laccase; VA, vanillin; AP, apocynin; DA, daidzein. Reaction conditions were the same as Figure 1B.

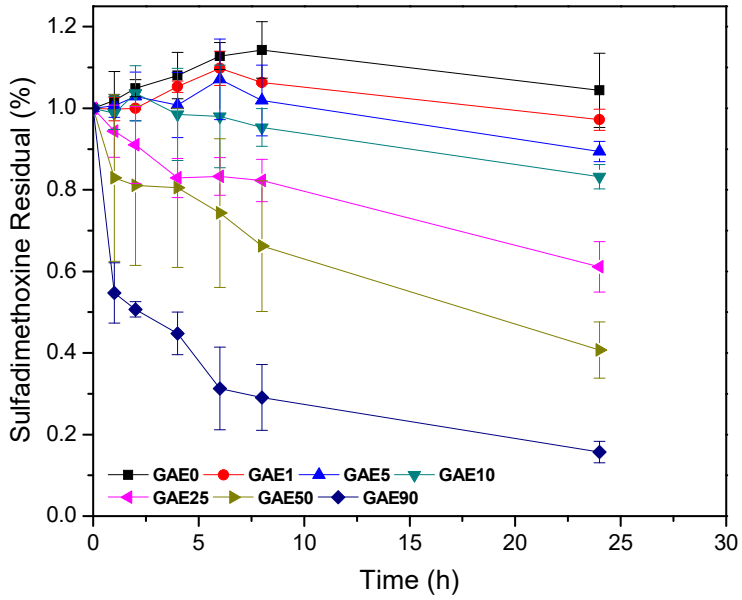

Figure 2.4. The removal of sulfadimethoxine (SDM) in SBE diluents at various total phenolic content expressed as gallic acid equivalent (GAE). The initial SDM concentration was 1 mg L^{-1}, and the initial enzyme activity was 0.5 unit mL^{-1}.

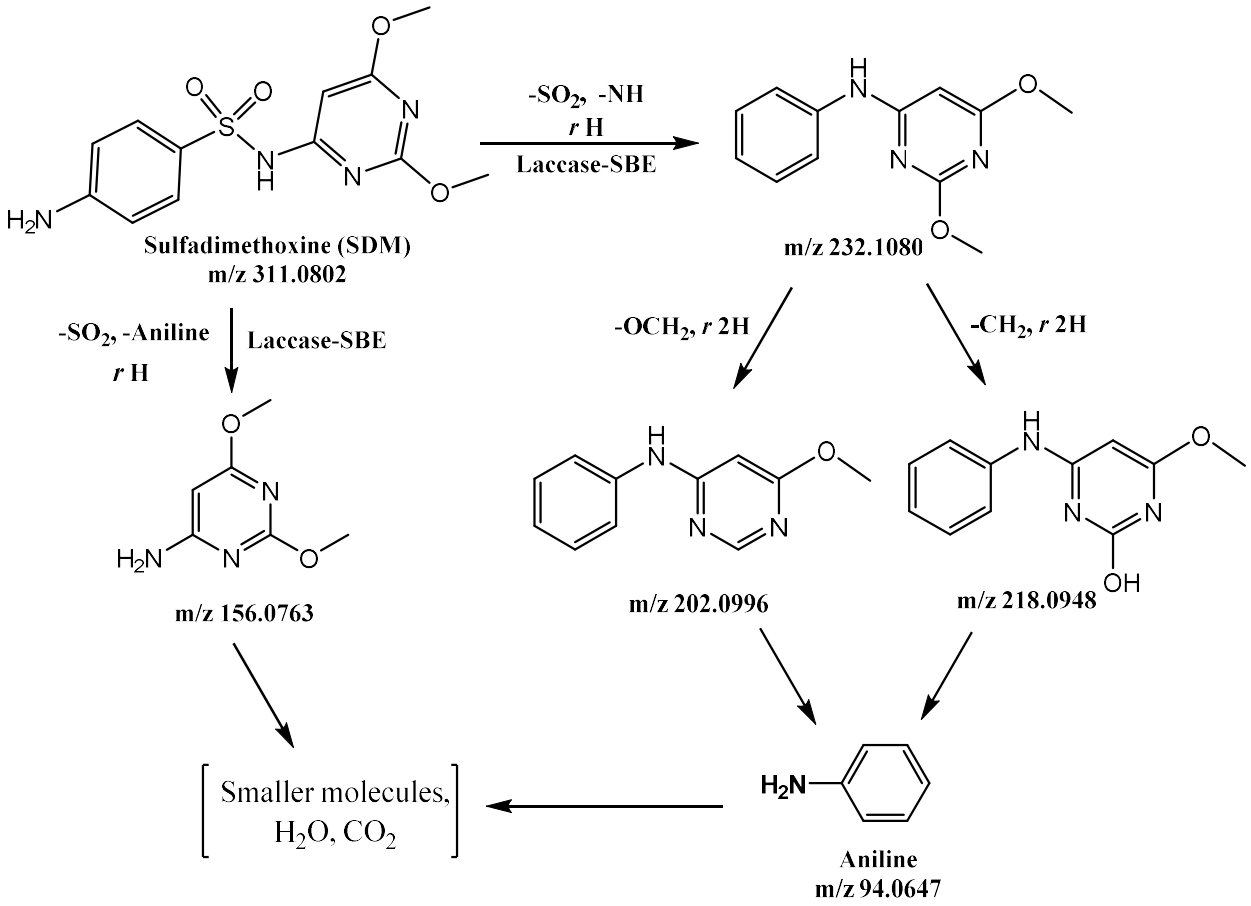

Figure 2.5. Proposed transformation pathways of sulfadimethoxine in laccase-SBE treatment system. *r* H stands for proton rearrangement.

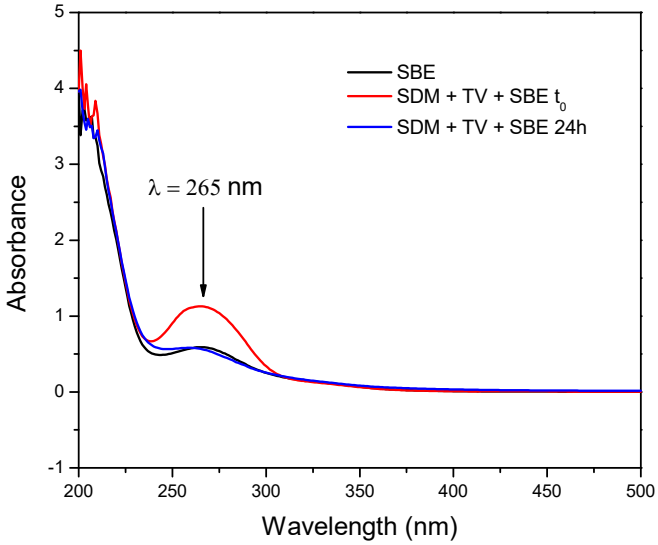

Figure 2.6. UV-Vis scan spectrum of 10 mg L^{-1} SDM before and after laccase-SBE treatments. Reaction conditions were the same as Figure 1B.

CHAPTER 3

COUPLING GRANULAR ACTIVATED CARBON WITH LACCASE CATALYZED HUMIFICATION REACTION FOR SEPARATION AND DESTRUCTION OF PFAS[2]

[2] Liang, S., Robel, A., Field, J., Pierce, D., Zhang, D., Huang, Q., Pohlman, D., Varley, C., Bodour, A., Chiang, D. To be submitted to *Environmental Pollution.*

ABSTRACT

Granular activated carbon adsorption of PFOA and PFOS is a prevailing technique that removes per- and polyfluoroalkyl substances (PFAS) from the contaminated water. However, GAC filtration technique simply removes PFOS and PFOA mass from one media (water phase) onto another (solid GAC) phase without destructing the contaminants. This study proposed a trap and treat technology that couples GAC with enzyme catalyzed oxidation humification reaction (ECOHR) to degrade PFOS and PFOA in the GAC column. Both batch study and a flow-through column study were conducted to demonstrate the effeciency. The GAC batch study results reveal that 32.4 % of PFOA was degraded at the tested optimal ECOHR conditions over 60 days of incubation. About 24% PFOA removal was also observed in a 60-d batch study using groundwater collected at Air Force Base. For the flow-through GAC column experiment, we have observed a significant decrease of PFOA (up to 65% removal) in the effluents of the reaction columns treated with ECOHR after about 40 days. The results suggest that the combination of GAC column and ECOC treatment is a potential approach for PFOA and PFOS groundwater remediation. The GAC trap treatment removes PFOA and PFOS from the groundwater, and concurrent/subsequent ECOC treatment breaks down the PFOA and PFOS adsorbed on the GAC to achieve detoxification of the contaminants and regeneration of the GAC.

Keywords: GAC, PFCs, laccase, groundwater, remediation

INTRODUCTION

Poly- and perfluorinated substances (PFASs) compounds are pollutants of emerging concern due to their world-wide distribution, environmental persistence and bioaccumulation potential (Fujii, Polprasert, Tanaka, Lien, & Qiu, 2007; Giesy & Kannan, 2001). Wildlife and human monitoring services have identified perfluoroalkyl acids (PFAAs) in mammal populations

across the globe (Lau et al., 2007). Toxicological research of PFASs in mammals is still in its infancy, but studies suggest they are particularly related to developmental toxicity, immunotoxicity, and hepatotoxicity (Lau et al., 2007). PFASs have been used in industrial applications since the latter half of the 20th century primarily as surfactants suited for harsh conditions because of their extreme chemical and thermal stability (J. Guo, Resnick, Efimenko, Genzer, & DeSimone, 2008). Since the 1950's, USAF bases and commercial airports have used AFFF (aqueous film forming foams) to combat fuel fires. Many AFFF products contain PFASs as well as many other organic pollutants. USAF base Wurtsmith, Michigan has used these AFFFs in training exercises since 50's till its decommission in 93. Studies in early 2000s showed levels of groundwater contamination from 3 to 120 μg L^{-1} of perfluorooctanesulfonate (PFOS), perfluorohexanesulfonate (PFHxS); perfluorooctanoate (PFOA), and perfluorohexanoate (PFHxA) (Moody, Hebert, Strauss, & Field, 2003).

Treatment methods for the removal of PFAS surfactants from industrial effluents are needed to minimize the environmental release of these pollutants, but have been particularly difficult to develop and apply. Due to the stability of PFASs, a combination of multiple treatment technologies will likely be required to effectively address PFAS contaminations which often exist in mixtures with co-contaminants present in complex environmental matrices (Merino et al., 2016). Removal of PFAS surfactants from contaminated groundwater by sorption onto granular activated carbon (GAC) has been heavily investigated (Ochoa-Herrera & Sierra-Alvarez, 2008). The presence of a variety of functional groups on the GAC's surfaces allow negative charge-assisted H-bonds to form with the acid groups of PFAAs, thus facilitating sorption (Zhang et al., 2016). However, GAC sorption is not a destruction approach, requires frequent change-outs, and the spent GAC needs to be disposed through incineration. The high stability of PFAA renders current *in situ*

treatment technologies involving oxidation and microbial degradation not so effective for their destruction (C. Vecitis, Park, Cheng, Mader, & Hoffmann, 2009). Advanced oxidation processes (AOPs), such as alkaline ozonation, peroxone, or Fenton's reagent, have been shown effective to degrade a wide range of organic contaminants. However, those techniques have very limited success in destructing PFASs from studies reported so far. A couple of direct and indirect photolytic oxidation pathways (Hori et al., 2005; Kormann, Bahnemann, & Hoffmann, 1991; Kutsuna & Hori, 2007), sonochemistry (Cheng et al., 2008; Cheng, Vecitis, Park, Mader, & Hoffmann, 2010), and reductive dehalogenation achieved some PFAS degradation, but are not applicable for *in situ* treatment applications.

Our previous work (Luo et al., 2015) shows promise in the decomposition of perfluorooctanoic acid (PFOA) by enzyme-catalyzed oxidative humification reactions (ECOHRs). These reactions are ubiquitous in, usually catalyzed by certain naturally occurring extracellular enzymes (lignin peroxidase, manganese peroxidase and laccases, etc) that are produced by certain white/brown rot fungi. During ECOHRs, these enzymes effectively catalyze conversion of natural or anthropogenic chemicals containing phenolic or anilinic moieties into active intermediates such as radicals or quinones that can subsequently attack NOM or a persistent organic chemical, causing its activation and consequent incorporation into the natural humification process (Lisa M. Colosi, Pinto, Huang, & Weber, 2009; Q. Huang & Weber, 2004a, 2004b; Park, Dec, Kim, & Bollag, 1999; Walter J. Weber & Qingguo Huang, 2003),. We have shown in our earlier studies that such mediator-facilitated mechanism can lead to degradation of PFOA during ECOHR. Approximately 50% removal of PFOA was achieved in a mineral buffer solution upon addition of laccase and 1-hydroxybenzotriazole (HBT) after a total treatment of 157 days. The synthetic mediator, HBT, plays a crucial role in the process, as the addition of laccase alone did not induce any discernible

PFOA decomposition (Luo et al., 2017). Similar to HBT, a number of naturally occurring phenolic chemicals, such as 4-methoxyphenol, guaiacol, catechol, and even soil organic matter itself can serve as such mediators by generating free radicals under humification enzyme catalysis (Lisa M Colosi, Burlingame, Huang, & Weber, 2007; Lisa M. Colosi et al., 2009; Walter J. Weber & Qingguo Huang, 2003). It may be hypothesized that granular activated carbon, which contains various types of functional groups (e. g., free and hydrogen bonded OH groups (Wasewar, Prasad, & Gulipalli, 2009), can serve the role as a laccase mediator, and therefore humification enzymes may be loaded to GAC and induce ECOHRs that can lead to PFAA destruction. The study herein was intended to tested such an hypothesis, and thus prove the concept of coupling GAC sorption and ECOHR destruction as an alternative scheme for remediation of PFASs in groundwater.

The coupling of GAC and ECOHR treatments is a "Trap and Treat" setup in nature, which is considered promising given the inherent synergy of the two treatment techniques. Since PFOS and PFOA concentrations in groundwater are at μg L^{-1} levels, a "trap" technique, like GAC sorption, will be essential to concentrate PFOS and PFOA in groundwater, making the ECOHR "treat" process more effective. The GAC trap treatment removes PFOA and PFOS from the groundwater, and concurrent/subsequent ECOHR treatment breaks down the PFOA and PFOS adsorbed on GAC to achieve detoxification of the contaminants, and potentially extend the service time of GAC.

In this study, we investigated the degradation of PFASs in spiked water samples and PFASs-containing groundwater with GAC and humification enzyme added to induce ECOHR in a batch reactor experiment. Flow through column experiment was also performed with GAC micro-column with either spiked solution or groundwater samples, with humification enzymes loaded to the columns in some treatments to investigate the degradation of PFASs by ECOHR on

GAC. A pilot-scale GAC column test was conducted at Wuftsmith Air Force Base in Michigan to study the effectiveness of the treatment scenarios with or without ECOHR induced. GAC sorption isotherms and column breakthrough behaviors were characterized for selected PFAAs to provide necessary fundamental information to assist data interpretation, and identification of degradation products were attempted using High Resolution Mass Spectrometry for samples where ECHOR was induced. In addition, FTIR spectra of GAC with or without ECOHR treatment was obtained to help elucidate the role of functional groups on the GAC surface.

MATERIALS AND METHODS

Chemicals and water samples

The perfluorooctanoic acid (PFOA) and perfluorooctanesulfonic acid (PFOS) were purchased from Sigma Aldrich (St. Louis, MO). The surrogate standard perfluoro-n-[^{13}C8]-octanoic acid (M8PFOA) and perfluoro-n-[^{13}C8]-octanesulfonic acid (M8PFOS) were obtained from Wellington Laboratories (Ontario, Canada). Sand, 1-hydroxybenzotriazole (HBT), and 2,6-dimethoxyphenol (DMP) were purchased from Sigma Aldrich (St. Louis, MO). HPLC grade acetonitrile, methanol, and dichloromethane were from Fisher Scientific (Waltham, MA). All solutions were prepared in nanopure water generated from Barnstead NANOpure® water purification system (Thermo Scientific, Waltham, MA). The 0.2µm Cellulose Acetate Membrane and 4-mL Reservoir were purchased from VWR International (Radnor, PA). Laccase was produced from fermentation with fungal strain *Pycnoporus sp* SYBC-L3 (PS) in the form of a crude concentrate (~900 U/mL) of the fermentation broth (J. Liu, Y. Cai, et al., 2013). We have previously conducted studies to characterize this enzyme and to study its uses in decontamination and biofuel production (J. Liu, M. L. Wang, et al., 2013; J. Y. Liu et al., 2012). The granular activated carbon (GAC) obtained from Sigma Aldrich (St. Louis, MO) was 20-40 mesh particle

size, and DSR A 8x40 GAC was acquired from CalgonCarbon (Pittsburgh, PA). Groundwater samples were collected at the Wurtsmith U.S. Air Force Base.

Batch experiments

The experiment with PFOA-spiked water samples was conducted in 20 mL polypropylene vials containing 15 mL reaction solution and 20 mg granular activated carbon purchased from Sigma Aldrich. The original concentrations of PFOA, HBT and laccase in each treatment container are listed in **Table S1.** The solution was incubated in dark at 30ºC for 60 days with triplicate water samples taken at 0, 15, 30, and 60 days. The HBT and enzyme were re-dosed at the original dosages after 30 days of incubation. After the incubation was completed, PFOA concentrations in the aqueous phase and sorbed on GAC were quantified as described below, and the total amount remaining was calculated and expressed as concentration as if all in solution.

For the batch experiment with groundwater, the test was conducted in 50 mL polypropylene centrifuge tube that contained 45 mL groundwater containing 10 mg GAC (from CalgonCarbon), 2 Unit/mL PS laccase, and w/wo 20 μM HBT. Control reactors were prepared and tested at the same time that contained 10 mg GAC but not HBT or laccase in 45 mL groundwater. The reactors were incubated at 30ºC for 60 days, and triplicate reactors were sampled on the last day of incubation, and analyzed as described above for PFOA concentrations.

GAC extraction

To quantify the amount of PFOA adsorbed on GAC, a multi-step extraction was performed on the GAC collected from each sample. Firstly, the GAC particles were dried in an oven at 45 ºC for 24 hrs until reaching constant weight. Ten or twenty milligrams of GAC were extracted with 4 mL mixture of dichloromethane and methanol (V:V=2:1) in a 10-mL glass tube, and then the tube was held in the ultrasonic processor (Cole Parmer, Vernon Hills, IL) for 45 min in a water to ensure

the temperature of solution below 50 °C through the extraction process. After extraction, the extracted slurry was centrifuged at 4200 rpm/min for 20 min to collect the supernatant. The GAC residue was extracted again for another two times as described above, and all supernatants collected during extraction were combined to about 10 mL. The supernatant was then concentrated to nearly dry using a nitrogen flow. The resulting solution was mixed with 2 mL methanol (HPLC grade Methanol final concentration, 99.9%) and filtered through 0.2 μm cellulose acetate membrane before being transferred to HPLC vial for subsequent analysis. The average recovery was 56%-60% with a Relative Standard Deviation (RSD) of 3.23%.

Micro-column experiments

The setup of the flow-through column experiment is schematically represented in **Figure 3.1**. First, a micro cartridge was packed with 0.1 g GAC and 0.5 g quartz sand, and the filling materials were compacted by two frits on both ends. The column was periodically tapped and the water level in the column was maintained above the solid fillings through the packing process to ensure packing quality. After packing, the column was flushed with HPLC water at 0.1 mL/min for 24 hrs before use. For the experiment with PFOA spiked solution, a solution containing 1 μmol L^{-1} PFOA, 20 μmol L^{-1} HBT, and 4 or 2 Unit/mL PS laccase was continuously passed through a column at a flow rate of 0.1 mL/min driven by a Cole Parmer Masterflex L/S pump. A control treatment was also conducted at the same time under the same condition with a solution containing only 1 μmol L^{-1} PFOA. The effluent was collected at pre-selected time intervals for PFOA quantification. A total of 6 L solution was passed through the column, and the procedure lasted for about 40 days. PS enzyme and HBT were used as a model enzyme and mediator in this study.

Column experiments were also conducted to test effectiveness of using the GAC column with and without ECOHR to treat low concentrations levels of PFOA in groundwater collected at

Wuftsmith Air Force Base in Michigan, which was intended to provide information for designing a pilot scale column test on site. Each column was packed with 0.5 g CalgonCarbon GAC, and the flow rate was 0.14 mL/min. Instead of mixing prior to loading onto column, the groundwater, the solutions containing HBT, and the solution containing PS laccase were passed through GAC column in sequence at flow rate of 0.14 mL/min until the effluent concentration of each component reached 80% of its influent concentration. Meanwhile, control columns were prepared tested by passing groundwater and PS laccase (without HBT), or groundwater and HBT (without PS). In such scenarios, it is expected that PFAS, HBT and laccase are distributed evenly in GAC column, which ensures better contact between reactants and effective reaction, and when laccase was loaded to the column as the last component, ECOHR was initiated to degrade PFASs. After loading process, all columns were set aside to allow laccase degradation of PFAS to happen on GAC. After 45 days, the columns were flushed by the original groundwater sample, and the different elution curves between treatment and control were used to indicate the PFOA/S degradation, if any, happened on GAC.

Quantification methods

PFOA and PFOS were quantified using the Waters ACQUITY I-class UPLC coupled with XEVO TQD tandem quadrupole mass spectrometry (Milford, MA). An Acquity UPLC BEH 1.7 μm C18 column (Waters, Milford, MA) was used for UPLC separation with a mobile phase consisting of 5 mM ammonium acetate in water (A) and 5 mM ammonium acetate in methanol (B) at a flow rate of 0.3 mL/min by a 10-minute gradient program: 90% A and 10% B at time 0, linearly change to 10% A and 90% B, and then held for 2 min. Electrospray ionization was operated in a negative mode for PFOA and PFOS detection with the capillary voltage at 3 kV and the source temperature at 400 ^{o}C. Ultra high purity nitrogen was used as the desolvation and cone gas with

the flow rates at 550 and 50 L/hour, respectively. Multiple reaction monitoring (MRM) was used to quantify PFOA, PFOS, and their isotope labeled standards based on the transition patterns m/z = 413 > 369 for PFOA, m/z = 421 > 376 for M8PFOA, m/z = 499 > 99 for PFOS, and m/z = 507 > 99 for M8PFOS. Concentrations were calculated based on the ratio between PFOA or PFOS and its isotope labeled standard in reference to a five-point calibration curve.

Solid phase extraction

The effluent samples were purified and concentrated by Waters Oasis HLB cartridges (60 mg) before chemical analysis for PFAS and HBT. The SPE cartridges were conditioned with 3 mL methanol, 3 mL HPLC water, and then another 3 mL HPLC water before loading samples. Thirty milliliter of water samples were loaded on the cartridge slowly, and the cartridges were washed by 3 mL HPLC water to elute interferences. The SPE column was then vacuum dried for 10 minutes before being eluted with 3 x 1 mL methonal and 2 x 1 mL acetonitrile to collect the analytes. At the end of elution, vacuum was applied to the system for another 10 minutes to allow complete elution. The effluents were combined, and then dried under a gentle nitrogen flow, followed by reconstitution to 300 μL with methanol. The sample for HPLC-MS/MS quantification was prepared by mixing 100 μL reconstitute sample with 50 μL M8PFOA and 50 μL M8PFOS.

Laccase Activity Measurements.

Laccase activity was determined spectrometrically by adding 20 μL of sample to 3.4 mL of 1 mM 2, 6-dimethoxyphenol in a citrate phosphate buffer (pH 3.8) in a cuvette with 1 cm light path, the absorbance of which was measured at 468 nm, and one unit is defined as the amount of enzyme that causes a unit absorbance change per minute (I.-Y. Lee, Jung, Lee, & Park, 1999).

Product identification

Product identification was performed on the supernatant sample extracted from GAC samples that have been used for different treatments. MS full scan (m/z 50 – 1000, resolution R = 120,000) were performed on both treatment and control samples using an Orbitrap Elite high-resolution tandem mass spectrometer (Thermo Scientific, Waltham, MA) in electrospray negative (ESI-) mode. Mass filtration function (Xcalibur 2.1, Thermo Fisher Scientific) was then performed to identify possible products by screening peaks only present in treatment samples but not in controls. For each m/z peak identified, a molecular formula was assigned using Formula Finder with 5 mg L^{-1} mass error allowed. Subsequently, tandem MS (MS/MS) was performed on the possible products (resolution R = 30,000), and their molecular structures were deduced based on the fragment peaks and general MS fragmentation rules (McLafferty & Tureček, 1993).

GAC characterization

The chemical functionality of GAC samples after batch incubation was qualitatively identified by Fourier Transform Infrared Spectroscopy (FTIR). FTIR spectra were recorded between 4000 and 500 cm^{-1} using an AVATAR 360 spectrophotometer (Thermo Nicolet Co., Waltham, MA).

RESULTS AND DISCUSSION

Sorption isotherm

Two types of granular activated carbon have been used in this study for different experiments. GAC purchased from Sigma Aldrich was used to treat spiked solution, because this GAC has been used widely in previous studies to enable data comparison. GAC DSR A 8x40 produced by Calgon Carbon is a product having been used in numerous groundwater remediation applications. Therefore, lab scale tests were performed using this GAC to offer guidance for pilot

scale field test. The sorption isotherms of PFOA on both Sigma Aldrich GAC and Calgon Carbon GAC were studied, and the results were fitted well by the Langmuir models (**Figure S3.1**). The Sigma Aldrich GAC (qm = 39.4 mg/g) presented a slightly higher sorption capacity than Calgon Carbon GAC (qe = 31.08 mg/g), but has a much lower affinity (Kl = x) than the latter (Kl = y). The sorption capacity values were slightly lower than the results of a previous report using GAC from SigmaAldrich (Zhang et al., 2016), and this difference is likely due to variation in granule size.

Sorption of PS laccase on the two GACs was also investigated. The results (**Figure S3.2**) reveals a much larger sorption capacity on Calgon Carbon GAC (174.97 U/mL) than on Sigma Aldrich GAC (1.70 U/mL). Previous studies have demonstrated activated carbon as an effective adsorbent for enzymes through different proposed mechanisms such as ionic interaction, covalent binding, and physical adsorption (Daâssi, Rodríguez-Couto, Nasri, & Mechichi, 2014; Y. Liu et al., 2012). Among those mechanisms, some may require addition of external binding agents to ensure stable immobilization. The high sorption capacity on Calgon Carbon GAC is beneficial because laccase can be immobilized in large amount without the use of binding agents. As demonstrated in literature, sorption of laccase on activated carbon will not alter the structure and oxidative ability of the enzyme, and moreover, the enzyme activity remains stable after multiple usage (20 cycles) (Nguyen et al., 2016).

Treatment of spiked PFOA solution with SigmaAldrich GAC in batch reactor

In batch reactors, the concentrations of PFOA remained stable in control at the end of 15d, 30d, and 60d incubation, while it was reduced by 15.6%, 30.7%, and 32.4% with the addition of PS laccase, HBT, and ferric ion (**Figure 3.2**). Laccase-mediator system has been proven effective in degrading numerous contaminants such as antibiotics, PAHs, and PCBs (Lisa M Colosi et al.,

2007; Liang et al., 2017; Walter J Weber & Qingguo Huang, 2003), and recently its capability to oxidize PFOA during long-term incubation was also shown(Luo et al., 2015). Unlike other contaminants, which usually degraded to negligible levels within hours or a few days, the reduction of PFOA happened slowly over time. It took about 40 days to reach 30% reduction in aqueous sample in our earlier study (Luo et al., 2015), which was comparable to the present observation. This is mainly ascribed to the chemical structures of perfluorinated compounds, which consist of no hydrogen for abstraction and no double bond for addition, leaving direct electron transfer the only possible mechanism. It was found that the presence of certain multi-valent cations (Fe^{3+} and Cu^{2+}) is essential for the laccase-mediator reaction systems being effective towards PFOA degradation, because they bridge negatively charged laccase and PFOA in solution so that the free radicals of mediator produced from laccase surface can reach and react with PFOA before they are scavenged (Luo et al., 2017). Therefore, ferric ion was included in this ECOHR reaction system for the experiment.

Interestingly, the reduction in PFOA concentration was also observed in the treatment with the addition of PS laccase and HBT but no ferric ion, and the removal reached 2%, 25.2%, and 26.8% after 15d, 30d, and 60d of incubations, respectively. Except for 15-day results, the removal of PFOA in the samples without the addition of ferric ions was only slightly less than the removal in the treatments with them added. This is interesting because in all our previous experiments with ECOHR in aqueous solutions, PFOA did not degrade if an external multi-valent cation were not added (Luo et al., 2015; Luo et al., 2017). Several possible reasons can be proposed: 1) GAC itself contains some metal ions (Clark & Lykins, 1990) that can serve the role of bridging laccase and PFOA for the ECOHR reaction of PFOA to happen; and/or 2) the aromatic carbon structure in

GAC, having affinity to both laccase and PFOA, can serve a similar role as the multi-valent cations to bridge laccase and PFOA.

It is noted that extending reaction time from 30d to 60d did not lead to significantly greater PFOA reduction in all the treatments (**Figure 3.2**). This suggested that one or more of the factors supporting ECOHR were exhausted after 30 days of incubation. In laccase-mediator systems, mediators was consumed during ECOHR, and the activity of laccase can be inactivated along the reaction as well (Viswanath, Rajesh, Janardhan, Kumar, & Narasimha, 2014). As found in the previous test with periodical laccase and HBT dosing, laccase activity reduced between two enzyme additions, and HBT was gradually consumed over time (Luo et al., 2015). However, laccase activity is expected to be more stable when immobilized on GAC (Y. Liu et al., 2012; Nguyen et al., 2016).

Treatment of groundwater with Calgon GAC in batch reactor

An additional batch experiment was performed to test PFOA degradation by laccase-induced ECOHR in PFAS-containing groundwater and CalgonCarbon GAC. Based on the assumption that GAC, rich in phenolic surface functionalities, may provide mediators for ECOHR reactions, we also included a treatment with only PS laccase and GAC, but not HBT, added to the groundwater sample. Considering the metal ions naturally present in groundwater and GAC, external metal ion was not introduced to any treatment. The PFAS concentrations in groundwater (GW) sample were listed in **Table 3.1**. After 60 days of reaction, the PFOA concentration in GW+GAC+PS treatment was the lowest among all four conditions, reaching 23.6% removal comparing to the GW+GAC control, while the treatment with HBT addition led to a reduction of 15.2%. This confirms that GAC has components that can serve as mediators. whereas the added HBT did not further enhance ECOHR reactivity, but limited PFOA reactions, probably because

the self-coupling of the mediator radicals was promoted as mediator concentrations increased beyond optimum (Luo et al., 2015). The finding of GAC itself provides ECOHR mediators is of great application significance, as it eliminates the necessity of introducing an external chemical as mediator for field application of ECOHR. However, the percent removal in groundwater sample was not as great as that in the spiked samples, which was most likely due to the low PFOA concentration (0.872 μg L^{-1}) in groundwater that limited the contact between PFOA and free radicals, leading to slower reaction. It is therefore beneficial to pass large volume of groundwater through GAC column and have the PFAS mass built up on the GAC surface to ensure better interactions with enzyme and the free radicals generated during ECOHR.

GAC characterization

The FTIR spectrum of GAC with PFOA adsorbed and w/wo PS laccase tretament was shown in **Figure 3.4**. The spectrum obtained for GAC with only PFOA adsorbed displays absorption bands centered at 2350 cm^{-1} and 1500 cm^{-1}. The peaks at 2350 cm^{-1} showed the C≡C binding groups due to symmetric or asymmetric stretching of aliphatic bond or the presence of ketones (Cooke, Fuller, & Gaikwad, 1986). The location of multiple small bands at 1700-1400 cm^{-1} in both samples are compatible with the presence of the PFOA characteristic functional groups, namely CF_2, CF_3, and COO^- (W. Chen, Zhang, Mamadiev, & Wang, 2017; Lin, Wang, Niu, Yue, & Huang, 2015). Compared to GAC+PFOA treatment, the addition of PS laccase resulted in two extra bands centered at 3000 cm^{-1} and 1200 cm^{-2}. According to reference, the alcohol/phenol OH-stretch absorb infrared radiation at 3500-3200 cm^{-1} and the carboxylic acid OH-stretch is at 3000-2500 cm^{-1} (Günzler & Gremlich, 2002). Hence, the band located at 3000 cm^{-1} may be caused by either type of OH-stretch, which is most likely a result of GAC surface functionality oxidation by laccase. The band at 1200 cm^{-2} is compatible with the presence of *ν*(C–O–C) vibration, likely

resulting from laccase catalyzed reactions to form ether (Weber, Huang, & Pinto, 2005). The alterations in GAC surface functionalities suggested the sorption of PFOA on the carbon surface as well as the occurrence of laccase-catalyzed oxidation reactions.

Treatment of spiked PFOA solution with SigmaAldrich GAC micro-column

The sketch and picture of the micro-column packed with GAC are shown in **Figure 3.1-A** and **3.1-B**, and the setup is shown in **Figure 3.1-C**. In this test with PFOA spiked solution (1 μmol L^{-1}), the enzyme dosages were 2 unit/mL or 4 unit/mL, and the mediator dose was 20 μmol L^{-1}. The breakthrough curves for the GAC micro-columns with or without ECOHR induced was displayed in **Figure 3.5**. For PFOA solution with the higher PS laccase dose (4 unit/mL) and HBT, the initial breakthrough of PFOA occurred at the very early stage of the experiment, suggesting high concentration of enzyme may block some of the sorption sites. It was noted in previous study that enzyme immobilization at certain level will result in smaller surface area on GAC (Daâssi et al., 2014). Therefore, having a high enzyme input is not always beneficial to the system.

The breakthrough of PFOA happened at similar points (~ 350 bed volume) for both the control treatment with only PFOA in solution and the ECOHR treatment with PFOA, laccase and HBT in solution. From the breakthrough points on, the effluent concentration of the control remained continuously higher than that of the ECOHR treatment. When PFOA reached 100% breakthrough with an effluent concentration of 1 μmol L^{-1}, the effluent concentration of the treatment column was still 0.4 μmol L^{-1}. This reduced breakthrough concentration demonstrated that PFOA has degraded during ECOHR on GAC column.

Treatment of groundwater with Calgon GAC micro-column

Micro-column experiment was also conducted with groundwater Wurftsmith AFB on CalgonCarbon GAC, in an attempt to provide basic information guiding ensuing pilot testing on

site. Because enzyme sorption on GAC is much less strong than PFOA, loading enzyme in the feed water along with PFOA is not practical in an application scenario, as enzyme will break much earlier than PFOA and wasted. As such, a different loading scheme was tested in this experiment, where groundwater was first passed through the column till 80% breakthrough of both PFOA and PFOS, and then HBT and PS were each mixed in groundwater and passed through the column in sequence until both reached 80% breakthrough (**Figure S3.3**). After loading all the reagents, the columns were set aside for reaction with parafilm covering both ends to allow air diffusion. After 45 days of incubation, the columns were flushed by groundwater again, and the PFOA and PFOS concentrations in effluent were determined and shown in **Figure 3.6**. For PFOA concentrations in effluents, no significant difference was observed among treatments. This was most likely due to the low PFOA concentration in groundwater, which limited the sorption on GAC and contact with mediator and enzyme. As for PFOS, the treatment effects were not remarkable within the first 400 BV, but the concentrations were much lower in PFOS+PS and PFOS+PS+HBT treatments than the control from 400 BV to 700 BV (~ 100% breakthrough). It is obvious that laccase treatment will delay the breakthrough of PFOS, and thus extend the service life of GAC column by 1/3 even without mediator added.

CONCLUSIONS

In this study, a coupling technology combines GAC adsorption with enzyme catalyzed oxidation reaction was tested in two application scenarios, batch reactor and column reactor, to remove and degrade PFOA and PFOS from water. Both laboratory prepared spiked solution and groundwater collected at contaminated sites were used as testing subject. Two kinds of granular activated carbon, including GAC obtained from scientific supplier and GAC used for common

remediation practice were applied in the study to assess the universal applicability of this technology.

In batch reactor study, more than 20% reduction in PFOA concentration was found using either spiked solution or groundwater after 60 days of incubation. FTIR spectra of GAC before and after incubation indicated the occurrence of oxidation reaction on GAC surface, leading to enriched functional groups on GAC after incubation with enzyme and PFOA solution. The column study using spiked PFOA solution showed lower PFOA effluent concentration in ECOHR implemented treatment than control until full breakthrough. However, when transferring the same setup to groundwater, the impact of ECOHR treatment was not significant, which was most likely due to the extremely low PFOA and PFOS concentrations in groundwater. In general, this environmentally benign coupling technology can be applied in future PFAS remediation practice to destruct PFAS *in situ* and potentially extend the service life of GAC vessel.

SUPPORTING INFORMATION AVAILABLE

Results of sorption isotherm; test conditions in batch reactors; ATR-FTIR spectrometer analysis; breakthrough curves of reagents.

ACKNOWLEDGEMENTS

The study was supported by U.S. Department of Defense AFCEC Contract No. FA8903-12-C-0005. We thank the Proteomics and Mass Spectrometry Core Facility at the University of Georgia for performing the high resolution mass spectrometry analysis for our samples.

LITERATURE CITED

Chen, W., Zhang, X., Mamadiev, M., & Wang, Z. (2017). Sorption of perfluorooctane sulfonate and perfluorooctanoate on polyacrylonitrile fiber-derived activated carbon fibers: in comparison with activated carbon. *Rsc Advances, 7*(2), 927-938.

Cheng, J., Vecitis, C. D., Park, H., Mader, B. T., & Hoffmann, M. R. (2008). Sonochemical Degradation of Perfluorooctane Sulfonate (PFOS) and Perfluorooctanoate (PFOA) in Landfill Groundwater: Environmental Matrix Effects. *Environmental Science & Technology, 42*(21), 8057-8063. doi: 10.1021/es8013858

Cheng, J., Vecitis, C. D., Park, H., Mader, B. T., & Hoffmann, M. R. (2010). Sonochemical Degradation of Perfluorooctane Sulfonate (PFOS) and Perfluorooctanoate (PFOA) in Groundwater: Kinetic Effects of Matrix Inorganics. *Environmental Science & Technology, 44*(1), 445-450. doi: 10.1021/es902651g

Clark, R. M., & Lykins, B. W. (1990). Granular activated carbon: design, operation and cost.

Colosi, L. M., Burlingame, D. J., Huang, Q., & Weber, W. J. (2007). Peroxidase-mediated removal of a polychlorinated biphenyl using natural organic matter as the sole cosubstrate. *Environmental Science and Technology, 41*(3), 891-896.

Colosi, L. M., Pinto, R. A., Huang, Q., & Weber, W. J., Jr. (2009). Peroxidase-mediated degradation of perfluorooctanoic acid. *Environmental Toxicology and Chemistry, 28*(2), 264-271. doi: 10.1897/08-282.1

Cooke, N. E., Fuller, O. M., & Gaikwad, R. P. (1986). FT-ir spectroscopic analysis of coals and coal extracts. *Fuel, 65*(9), 1254-1260.

Daâssi, D., Rodríguez-Couto, S., Nasri, M., & Mechichi, T. (2014). Biodegradation of textile dyes by immobilized laccase from Coriolopsis gallica into Ca-alginate beads. *International*

Biodeterioration & Biodegradation, 90, 71-78.

Fujii, S., Polprasert, C., Tanaka, S., Lien, N. P. H., & Qiu, Y. (2007). New POPs in the water environment: distribution, bioaccumulation and treatment of perfluorinated compounds–a review paper. *Journal of Water Supply: Research and Technology-AQUA, 56*(5), 313-326.

Giesy, J. P., & Kannan, K. (2001). Global distribution of perfluorooctane sulfonate in wildlife. *Environmental Science and Technology, 35*(7), 1339-1342.

Günzler, H., & Gremlich, H.-U. (2002). IR spectroscopy. An introduction.

Guo, J., Resnick, P., Efimenko, K., Genzer, J., & DeSimone, J. M. (2008). Alternative fluoropolymers to avoid the challenges associated with perfluorooctanoic acid. *Industrial & Engineering Chemistry Research, 47*(3), 502-508.

Hori, H., Yamamoto, A., Hayakawa, E., Taniyasu, S., Yamashita, N., Kutsuna, S., . . . Arakawa, R. (2005). Efficient Decomposition of Environmentally Persistent Perfluorocarboxylic Acids by Use of Persulfate as a Photochemical Oxidant. *Environmental Science & Technology, 39*(7), 2383-2388. doi: 10.1021/es0484754

Huang, Q., & Weber, W. J. (2004a). Interactions of Soil-Derived Dissolved Organic Matter with Phenol in Peroxidase-Catalyzed Oxidative Coupling Reactions. *Environmental Science & Technology, 38*(1), 338-344. doi: 10.1021/es0304289

Huang, Q., & Weber, W. J. (2004b). Peroxidase-Catalyzed Coupling of Phenol in the Presence of Model Inorganic and Organic Solid Phases. *Environmental Science & Technology, 38*(19), 5238-5245. doi: 10.1021/es049826h

Kormann, C., Bahnemann, D. W., & Hoffmann, M. R. (1991). Photolysis of chloroform and other organic molecules in aqueous *Environmental Science & Technology, 25*, 494-500.

Kutsuna, S., & Hori, H. (2007). Rate constants for aqueous-phase reactions of SO4− with

C2F5C(O)O− and C3F7C(O)O− at 298 K. *International Journal of Chemical Kinetics, 39*(5), 276-288. doi: 10.1002/kin.20239

Lau, C., Anitole, K., Hodes, C., Lai, D., Pfahles-Hutchens, A., & Seed, J. (2007). Perfluoroalkyl acids: a review of monitoring and toxicological findings. *Toxicological Sciences, 99*(2), 366-394.

Lee, I.-Y., Jung, K.-H., Lee, C.-H., & Park, Y.-H. (1999). Enhanced production of laccase in Trametes vesicolor by the addition of ethanol. *Biotechnology Letters, 21*(11), 965-968.

Liang, S., Luo, Q., & Huang, Q. (2017). Degradation of sulfadimethoxine catalyzed by laccase with soybean meal extract as natural mediator: Mechanism and reaction pathway. *Chemosphere, 181*, 320-327.

Lin, H., Wang, Y., Niu, J., Yue, Z., & Huang, Q. (2015). Efficient sorption and removal of perfluoroalkyl acids (PFAAs) from aqueous solution by metal hydroxides generated in situ by electrocoagulation. *Environmental Science and Technology, 49*(17), 10562-10569.

Liu, J., Wang, M. L., Tonnis, B., Habteselassie, M., Liao, X., & Huang, Q. (2013). Fungal pretreatment of switchgrass for improved saccharification and simultaneous enzyme production. *Bioresource Technology, 135*(0), 39-45. doi: http://dx.doi.org/10.1016/j.biortech.2012.10.095

Liu, J. Y., Cai, Y. J., Liao, X. R., Huang, Q. G., Hao, Z. K., Hu, M. M., & Zhang, D. B. (2012). Simultaneous Laccase Production and Color Removal by Culturing Fungus Pycnoporus sp SYBC-L3 in a Textile Wastewater Effluent Supplemented with a Lignocellulosic Waste Phragmites australis. *Bulletin of Environmental Contamination and Toxicology, 89*(2), 269-273. doi: 10.1007/s00128-012-0678-8

Liu, Y., Zeng, Z., Zeng, G., Tang, L., Pang, Y., Li, Z., . . . Ren, P. (2012). Immobilization of laccase

on magnetic bimodal mesoporous carbon and the application in the removal of phenolic compounds. *Bioresource Technology, 115*, 21-26.

Luo, Q., Lu, J., Zhang, H., Wang, Z., Feng, M., Chiang, S.-Y. D., . . . Huang, Q. (2015). Laccase-catalyzed degradation of perfluorooctanoic acid. *Environmental Science & Technology Letters, 2*(7), 198-203.

Luo, Q., Wang, Z., Feng, M., Chiang, D., Woodward, D., Liang, S., . . . Huang, Q. (2017). Factors controlling the rate of perfluorooctanoic acid degradation in laccase-mediator systems: The impact of metal ions. *Environmental Pollution, 224*, 649-657.

McLafferty, F. W., & Tureček, F. (1993). *Interpretation of mass spectra*: University science books.

Merino, N., Qu, Y., Deeb, R. A., Hawley, E. L., Hoffmann, M. R., & Mahendra, S. (2016). Degradation and removal methods for perfluoroalkyl and polyfluoroalkyl substances in water. *Environmental Engineering Science, 33*(9), 615-649.

Moody, C. A., Hebert, G. N., Strauss, S. H., & Field, J. A. (2003). Occurrence and persistence of perfluorooctanesulfonate and other perfluorinated surfactants in groundwater at a fire-training area at Wurtsmith Air Force Base, Michigan, USA. *Journal of Environmental Monitoring, 5*(2), 341-345.

Nguyen, L. N., Hai, F. I., Dosseto, A., Richardson, C., Price, W. E., & Nghiem, L. D. (2016). Continuous adsorption and biotransformation of micropollutants by granular activated carbon-bound laccase in a packed-bed enzyme reactor. *Bioresource Technology, 210*, 108-116.

Ochoa-Herrera, V., & Sierra-Alvarez, R. (2008). Removal of perfluorinated surfactants by sorption onto granular activated carbon, zeolite and sludge. *Chemosphere, 72*(10), 1588-1593.

Park, J.-W., Dec, J., Kim, J.-E., & Bollag, J.-M. (1999). Effect of Humic Constituents on the

Transformation of Chlorinated Phenols and Anilines in the Presence of Oxidoreductive Enzymes or Birnessite. *Environmental Science & Technology, 33*(12), 2028-2034. doi: 10.1021/es9810787

Vecitis, C., Park, H., Cheng, J., Mader, B., & Hoffmann, M. (2009). Treatment technologies for aqueous perfluorooctanesulfonate (PFOS) and perfluorooctanoate (PFOA). *Frontiers of Environmental Science & Engineering in China, 3*(2), 129-151. doi: 10.1007/s11783-009-0022-7

Viswanath, B., Rajesh, B., Janardhan, A., Kumar, A. P., & Narasimha, G. (2014). Fungal laccases and their applications in bioremediation. *Enzyme research, 2014*.

Wasewar, K. L., Prasad, B., & Gulipalli, S. (2009). Removal of selenium by adsorption onto granular activated carbon (GAC) and powdered activated carbon (PAC). *CLEAN–Soil, Air, Water, 37*(11), 872-883.

Weber, W. J., & Huang, Q. (2003). Inclusion of persistent organic pollutants in humification processes: direct chemical incorporation of phenanthrene via oxidative coupling. *Environmental Science and Technology, 37*(18), 4221-4227.

Weber, W. J., & Huang, Q. (2003). Inclusion of Persistent Organic Pollutants in Humification Processes: Direct Chemical Incorporation of Phenanthrene via Oxidative Coupling. *Environmental Science & Technology, 37*(18), 4221-4227. doi: 10.1021/es030330u

Zhang, D., Luo, Q., Gao, B., Chiang, S.-Y. D., Woodward, D., & Huang, Q. (2016). Sorption of perfluorooctanoic acid, perfluorooctane sulfonate and perfluoroheptanoic acid on granular activated carbon. *Chemosphere, 144*, 2336-2342.

Table 3.1. Groundwater PFAS concentrations and other properties.

Chemicals	**Molecular Formula**	**Detection limit (ng L^{-1})**	**Concentration (µg L^{-1})**
PFBA (C4)	$F\text{-}(CF_2)_3COOH$	0.18	0
PFPeA (C5)	$F\text{-}(CF_2)_4COOH$	0.27	0.212
PFHxA (C6)	$F\text{-}(CF_2)_5COOH$	0.22	0.487
PFHpA (C7)	$F\text{-}(CF_2)_6COOH$	0.08	0.085
PFOA (C8)	$F\text{-}(CF_2)_7COOH$	0.11	0.872
PFNA (C9)	$F\text{-}(CF_2)_8COOH$	1.5	0
PFDA (C10)	$F\text{-}(CF_2)_9COOH$	1.0	0
PFUA (C11)	$(CF_2)_{10}COOH$	0.12	0
PFOS (C8)	$F\text{-}(CF_2)_8SO_3H$	0.82	3.917
HBT	$C_6H_5N_3O$	0.19	0
TOC (mg L^{-1})			4.6
Conductivity (µs/cm)			258.5

Table 3.2. Wavenumbers and ascription of the principal bands in activated carbons with PFOA or PFOA+PS adsorbed.

Wavenumbers (cm^{-1})	**Assignments**	**PFOA+GAC**	**PFOA+GAC+PS**
3050-2850	alcohol/phenol OH-stretch carboxylic acid OH-stretch		*
2400-2300	C≡C binding or ketone	*	*
1700-1400	PFOA characteristic functional groups	*	*
1100-1000	*ν*(C–O–C) vibration		*

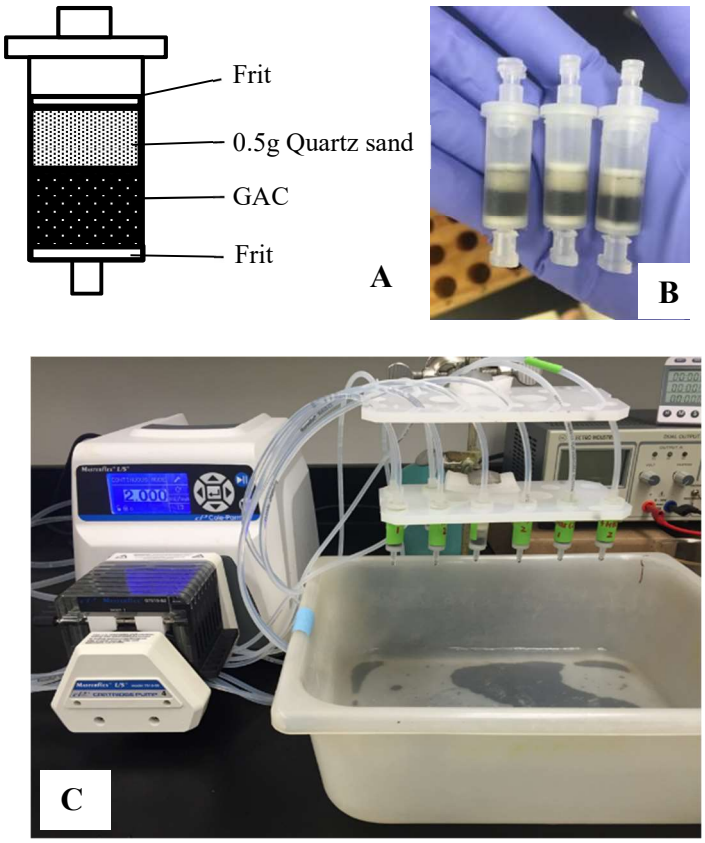

Figure 3.1. The sketch (A) and picture (B) of micro-column packed with GAC; The setup of bench scale "trap and treat" treatment system (C).

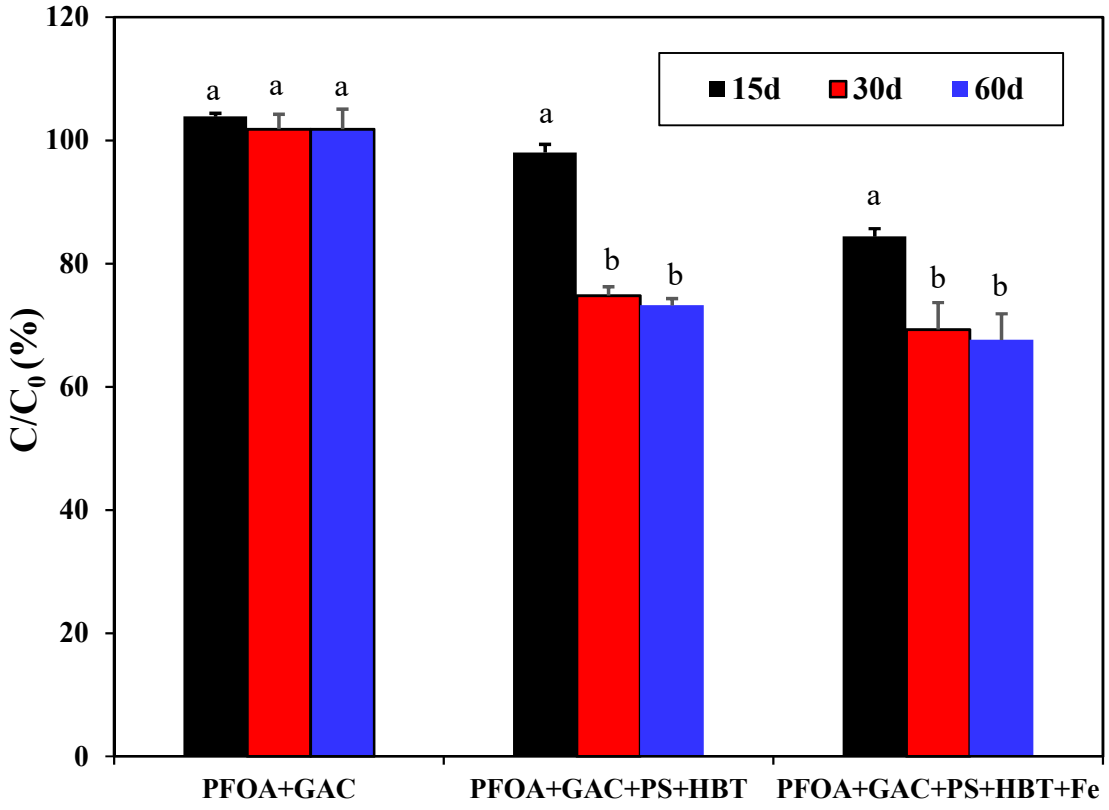

Figure 3.2. The removal of PFOA in spiked sample by laccase-mediator system immobilized on SigmaAldrich GAC in batch reactors. The total reaction volume is 15 mL with 20 mg GAC added. Concentrations of all the reagents were listed in **Table S1**. Means with different letters are significantly different ($p<0.05$).

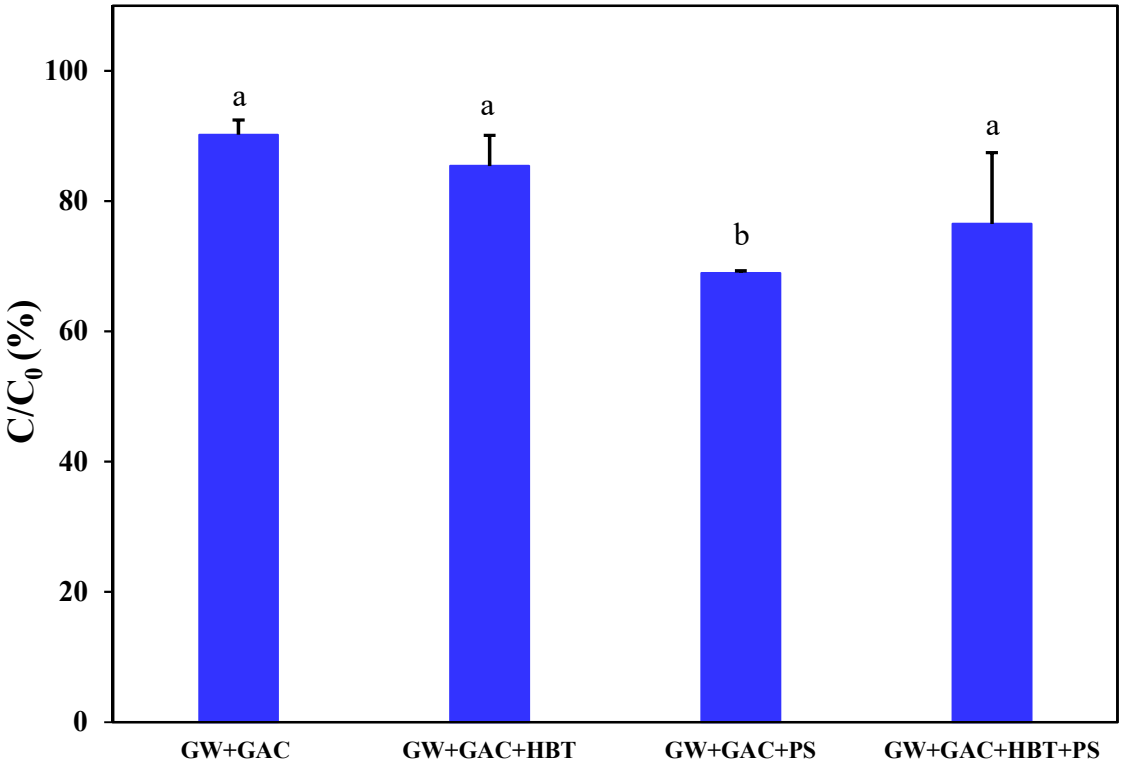

Figure 3.3. The removal of PFOA in groundwater by laccase-mediator system immobilized on CalgonCarbon GAC in batch reactors. The reaction volume is 45 mL containing 10 mg GAC (from CalgonCarbon), 2 Unit/mL PS laccase, and with 20 μmol L^{-1} HBT (GW+GAC+HBT+PS) or without HBT (GW+GAC+PS). Control reactors were prepared and tested at the same time that contained 10 mg GAC but not HBT and laccase (GW+GAC) or no laccase (GW+GAC+HBT) in 45 mL groundwater. Means with different letters are significantly different ($p<0.05$).

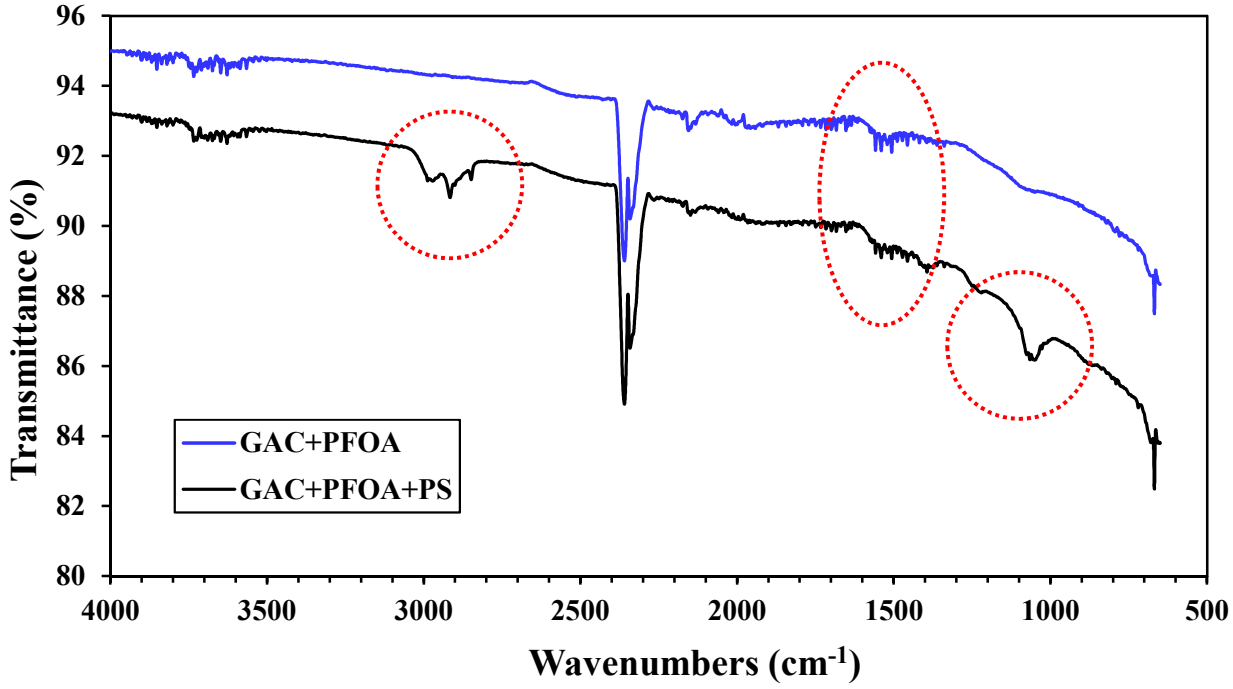

Figure 3.4. FTIR spectra of CalgonCarbon GAC adsorbed with PFOA only (1 μmol L^{-1} initial concentration) or PFOA and PS laccase with initial concentration of 1 μmol L^{-1} PFOA and 2 Unit/mL for laccase.

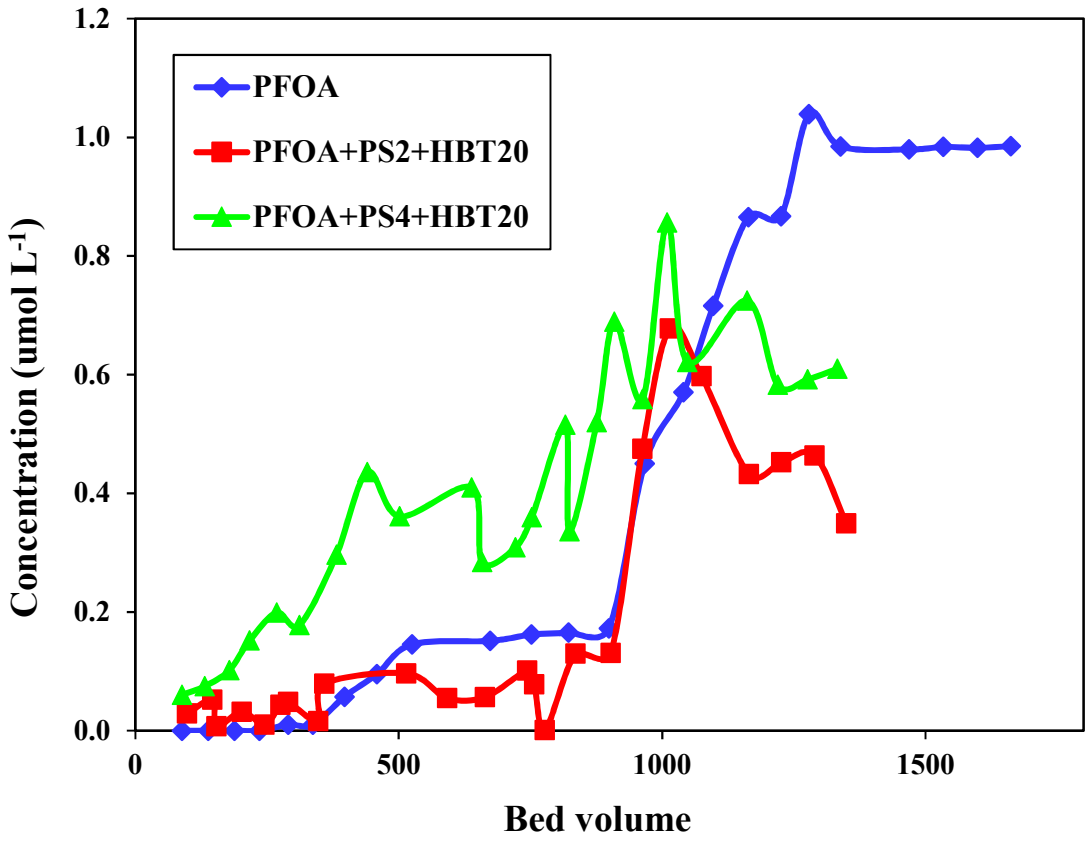

Figure 3.5. Breakthrough of PFOA on the GAC column packed with ECOHR induced and a blank control GAC column. The influents contained 1 μmol L^{-1} PFOA w/wo PS laccase added at two dosages (PS2: 2 Unit/mL; PS4: 4 Unit/mL) and w/wo HBT added at 20 μmol L^{-1}.

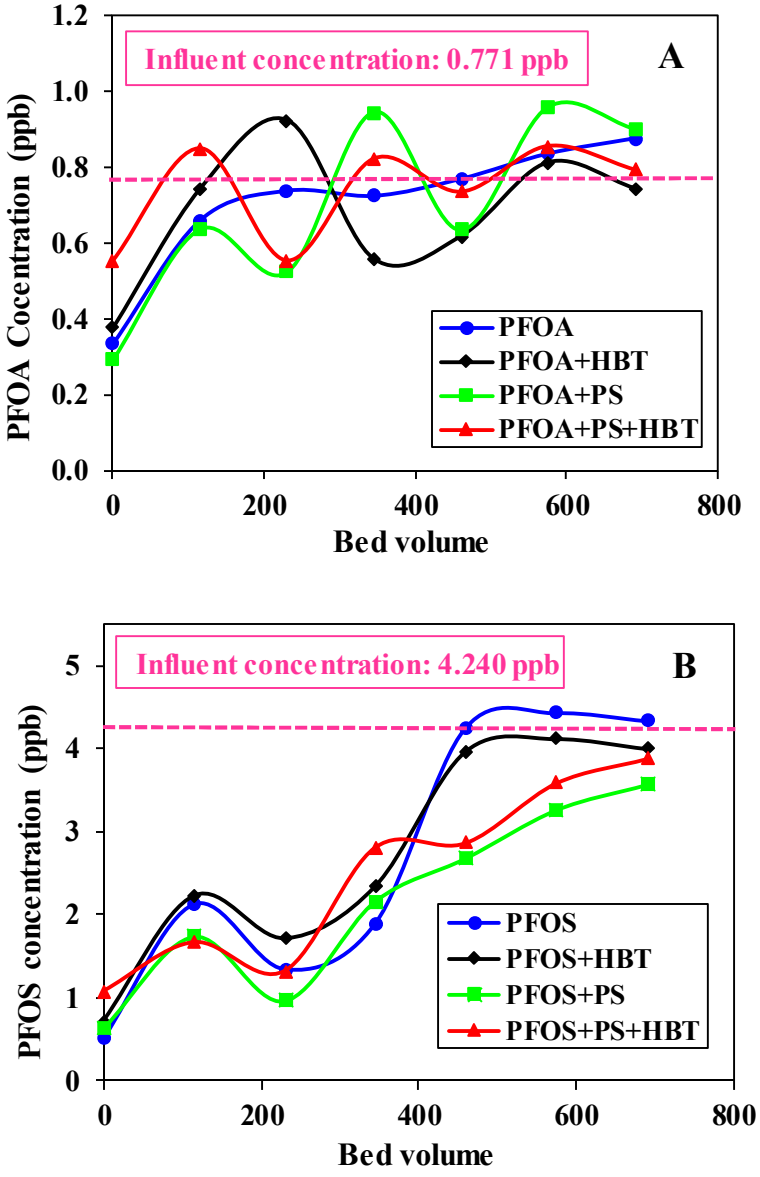

Figure 3.6. Breakthrough of PFOA (A) and PFOS (B) in groundwater on the GAC column packed with ECOHR induced and a blank control. The columns were packed with 0.5 g CalgonCarbon GAC, and the flow rate was 0.14 mL/min. The influent solutions contain groundwater, w/wo HBT at 20 μmol L^{-1}, and w/wo PS laccase at 2 unit/mL.

CHARPTER 4

ELECTRO-OXIDATION OF TETRACYCLINE BY A MAGNELI PHASE TI4O7 POROUS ANODE: KINETICS, PRODUCTS, AND TOXICITY[3]

[3] Liang, S., Lin, H., Yan, X., & Huang, Q. Accepted by *Chemical Engineering Journal*. Reprinted here with permission of publisher, November 1, 2017.

ABSTRACT

The goal of this study is to evaluate Magnéli phase titanium oxide (Ti_4O_7) as an anode material for potential application in electrochemical oxidation of organic pollutants in water. The removal of tetracycline (TC) was systematically investigated in terms of kinetics, reaction mechanisms and pathways, and multi-species toxicity. Application of 0.5 – 3 mA cm^{-2} current densities resulted in > 90% total removal of TC over a wide range of initial concentrations from 1 mg L^{-1} to 50 mg L^{-1} with half-lives between 28 mins and 75 mins. The oxidation mechanisms were further elucidated using salicylic acid (SA) as a hydroxyl free radical trap. At least 40% of total TC removal was attributable to reactions mediated by hydroxyl radicals, which were generated on Magnéli phase Ti_4O_7 at a rate of 2×10^{-9} mol cm^{-2} min^{-1} under 0.5 mA cm^{-2} applied current density. Tests on *Escherichia coli* culture indicated that electro-oxidation of TC by Magnéli phase Ti_4O_7 anode successfully reduced the original antimicrobial activity to a level below detection limit. However, for freshwater micro algae *Scenedesmus obliquus*, inhibitory effects persisted in the first couple of hours and then dramatically reduced during the last stage of treatment, likely due to intermediate products that later mineralized and detoxified. Reaction pathways were proposed based on the data of high-resolution mass spectrometry, and oxidation products with antibiotic potency similar to or greater than TC were identified in 1h treatment sample, but not detectable in the end-of-treatment solution.

Keywords: Magnéli phase Ti_4O_7; Ebonex; Electro-oxidation; Tetracycline; Toxicity

INTRODUCTION

Electrochemical processes are considered as the next-generation technologies for treating contaminated water owing to its ability to degrade a wide spectrum of pollutants (Radjenovic & Sedlak, 2015). Unlike traditional advanced oxidation processes, electrochemical oxidation

requires no addition of chemicals, and can be operated under ambient conditions. Electrochemical treatments are versatile, and therefore adaptive to various decentralized wastewater treatments, such as ballast water and wastewater from mobile facilities and rural homes and farms (Nanayakkara, Zheng, Alam, Zou, & Chen, 2011; Tsolaki, Pitta, & Diamadopoulos, 2010).However, its application has been hindered due to the relatively high cost, limited lifetime of electrodes, and possibility of releasing toxic metals during the treatment (Chaplin, 2014). After continuous operation, passivation may occur on electrode surface, where certain chemical species gradually accumulate and eventually cover the surface, blocking it from further reaction (Ferreira, Varela, Torresi, & Tremiliosi-Filho, 2006). Boron-doped diamond (BDD) electrode shows exceptional resistance to electrode passivation, and has been demonstrated to degrade refractory compounds efficiently, yet their costs are relatively high (Alfaro, Ferro, Martínez-Huitle, & Vong, 2006; W. Wu, Huang, & Lim, 2016). SnO_2- or PbO_2- based electrodes are economically feasible, but are at the risk of releasing toxic metals (Lin et al., 2013). Therefore, the environmental application of electrochemical treatment processes is hinged on the availability of appropriate electrode materials that is cost-effective, durable, and environmentally benign.

Magnéli phase titanium suboxides are substoichiometric titanium oxides with the general formula of Ti_nO_{2n-1}, where n is an integer between 4 and 10 (i.e., 4, 5, 6, and 8) (Miller-Folk, Noftle, & Pletcher, 1989). Magnéli phase titanium suboxides are typically manufactured by first heating titanium dioxide, a cheap, abundant and non-toxic metal oxide, to over 900^{o}C and then allowed to cool down using reducing agents (L. Guo, Jing, & Chaplin, 2016; Zhu, Santiago-Schübel, Xiao, Hollert, & Kueppers, 2016). Among various compositions produced, Ti_4O_7 exhibits the highest conductivity (1500 S cm^{-1}), comparable to that of graphite (Clarke & Harnsberger, 1988), as well as resistance to aggressive chemical conditions and corrosion (Graves, Pletcher,

Clarke, & Walsh, 1991). High conductivity, chemical stability and relatively low production cost make Magnéli phase titanium suboxide attractive as a promising electrode material. Therefore, the application of Magnéli phase titanium oxides has been intensively studied in the fields of chlorine generation, battery, fuel cell and cathodic protection.

The study on the use of Magnéli phase Ti_4O_7 in electrochemical oxidation for potential environmental applications is rather limited, despite its outstanding electrochemical properties. In addition to the many merits mentioned above, Magnéli phase Ti_4O_7 has high overpotential for hydrogen (~ -0.8 V *vs. RHE*) and oxygen (~ 2.5 V *vs. RHE*) evolution (Walsh & Wills, 2010), which allows for direct electrochemical treatment of pollutants in water over a wide range of redox potentials. Trichloroethylene (TCE) was removed from aqueous solution by oxidation with Magnéli phase Ti_4O_7 as the anode (G. Chen, Betterton, & Arnold, 1999). Removal of p-substituted phenol was achieved on Ti_4O_7 porous ceramic anode operated in either batch or cross-flow filtration mode (Zaky & Chaplin, 2013, 2014).

There is thus a great need to evaluate the use of Magnéli phase titanium oxides in anodic oxidation of various pollutants, and explore associated reaction behaviors and mechanisms to support its potential applications in water/wastewater treatment. This study systematically investigated the removal and transformation of tetracycline, a model antibiotic widely present in aqueous environments, on a Magnéli phase Ti_4O_7 anode. The electrode was synthesized by high-temperature reduction of TiO_2 and sintering, and characterized by X-ray diffraction (XRD), scanning electron microscopy (SEM), and Hg porosimetry. Electrochemical oxidation of tetracycline on Ti_4O_7 anode was investigated under various operation conditions. The rate behavior was examined and modeled, and the products were identified, with reaction mechanisms explored via free radical probing approach. The toxicity of the tetracycline solution, without and with

electro-oxidation treatment for different durations, was assessed using *Escherichia coli* and green algae *Scenedesmus obliquus* as receptors.

MATERIALS AND METHODS

Preparation of Magnéli phase Ti_4O_7 electrode

Magnéli phase Ti_4O_7 was produced through high temperature sintering. Magnéli phase Ti_4O_7 powder was produced by heating titanium oxide nano powder at 950 ºC and subsequently reduced under a hydrogen flow. The resulted Magnéli phase Ti4O7 powder was mixed (0.5%, m/m) with polyacrylamide/polyvinyl alcohol (95/5, m/m) and 5% of water. The spray drying process was performed by a PZL-15 spray drying granulation apparatus (YCdry, Inc., China) with a heating power at 54 kW to form granules (40~80 mesh). Then the granulates were pressed at 30 MPa for 5 min in a mold to form ceramic material before sintering in vacuum at 1350ºC for 11 hrs.

Material characterization

Scanning electron microscopy (SEM) of Magnéli phase Ti_4O_7 material was taken on a Hitachi's S-4800 FE-SEM system (Hitachi, Japan). The crystal structures of the samples were characterized by a PANalytical X'Pert PRO MRD X-ray diffractometer (XRD) (PANalytical, Netherlands) at an incidence angle of 2.5°. The XRD scans were recorded with a CuKα1 radiation (λ = 1.541 Å) in the 2θ range from 20° – 80° with a step size of 0.020° and a step time of 1s. The pore structure and porosity of the Magnéli phase Ti_4O_7 ceramic material was characterized using Micromeritics AutoPore IV 9500 mercury porosimetry (Norcross, GA).

Linear scan voltammetry (LSV) was conducted with a Ti_4O_7 ceramic plate (1 cm × 1 cm) as the anode, a platinum foil (2 cm × 2 cm) as the counter electrode, and a silver chloride electrode

(SCE) in an electrolysis cell containing 0.5 M H_2SO_4 background electrolyte, at a linear scan rate of 100 mV s^{-1} driven by a CHI 660E electrochemical workstation (Austin, TX)

Chemicals

Chemicals used in this study were reagent or higher grade. Tetracycline (TC), salicylic acid (SA), 2,3-dihydroxybenzoic acid (2,3-DHBA), 2,5-dihydroxybenzoic acid (2,5-DHBA), sodium sulfate (Na_2SO_4), HPLC grade acetonitrile, and formic acid were obtained from Sigma-Aldrich (St. Louis, MO). All solutions were prepared in Barnstead Nanopure water ($\geqslant$18 MΩ cm^{-1} at 20ºC).

Electro-oxidation procedure

Electrochemical oxidation experiments were conducted in an electrolytic cell (10 cm × 5 cm × 2.5 cm) with a Ti_4O_7 ceramic plate or a Ce-PbO_2 plate (8 cm × 5 cm) as the anode and a 304 stainless steel plate of the same size as the cathode. The thickness of the anode is 3 mm. The electrical connection was made directly from DC power source to electrodes using copper wire and alligator clamps. The Ce-PbO_2 electrode was prepared as previously described (Lin et al., 2013). In each treatment, 100 mL of a solution containing 1, 10, or 50 mg L^{-1} tetracycline and 100 mM Na_2SO_4 as background electrolyte was placed in the electrolytic cell with continuous stirring. A direct current was supplied at different current density (0.5, 1.0, 2.0 or 3.0 mA cm^{-2}) by a controllable DC power source (Electro Industries Inc., Monticello, MN), while the anode potential was monitored using a CHI 660E (CH Instruments, Inc., Austin, TX) electrochemical workstation with silver chloride electrode placed in the cell. Triplicate samples were withdrawn from each reactor at pre-selected time intervals and stored at 4ºC for subsequent analysis. The energy consumption for degrading one mole of TC molecules was calculated according to equation (1) (Raut et al., 2014):

$$E = 10^{-3} * (V \times I \times t)/M \quad (1)$$

where:

E = energy required for disinfection in kWh/mol TC

V = electrode voltage in volts

I = electrode current in amperes

t = time required for the removal of TC

M = treated molarity of TC (mol)

Free radical trapping

Experiments were conducted using salicylic acid as a hydroxyl radical probe to determine the role of hydroxyl radicals in the electrochemical oxidation of tetracycline, and validate the feasibility of using salicylic acid as a radical trapping agent in electro-oxidation processes. In brief, salicylic acid of a different dosage (0, 100 mg L^{-1} or 1000 mg L^{-1}) was added to a solution containing 10 mg L^{-1} tetracycline and 100 mM Na_2SO_4, and electrolyzed at the current density of 0.5 mA cm^{-2} with Ti_4O_7 ceramic anode and stainless steel cathode in the reactor described above. Triplicate samples were taken from each solution at pre-designated time points and stored at 4°C for future analysis.

Chemical analysis

Quantification methods

The aqueous samples were passed through 0.22 μM cellulose membrane, and 100 μL of the filtrate was reconstituted in 900 μL of an acetonitrile/water (50/50, v/v) mixture for analysis. Tetracycline, salicylic acid, 2,3-DHBA and 2,5-DHBA were quantified using a Waters ACQUITY UPLC system coupled with Xevo TQD tandem mass spectrometry (UPLC-MS/MS) (Milford, MA) with acetonitrile and water (0.1% formic acid) as mobile phases at a flow rate of 0.3 mL/min

for a total elution time of 6 mins. The mass spectrometer was operated as following: capillary voltage 2.60 kV, cone voltage 38.34 V, desolvation temperature 500°C, cone gas flow 50 L/Hr, and desolvation gas flow 500 L/Hr. Tetracycline was quantified using electron spray positive (ESI+) ionization and multiple reaction monitoring (MRM) mode based on the precursor ion (m/z 445)/daughter ion (m/z 410) transition. For salicylic acid, 2,3-DHBA, and 2,5-DHBA concentration determination, electro spray ionization negative mode (ESI-) was applied with transition patterns: salicylic acid (m/z 137 to 93), 2,3-DHBA and 2,5-DHBA (m/z 153 to 109).

Product identification

The sample used for product identification was obtained at 1 h during EO treatment at 0.5 mA cm^{-2} and 10 mg L^{-1} initial concentration. A positive control with 10 mg L^{-1} tetracycline in 100 mM Na_2SO_4 solution without EO treatment and a negative control containing water only were also processed along with the treatment samples for comparison. MS full scan (m/z 50 – 1000, resolution R = 120,000) were performed on both treatment and control samples using an Orbitrap Elite high-resolution tandem mass spectrometer (Thermo Scientific, Waltham, MA) in electrospray positive (ESI+) mode. Mass filtration function (Xcalibur 2.1, Thermo Fisher Scientific) was then performed to identify possible products by screening peaks only present in treatment samples but not in controls. For each m/z peak identified, a molecular formula was assigned using Formula Finder with 5 mg L^{-1} mass error allowed. Subsequently, tandem MS (MS/MS) was performed on the possible products (resolution R = 30,000), and their molecular structures were deduced based on the fragment peaks and general MS fragmentation rules (McLafferty & Tureček, 1993).

UV-Vis absorption spectrum study

The absorption spectra of treatment samples taken at the time 0 (t_0), 2h and 5 h during EO treatment (10 mg L^{-1} initial concentration, 0.5 mA cm^{-2}) were scanned at 1,200 nm/min from 250 nm to 400 nm with a Beckman Coulter DU 800 spectrophotometer (Brea, CA).

Toxicity assessment

Growth inhibition on green algae

The growth inhibition assay with freshwater microalgae *Scenedesmus obliquus* (UTEX, University of Texas, Austin, TX) was conducted according to a modified version of OECD NO. 201 guideline. *S. obliquus* stock solution was prepared by culturing algae in 250 mL flask containing 100 mL of modified 3N medium (UTEX, University of Texas, Austin, TX) on an orbital agitator at 22ºC under continuous light for 7 – 10 days. Then, an aliquot (1 mL) of exponentially-growing algae stock suspension and 1 mL of treatment sample taken at different time points during electrolysis of a solution with10-mg L^{-1} initial tetracycline concentration (0.5 mA cm^{-2}) were added to 8 ml 3N medium in 50 mL sterilized culture tubes. Control samples with no algae stock addition but all the other reagents added were prepared along with treatment samples. All the culture tubes were incubated at 20°C with continuous illumination, and the algae biomass was determined at 0, 24, 48, 72, 96 h by measuring optical densities at 680 nm using Beckman Coulter DU 800 spectrophotometer (Brea, CA). The assay was performed in triplicate per treatment and control sample. The average specific growth rate and percent inhibition of growth rate was calculated according to equation (1) and (2):

Average specific growth rate: $\mu_{i-j} = \frac{\ln B_j - \ln B_i}{t_j - t_i}\ d^{-1}$ (1)

Where: $\mu_{i\text{-}j}$ is the average specific rate from time i to j; B_i is the biomass concentration at time i (t_i), and B_j is the biomass concentration at time j (t_j).

Percent inhibition of growth rate: $\%I = \frac{\mu_0 - \mu_t}{\mu_0} \times 100$ (2)

Where: $\%I$ is the percent inhibition in average specific growth rate; μ_0 is the mean value for μ in the control; μ_t is the mean value for μ in the treatment.

Antimicrobial activity

Disk agar-diffusion biocidal susceptibility method (Balouiri, Sadiki, & Ibnsouda, 2016) was performed by dropping 100 µl electrolysis treatment or control samples to blank filter disks, and then placing the disks onto Lysogeny Broth (LB) plates inoculated with *Escherichia coli* (*E. coli*) cells. After incubating the plates at 37ºC for 24 hrss, antimicrobial activity of treatment samples was compared with the control samples by the presence and diameters of their inhibition zones. Completely detoxified and the negative control samples would not show visible inhibition zone surrounding the filter disks, yet it is supposed to be seen around the positive control samples containing tetracycline.

RESULTS AND DISCUSSION

Characterization of Magnéli phase Ti_4O_7 material

The XRD patterns of the anode material and reference Ti_4O_7 powder are shown in **Figure 4.1-A** and **Figure 4.1-B**, respectively. The major peaks matching those of the characteristic peaks of the reference Ti_4O_7 material occur at 20.7º, 26.3º, 29.5º, 31.7º, 34.0º, 36.3º, 40.5º, 53.1º, 55.0º, 63.8º, and 66.4º (indicated by red points), confirming the presence of Magnéli phase Ti_4O_7 as the major composition (**Figure S4.1**). The high percentage of Ti_4O_7 ensures outstanding electrical conductivity, because Ti_4O_7 exhibits the best conductivity among all different phases of titanium suboxides (L. Guo, Jing, et al., 2016; J. Smith, Walsh, & Clarke, 1998). The scanning electron

microscopy (SEM) image (Figure **4.1-C)** on the surface of Magnéli phase Ti_4O_7 anode material shows rather uniform interconnecting pores with diameters smaller than 10 μm. Mercury intrusion porosimetry analysis (**Figure 4.1-D**) indicates a porosity of 23% with an average pore diameter of 2.6 μm. In a previous study, increase of the macropore volume in the electrode material significantly reduced the performance loss caused by mass transport limitations (Kong, Kim, Lee, Shul, & Lee, 2002). Therefore, the dominant volume of macropores in the Magnéli phase titanium oxide (Ti_4O_7) in this study is beneficial to the removal of TC. The interconnected macro-pore structure is advantageous for an electrode, because it provides pathways for the electrolytes and the pollutants to diffuse, and more active sites for them to interact with, leading to greater electrochemical accessibility and efficiency than smooth non-porous electrodes (Janssen & Koene, 2002). In addition, roughness factor can be calculated based on the voltammetric charge and double-layer capacitance obtained from cyclic voltammetry scanning at various frequencies (**Figure S4.3-b**) as described (Xu & Scantlebury, 2003). The roughness factor of the electrode utilized in this study was determined to be 1075.5 ± 66.8. This large roughness factor suggested more reactive sites and greater effective surface area on porous electrodes than smooth surface electrodes (C. W. Li, Ciston, & Kanan, 2014).

The linear scan voltammetry (LSV) of Magnéli phase Ti_4O_7 electrode (**Figure S4.2**) revealed a high oxygen evolution potential (OEP) at 2.3 V *vs.* SCE, which is comparable to BDD electrode (2.2 – 2.6 V *vs.* NHE) and higher than metal oxides based hybrid electrodes (1.4 – 2.0 V *vs.* NHE) (Martínez-Huitle & Andrade, 2011). The high overpotential for oxygen evolution makes Magnéli phase Ti_4O_7 electrode suitable for oxidizing a wide range of organic pollutants with no or less water hydrolysis competition. In addition, the low activity of an anode towards oxygen evolution (high OEP) is associated with weaker interaction between hydroxyl radical and the

electrode surface, thus leading to higher reactivity for the $OH^{\bullet}$ to oxidize target pollutants (Alfaro et al., 2006). In addition, as shown in **Figure S4.3-a**, the electrochemical activity of Magnéli phase Ti_4O_7 remained unchanged after 200 cycles of cyclic voltammetry scanning in 10 mM $K_4Fe(CN)_6$ + 0.1 M KNO_3 solution. This result suggested the high stability and reusability of the testing electrode.

Electrochemical degradation of tetracycline

Electrochemical degradation of tetracycline by Magnéli phase Ti_4O_7 anode was conducted at current densities ranging from 0.5 to 3.0 mA cm^{-2} with the initial TC concentrations at 10 mg L^{-1} and 50 mg L^{-1}. The time-dependent TC concentration in the electrolytic cell is shown in **Figure 4.2**. Pseudo-first order rate constants were obtained by model fit and listed in **Table 4.1**. For the initial concentration at 10 mg L^{-1}, the removal rate of 75.2%, 89.3%, 95.2% and 97.6% was achieved after 120-min treatment at the current densities of 0.5, 1.0, 2.0, and 3.0 mA cm^{-2}, respectively. The pseudo-first order rate constants (k) ranged from 1.05×10^{-2} to 1.87×10^{-2} min^{-1} with half-lives between 37 ~ 66 minutes. Although in general, TC decay rate was positively related to the current density applied, enhanced removal was not evident when increasing the current density from 2.0 mA to 3.0 mA cm^{-2}, likely indicative of mass-transfer limit, especially when TC concentrations dropped to relatively low level as the treatment went on. Unlike treatments at the lower initial TC concentrations, differences among rate constants at various current densities were more evident for experiments with the 50-mg L^{-1} initial concentration (**Figure 4.2-B**), suggesting that mass transfer was no longer a limiting factor. Based on the energy consumed per mole of TC removal (**Table 4.1**), the optimum treatment condition was 0.5 mA cm^{-2} at 50 mg L^{-1} initial concentration. The energy consumption for the solution with the initial concentration of 50 mg L^{-1} was only ¼ of that with 10-mg L^{-1} initial concentration, which was also

benefited from the greater mass transfer rates at higher concentrations. Additionally, electro-oxidation of TC with the initial concentration at 1 mg L^{-1} was evaluated (**Figure S4.5**). The 2-h removal rate was >90% at 0.5 to 3.0 mA cm^{-2}, and the average pseudo-first order rate constant was 1.59×10^{-2} min^{-1}.

The electrochemical performance of Magnéli phase Ti_4O_7 anode was compared with the Ce-PbO_2 electrode, a "non-active" electrode previously reported to effectively remove refractory contaminants (Niu et al., 2012). Electro-oxidation experiments were conducted at 2.0 mA cm^{-2} with the initial TC concentration at 10 mg L^{-1} and 50 mg L^{-1}. The results revealed a slightly faster TC degradation with Ce-PbO_2 electrode at 10-mg L^{-1} initial concentration (**Figure 4.3-A**), but the performance of Magnéli phase Ti_4O_7 anode was significantly better than Ce-PbO_2 electrode at 50 mg L^{-1} initial TC concentration (**Figure 4.3-B**). The difference was most likely attributed to more active reaction sites provided by the 3D porous Ti_4O_7 anode than the two-dimensional Ce-PbO_2 electrode, as diffusion was no longer a limiting factor when TC concentration was sufficiently high. Thus, Magnéli phase Ti_4O_7 anode is a great candidate for treating organic pollutants at high concentration or at enhanced diffusion rate.

The EO experiment was also carried out using constant anode potential ranged from 2.5 V to 4.9 V. The surface-area normalized reaction rate constants (k_{ob}) can be obtained via the time course data of TC degradation at different anode potential (**Figure S4.6-A**). The k_{ob} values thus obtained were fit to a kinetic model established on the assumption of substrate transformation via consecutive mass transfer and electron transfer that reach steady state (**Text S4.1**). The mass transfer rate constant of TC in the reaction system was determined to be 1.27×10^{-3} cm s^{-1} by model fit (**Figure S4.6-B**). It should however be noted that the model did not fully capture the measured k_{ob} values with evident deviation particularly at the relatively lower anodic potential

(<3.5 V vs SCE), probably because that the model only accounts for the substrate transformation via direct electron transfer, but disregards hydroxyl radical initiated reactions, which tends to have more significant contribution in substrate degradation process at lower anode potential.

In addition, a preliminary experiment was conducted to assess the performance of Ti_4O_7 material as a reactive electrochemical membrane (REM) using a dead-end filtration system (**Figure S4.12**). With this REM system, the energy consumption was calculated to be 7.3, 14.0, 30.9, and 50.3 kWh/mol TC removal under 1, 2, 3, and 5 mA/cm^{-2} respectively at the flow rate of 10 mL/min, which was about only 1/25 of those for the batch operation at the same current density (**Figure S4.13**). This markedly enhanced energy efficiency is mainly contributed by the high mass transfer rate during filtration, which ensures better contact between contaminates and reactive sites on electrode. The relative independence of the performance on the tested current densities suggested that the reaction was controlled by mass transfer rate under these conditions. Our future study will be focused on investigating and optimizing the Ti_4O_7 REM systems. The pure water flux of Magnéli phase Ti_4O_7 electrode was tested to be12,895 LMH Bar^{-1} (**Figure S4.11**), about five times higher than the general ultra filtration membranes used for drinking water filtration.

Production of free radicals on electrode

It is proposed that organic chemicals may be oxidized electrochemically at anode through two pathways: 1) direct electron transfer from the chemical to electrode, which dominates at low anodic potential; and 2) hydroxyl radical ($OH^{\bullet}$) mediated reactions, which prevails when anode potential is greater than 2.38 V (vs SCE), the standard potential for $OH^{\bullet}$ generation from water electrolysis (Kapałka, Fóti, & Comninellis, 2009). In the case of "non-active" anode, hydroxyl radicals are weakly adsorbed on the electrode surface through physical interactions, thus able to more effectively oxidize the organic chemical via radical chain reactions, as opposed to the

"active" anode where hydroxyl radicals are chemisorbed (Marselli, Garcia-Gomez, Michaud, Rodrigo, & Comninellis, 2003). Magnéli phase Ti_4O_7 anode was characterized as a non-active electrode given its superior stability and ability to produce free hydroxyl radicals (Bejan, Guinea, & Bunce, 2012). Understanding the quality and quantity of hydroxyl radicals generated on the Magnéli phase Ti_4O_7 anode is however necessary and important to assess its electrochemical reactivity, and elucidate the reaction pathways, and help with future modification and improvement of the material for better efficiency.

Spin trapping has been used to detect hydroxyl radicals in chemical systems, since free radicals are too reactive and short-lived to be directly determined (Janzen, Radicals, & Traps, 2012). A spin trapping probe ideal for electrolysis systems should have the following properties: 1) inert to direct electron transfer process; 2) react fast with free radicals; and 3) the products (also called spin adducts) are persistent, so that it can be properly quantified. Salicylic acid (SA) was selected and used in this study as a spin trapping probe (Ai, Wang, Li, & Jin, 2005; Jen, Leu, & Yang, 1998; Marselli et al., 2003; Peralta et al., 2014) to examine the production of $OH^{\bullet}$ on Magnéli phase Ti_4O_7 electrode and the extent of hydroxyl radical mediated substrate oxidation. SA reacts with hydroxyl radical to form two hydroxylation products (2,3-DHBA and 2,5-DHBA) (Eq. 8).

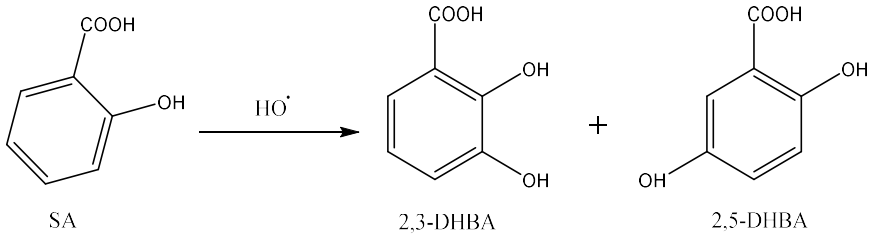

[8]

TC removal, SA consumption, and accumulation of the spin adducts were monitored in an EO system (0.5 mA cm^{-2}) with SA added at several concentration levels (0 pm, 100 mg L^{-1} and

1000 mg L^{-1}). Interestingly, the results (**Figure 4.4**) revealed enhanced TC removal with 100-mg L^{-1} SA addition in comparison to the treatment without SA in solution. This indicates that 100-mg L^{-1} SA did not compete with TC reaction on the anode surface, and the increased removal of TC was most likely attributed to enhanced ionic strength caused by SA addition. The absence of SA competition suggests that 1) the mass transfer rate of SA at 100 mg L^{-1} is lower than TC at 10 mg L^{-1}, and/or 2) the rate of hydroxyl radicals generated on electrode was excessive than needed for converting both SA and TC. The excessive generation of hydroxyl radicals was evidenced by continuous consumption of 2,3-DHBA and 2,5-DHBA as shown in **Figure 4.5-A** and **Figure 4.5-C**. Similar concentration profiles were observed in a previous work conducted using platinum anode with the initial SA concentration around 100 mg L^{-1} (Peralta et al., 2014). Therefore, when insufficient SA dosage was used, the generation of 2,3-DHBA and 2,5-DHBA would significantly underestimate the production of hydroxyl radicals on anode. When the SA dosage was raised to 1000 mg L^{-1}, the following results were observed: 1) TC removal was inhibited by about 40% (**Figure 4.4**), which would be greater if TC removal had not been enhanced by the change in ionic strength caused by SA addition; 2) SA was consumed at a constant rate over the testing period (**Figure 4.5-B**); and 3) 2,3-DHBA and 2,5-DHBA were continuously accumulated at a constant rate (**Figure 4.5-B**). These suggested that SA was in excess, and thus consumed all free radicals, so that 2,3-DHBA and 2,5-DHBA did not further degrade by hydroxyl radicals. Hence, the rate of hydroxyl radical generation on Magnéli phase Ti_4O_7 anode was calculated by assuming that the sum of 2,3-DHBA and 2,5-DHBA formations was equal to the hydroxyl radical formation in the case of 1000-mg L^{-1} SA addition. The production rate of $OH^{\bullet}$ was thus determined to be 2×10^{-9} mol cm^{-2} min^{-1} at the tested condition (0.5 mA/cm^2).

It is noteworthy that the total generation of 2,3-DHBA and 2,5-DHBA only accounted for ~30% of the SA reduction over the duration of experiment (**Figure 4.5-D**), which indicated other routes of SA consumption. For example, other products, such as catechol and 2,6-dihydroxybenzoic acid (2,6-DHBA), were also detected during SA hydroxylation, but was reported to occur in very small quantities (Guinea et al., 2008; D. Wu, Liu, Dong, & Zhou, 2007). In addition, SA is not completely inert to direct electron transfer, and conversion of SA was previously observed at low current densities (Marselli et al., 2003). It therefore would be mistaken if using SA reduction (instead of spin adduct formation) to estimate the production of hydroxyl free radicals during electrochemical reactions, although this method was proven effective in other $OH^{\bullet}$ generation systems, such as Fenton reaction (Gruber, Wiesner, Burger, & Lindner, 2006; Jen et al., 1998; Tomita, Okuyama, Watanabe, & Watanabe, 1994).

Reaction pathways

Possible reaction products were identified in a sample after one hour of EO treatment (0.5 mA/cm^2, 10 mg L^{-1} initial concentration) with about 50% TC removal by screening the m/z peaks present in its HRMS spectra but not in those of the control samples (**Figure S4.7 and S4.8**). Five products with molecular ions of *m/z* 402.1553 (P1), 461.1562 (P2), 477.1515 (P4) and 442.1140 (P5) were identified in the treatment sample (**Table 4.2)**. It should be noted that none of these five products were detectable in the sample at the end of 5-h EO treatment with 97.5% TC removal, indicating that these products are intermediates in nature.

The molecular structures of the products were further deduced based on their tandem MS spectra according to common fragmentation rules. The reaction pathways of TC oxidation to form the five products were then proposed as depicted in **Figure 4.6**. The electronic structure of tetracycline was calculated using density functional theory (DFT) (**Text S4.2 in SI**) to assist with

interpretation of the reaction mechanism. Conjugation can form between C=C bond and the oxygen on its adjacent hydroxyl group that is electron-donating with negative charge (atom 25C, 22O, 40C and 38O in **Table S4.1**). This weakens 8C–9C and 14C–15C double bonds, thus making them the most vulnerable sites on the TC molecule for $OH^{\bullet}$ attack to add -OH groups at these positions, as also observed in a previous study (Khan, Bae, & Jung, 2010), and such addition tends to occur on the more positively charged carbons in the double bonds (8C and 14C), leading to the formation of products P2 and P3 (**Figure 4.6)**. Consistent with previous oxidation studies (Dalmázio, Almeida, Augusti, & Alves, 2007; Yan Wang et al., 2011), loss of NH_3 subsequently happened at the amino group at 14C, resulting in a degradation product with lactone ring (P4).

It is known that the ketone and enol groups play an important role in the antimicrobial activity of tetracycline antibiotics (Brodersen et al., 2000). Thus, the electro-oxidation products P1, P2 and P3 may exhibit similar antimicrobial activity as the parent compound, because these critical functional groups are preserved in their structures. Previous studies revealed that several common degradation products had potency at the same level as or greater than tetracycline; for example, 5a,6-anhydrotetracycline and 5a,6-anhydrochlortetracycline even caused growth inhibition on tetracycline-resistant bacteria (Halling-Sørensen, Sengeløv, & Tjørnelund, 2002; Jiao, Zheng, Yin, Wang, & Chen, 2008). Apart from antibacterial activity, tetracycline also had adverse effects on the growth and reproduction of other aquatic organisms, such as freshwater green algae and crustacean *Daphnia magna* (Wollenberger et al., 2000; Yang, Tang, Zhou, Zhang, & Song, 2013). TC degradation products may have higher degree of potency towards those species considering their enhanced antimicrobial activity, but related information is very limited so far. Hence, multi-species toxicity assessment of TC and its electro-oxidation products is of great importance for comprehensive evaluation of the treatment effects on environmental ecosystem.

Toxicity assessment

Inhibition on the growth of *E. coli*

In order to evaluate the effects of electrochemical treatment on the antimicrobial activity of TC, an agar diffusion test was performed on a sample after EO treatment (0.5 mA cm^{-2}, 10 mg L^{-1} initial concentration) for 0 and 5 hrs as well as the TC stock solution (10 mg L^{-1}) and the background electrolyte solution (100 mM Na_2SO_4). The t_0 treatment solution and the positive control TC stock solution resulted in significant inhibitions zones around the spiked filter disks, while the inhibition zone was not visible for the 5-h treatment sample and the background electrolyte control sample (**Figure 4.7-A**). This indicates that the antibacterial activity of the TC solution had been eliminated during the electro-oxidation process, or at least reduced to a level below the minimum inhibitory concentration of *E. coli*. This is consistent with the change in UV absorption spectrum of TC solution over treatment, showing diminished intensities of the peaks corresponding to the keto (275 nm) and enol (360 nm) groups over time (**Figure S4.10**).

Toxic effects on green algae

A toxicity assessment was also performed on freshwater green algae *Scenedesmus obliquus* with samples taken from a TC solution after different durations of EO treatment, and the percent inhibition of specific growth rate was shown in **Figure 4.7-B**. For the sample after four hrs of EO treatment with 91% TC removal, the percent inhibition on algae only reduced from 50% to 44%. This was likely due to the generation of equally or more toxic products by electro-oxidation, consistent with the findings reported by Zhu et al (Zhu et al., 2016) on increased algal toxicity of fluoroquinolone antibiotics after electrochemical oxidation. However, the adverse effect was

reduced remarkably after 6 hrs of treatment, dropping to 6.2%. This can be justified by a common product evolution pattern during electro-oxidation observed in previous studies (Barhoumi et al., 2015; Kapałka, Fóti, & Comninellis, 2008; Niu et al., 2012; Zhu et al., 2016): reactions with hydroxyl radicals during the initial stage of treatment lead to rapid degradation of the parent chemical and accumulation of the intermediates, which are then destroyed via step-wise mineralization, resulting in destruct of the functional structures of the intermediates and thus elimination of the toxicity. In order to study the mineralization degree, the total organic carbon (TOC) contents in the samples with 10-mg L^{-1} initial concentration that had been treated at 0.5 mA cm^{-2} for 0 and 2h were measured using Shimadzu TOC-Vcsh total organic carbon analyzer (Columbia, MD). The TOC contents at time zero and 2 h were 6.81 mg L^{-1} and 4.94 mg L^{-1}, respectively. This indicated a 27.5% mineralization rate when 75.2% TC was removed in the system. Besides complete mineralization into carbon dioxide, other routes of TC removal include being oxidized into less toxic coupling products or smaller molecules. Thus, the toxicity of the solution is gradually reduced during EO treatment process.

CONCLUSIONS

Electrochemical oxidation by Magnéli phase Ti_4O_7 anode, a porous material with high conductivity and chemical stability, is able to effectively remove tetracycline (TC) in water, EO by the Ti_4O_7 anode achieved faster TC removal than Ce-PbO_2 anode when the substrate concentration was high (> 50 mg L^{-1}), while the removal rates were similar between the two electrodes at relatively lower substrate concentration.

When salicylic acid (SA) was used as free radical probe in excess, TC removal was significantly inhibited, indicating that reactions initiated by hydroxyl radicals dominate TC degradation. SA concentration was reduced linearly over time and the hydroxylation products 2,3-

DHBA and 2,5-DHBA accumulated, suggesting negligible subsequent reactions with hydroxyl radicals. However, when SA was used at lower concentration, 2,3-DHBA and 2,5-DHBA were continuously consumed at anode, in which case, hydroxyl radical generation cannot be properly quantified.

Several oxidation products of TC were formed during electro-oxidation through the addition of oxygen or loss of -NH_3 or -CONH groups. Some of those products may exhibit similar or higher antimicrobial activity and toxicity compared to the parent compound, since their core functional groups (ketone and enol) remained intact in structure, while such products were further degraded at longer treatment time.

The result of agar diffusion test revealed that the inhibitory effect of TC on the growth of *E coli* cell was eliminated or reduced to non-detectable level after 5h of electrochemical treatment. Yet, the adverse effects on green algae *S obliquus* was essentially unchanged at the beginning, but significantly reduced during the last two hrs of treatment, which suggested the generation of primary oxidation products with equal or higher potency in comparison to TC.

Future work is needed to overcome the rate limiting mass transfer process, which may be achieved by developing porous Magnéli phase Ti_4O_7 material into membrane filtration system to boost convection dispersion of substrates.

SUPPORTING INFORMATION AVAILABLE

XRD plots including reference titanium suboxides with various composition; The electrochemical stability, electrical resistance, and linear scan voltammetry (LSV) plot of Magnéli phase Ti_4O_7; Removal of TC at 1 mg L^{-1} initial concentration; Mass spectrum of reaction products; Kinetic modeling; Density functional theory; UV absorption spectrum of treatment solution; Membrane permeability; Filtration device setup; Filtration treatment efficiency.

ACKNOWLEDGEMENTS

The study was supported in part by U.S. Department of Defense SERDP ER 2717. We thank the Proteomics and Mass Spectrometry Core Facility at the University of Georgia for performing the high-resolution mass spectrometry analysis for our samples.

LITERATURE CITED

J. Radjenovic, D.L. Sedlak, Challenges and opportunities for electrochemical processes as next-generation technologies for the treatment of contaminated water, Environ. Sci. Technol. 49 (2015) 11292-11302.

E. Tsolaki, P. Pitta, E. Diamadopoulos, Electrochemical disinfection of simulated ballast water using Artemia salina as indicator, Chem. Eng. J. (Lausanne) 156 (2010) 305-312.

K.N. Nanayakkara, Y.-M. Zheng, A.K. Alam, S. Zou, J.P. Chen, Electrochemical disinfection for ballast water management: technology development and risk assessment, Mar. Pollut. Bull. 63 (2011) 119-123.

B.P. Chaplin, Critical review of electrochemical advanced oxidation processes for water treatment applications, Env. Sci. Process. Impact 16 (2014) 1182-1203.

M. Ferreira, H. Varela, R.M. Torresi, G. Tremiliosi-Filho, Electrode passivation caused by polymerization of different phenolic compounds, Electrochim. Acta 52 (2006) 434-442.

W. Wu, Z.H. Huang, T.T. Lim, A comparative study on electrochemical oxidation of bisphenol A by boron-doped diamond anode and modified SnO2-Sb anodes: Influencing parameters and reaction pathways, J. Environ. Chem. Eng. 4 (2016) 2807-2815.

M.A.Q. Alfaro, S. Ferro, C.A. Martínez-Huitle, Y.M. Vong, Boron doped diamond electrode for the wastewater treatment, J. Braz. Chem. Soc. 17 (2006) 227-236.

H. Lin, J. Niu, J. Xu, H. Huang, D. Li, Z. Yue, C. Feng, Highly efficient and mild electrochemical mineralization of long-chain perfluorocarboxylic acids (C9–C10) by Ti/SnO_2–Sb–Ce, Ti/SnO_2–Sb/Ce–PbO_2, and Ti/BDD electrodes, Environ. Sci. Technol. 47 (2013) 13039-13046.

R.R. Miller-Folk, R.E. Noftle, D. Pletcher, Electron transfer reactions at Ebonex ceramic

electrodes, J. Electroanal. Chem. Interfacial Electrochem. 274 (1989) 257-261.

L. Zhu, B. Santiago-Schübel, H. Xiao, H. Hollert, S. Kueppers, Electrochemical oxidation of fluoroquinolone antibiotics: Mechanism, residual antibacterial activity and toxicity change, Water Res. (2016).

L. Guo, Y. Jing, B.P. Chaplin, Development and characterization of ultrafiltration TiO_2 Magnéli phase reactive electrochemical membranes, Environ. Sci. Technol. 50 (2016) 1428-1436.

R. Clarke, S. Harnsberger, New electrically conductive ceramic--a fundamental advance in electrode technology, Am. Lab. 20 (1988) 8.

J. Graves, D. Pletcher, R. Clarke, F. Walsh, The electrochemistry of Magnéli phase titanium oxide ceramic electrodes Part I. The deposition and properties of metal coatings, J. Appl. Electrochem. 21 (1991) 848-857.

F. Walsh, R. Wills, The continuing development of Magnéli phase titanium sub-oxides and Ebonex® electrodes, Electrochim. Acta 55 (2010) 6342-6351.

G. Chen, E. Betterton, R. Arnold, Electrolytic oxidation of trichloroethylene using a ceramic anode, J. Appl. Electrochem. 29 (1999) 961-970.

A.M. Zaky, B.P. Chaplin, Mechanism of p-substituted phenol oxidation at a Ti_4O_7 reactive electrochemical membrane, Environ. Sci. Technol. 48 (2014) 5857-5867.

A.M. Zaky, B.P. Chaplin, Porous substoichiometric TiO_2 anodes as reactive electrochemical membranes for water treatment, Environ. Sci. Technol. 47 (2013) 6554-6563.

A.S. Raut, G.B. Cunningham, C.B. Parker, E.J. Klem, B.R. Stoner, M.A. Deshusses, J.T. Glass, Disinfection of E. coli contaminated urine using boron-doped diamond electrodes, J. Electrochem. Soc. 161 (2014) G81-G85.

F.W. McLafferty, F. Tureček, Interpretation of mass spectra, University science books 1993.

M. Balouiri, M. Sadiki, S.K. Ibnsouda, Methods for in vitro evaluating antimicrobial activity: A review, J. Pharm. Anal. 6 (2016) 71-79.

J. Smith, F. Walsh, R. Clarke, Electrodes based on Magnéli phase titanium oxides: the properties and applications of Ebonex® materials, J. Appl. Electrochem. 28 (1998) 1021-1033.

C.S. Kong, D.-Y. Kim, H.-K. Lee, Y.-G. Shul, T.-H. Lee, Influence of pore-size distribution of diffusion layer on mass-transport problems of proton exchange membrane fuel cells, J. Power Sources 108 (2002) 185-191.

L. Janssen, L. Koene, The role of electrochemistry and electrochemical technology in environmental protection, Chem. Eng. J. (Lausanne) 85 (2002) 137-146.

L. Xu, J. Scantlebury, Electrochemical Surface Characterization of IrO_2-Ta_2O_5 Coated Titanium Electrodes in Na_2SO_4 Solution, J. Electrochem. Soc. 150 (2003) B288-B293.

C.W. Li, J. Ciston, M.W. Kanan, Electroreduction of carbon monoxide to liquid fuel on oxide-derived nanocrystalline copper, Nature 508 (2014) 504-507.

C.A. Martínez-Huitle, L.S. Andrade, Electrocatalysis in wastewater treatment: recent mechanism advances, Quim. Nova 34 (2011) 850-858.

J. Niu, H. Lin, J. Xu, H. Wu, Y. Li, Electrochemical mineralization of perfluorocarboxylic acids (PFCAs) by Ce-doped modified porous nanocrystalline PbO_2 film electrode, Environ. Sci. Technol. 46 (2012) 10191-10198.

A. Kapałka, G. Fóti, C. Comninellis, The importance of electrode material in environmental electrochemistry: formation and reactivity of free hydroxyl radicals on boron-doped diamond electrodes, Electrochim. Acta 54 (2009) 2018-2023.

B. Marselli, J. Garcia-Gomez, P.-A. Michaud, M. Rodrigo, C. Comninellis, Electrogeneration of hydroxyl radicals on boron-doped diamond electrodes, J. Electrochem. Soc. 150 (2003)

D79-D83.

D. Bejan, E. Guinea, N.J. Bunce, On the nature of the hydroxyl radicals produced at boron-doped diamond and Ebonex® anodes, Electrochim. Acta 69 (2012) 275-281.

E.G. Janzen, S.F. Radicals, D. Traps, A critical review of spin trapping, Free radicals in biology 4 (2012) 116-154.

S. Ai, Q. Wang, H. Li, L. Jin, Study on production of free hydroxyl radical and its reaction with salicylic acid at lead dioxide electrode, J. Electroanal. Chem. 578 (2005) 223-229.

J.-F. Jen, M.-F. Leu, T.C. Yang, Determination of hydroxyl radicals in an advanced oxidation process with salicylic acid trapping and liquid chromatography, J. Chromatogr. A 796 (1998) 283-288.

E. Peralta, G. Roa, J. Hernandez-Servin, R. Romero, P. Balderas, R. Natividad, Hydroxyl radicals quantification by UV spectrophotometry, Electrochim. Acta 129 (2014) 137-141.

E. Guinea, C. Arias, P.L. Cabot, J.A. Garrido, R.M. Rodríguez, F. Centellas, E. Brillas, Mineralization of salicylic acid in acidic aqueous medium by electrochemical advanced oxidation processes using platinum and boron-doped diamond as anode and cathodically generated hydrogen peroxide, Water Res. 42 (2008) 499-511.

D. Wu, M. Liu, D. Dong, X. Zhou, Effects of some factors during electrochemical degradation of phenol by hydroxyl radicals, Microchem. J. 85 (2007) 250-256.

M. Tomita, T. Okuyama, S. Watanabe, H. Watanabe, Quantitation of the hydroxyl radical adducts of salicylic acid by micellar electrokinetic capillary chromatography: oxidizing species formed by a Fenton reaction, Arch. Toxicol. 68 (1994) 428.

M. Gruber, G. Wiesner, R. Burger, R. Lindner, The salicylate trapping method: Is oxidation of salicylic acid solution oxygen and time dependent and metal catalysed?, J. Chromatogr. B

831 (2006) 320-323.

M.H. Khan, H. Bae, J.-Y. Jung, Tetracycline degradation by ozonation in the aqueous phase: proposed degradation intermediates and pathway, J. Hazard. Mater. 181 (2010) 659-665.

I. Dalmázio, M.O. Almeida, R. Augusti, T.M. Alves, Monitoring the degradation of tetracycline by ozone in aqueous medium via atmospheric pressure ionization mass spectrometry, J. Am. Soc. Mass Spectrom. 18 (2007) 679-687.

Y. Wang, H. Zhang, J. Zhang, C. Lu, Q. Huang, J. Wu, F. Liu, Degradation of tetracycline in aqueous media by ozonation in an internal loop-lift reactor, J. Hazard. Mater. 192 (2011) 35-43.

D.E. Brodersen, W.M. Clemons, A.P. Carter, R.J. Morgan-Warren, B.T. Wimberly, V. Ramakrishnan, The structural basis for the action of the antibiotics tetracycline, pactamycin, and hygromycin B on the 30S ribosomal subunit, Cell 103 (2000) 1143-1154.

B. Halling-Sørensen, G. Sengeløv, J. Tjørnelund, Toxicity of tetracyclines and tetracycline degradation products to environmentally relevant bacteria, including selected tetracycline-resistant bacteria, Arch. Environ. Contam. Toxicol. 42 (2002) 263-271.

S. Jiao, S. Zheng, D. Yin, L. Wang, L. Chen, Aqueous photolysis of tetracycline and toxicity of photolytic products to luminescent bacteria, Chemosphere 73 (2008) 377-382.

L. Wollenberger, B. Halling-Sørensen, K.O. Kusk, Acute and chronic toxicity of veterinary antibiotics to Daphnia magna, Chemosphere 40 (2000) 723-730.

W. Yang, Z. Tang, F. Zhou, W. Zhang, L. Song, Toxicity studies of tetracycline on Microcystis aeruginosa and Selenastrum capricornutum, Environ. Toxicol. Pharmacol. 35 (2013) 320-324.

N. Barhoumi, L. Labiadh, M.A. Oturan, N. Oturan, A. Gadri, S. Ammar, E. Brillas,

Electrochemical mineralization of the antibiotic levofloxacin by electro-Fenton-pyrite process, Chemosphere 141 (2015) 250-257.

A. Kapałka, G. Fóti, C. Comninellis, Kinetic modelling of the electrochemical mineralization of organic pollutants for wastewater treatment, J. Appl. Electrochem. 38 (2008) 7-16.

M. Bowden, G. White, I. Brown, M. Ryan, G. Gainsford, Improved powder diffraction patterns for the titanium suboxides Ti_nO_{2n-1} ($4 \leq n \leq 9$), Powder Diffr. 11 (1996) 60-68.

Table 4.1. Degradation parameters of electro-oxidation of tetracycline at Magnéli phase Ti_4O_7 anodes.

Initial concentration (mg L^{-1})	Current Density (mA cm^{-2})	Cell Voltage (V)	Anode Potential (V)	Removal at 120 min	k (min^{-1})	$t_{1/2}$ (min)	R^2	Energy Consumption (kWh/mol)
10	0.5	3.8	2.4	75.2%	1.05×10^{-2}	66.0	0.989	89.7
	1.0	4.4	3.5	89.3%	1.59×10^{-2}	43.6	0.979	175.0
	2.0	4.8	3.6	95.2%	1.83×10^{-2}	37.9	0.743	358.2
	3.0	5.9	4.2	97.6%	1.87×10^{-2}	37.1	0.618	644.2
50	0.5	4.2	3.1	69.0%	0.93×10^{-2}	74.5	0.927	21.6
	1.0	4.9	3.3	92.5%	1.82×10^{-2}	38.1	0.808	37.6
	2.0	5.4	3.3	93.9%	1.93×10^{-2}	35.9	0.951	81.7
	3.0	5.8	3.9	98.4%	2.46×10^{-2}	28.2	0.706	125.6

Table 4.2. High resolution mass spectrometry data of TC degradation products.

Product	Short Written	Elemental Composition	$[M+H]^+$		Error (mg L^{-1})
			Measured Mass	Theoretical Mass	
TC	$[M+H]^+$	$C_{22}H_{25}O_8N_2$	445.1615	445.1605	0.94
P1	$[M-CONH+H]^+$	$C_{21}H_{24}O_7N$	402.1553	402.1547	0.59
P2	$[M+H+O]^+$	$C_{22}H_{25}O_9N_2$	461.1562	461.1555	0.78
P3	$[M+H+2O]^+$	$C_{22}H_{25}O_{10}N_2$	477.1515	477.1504	1.19
P4	$[M+H+O-2H-NH_3]^+$	$C_{22}H_{20}O_9N$	442.1140	442.1133	0.79

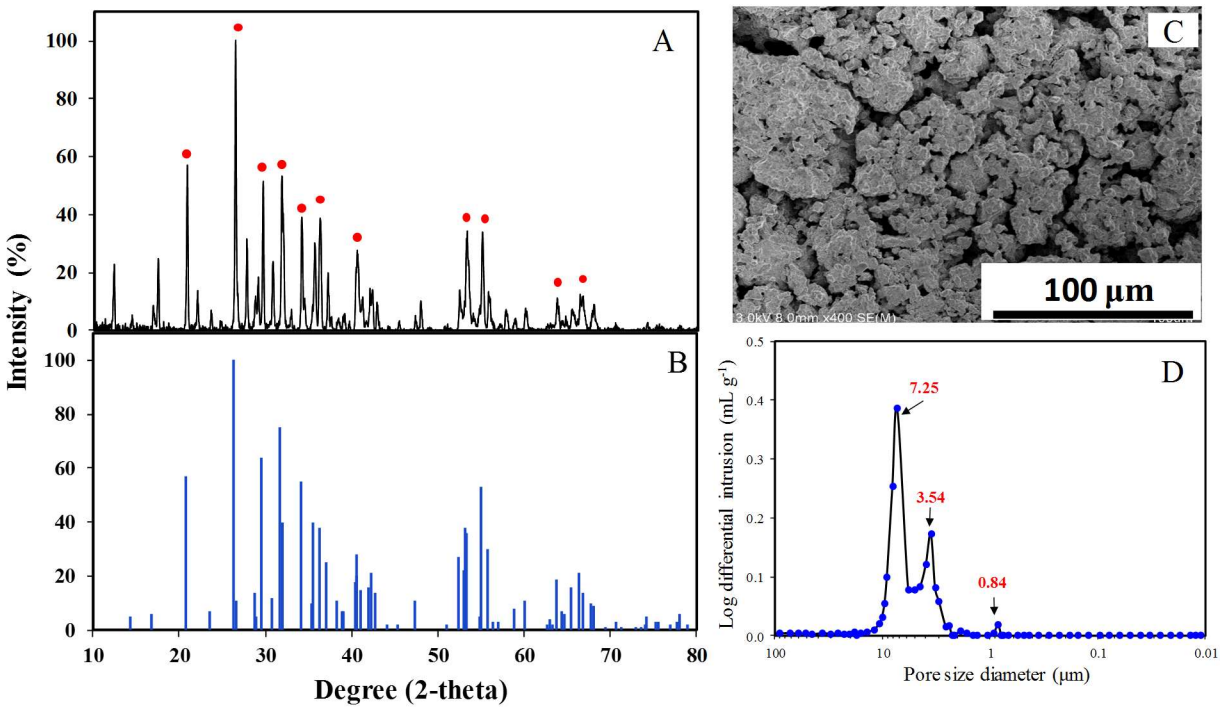

Figure 4.1. (A) XRD spectrum of Magnéli phase Ti_4O_7 electrode material (red dots indicate matching peaks compared with reference spectrum); (B) XRD spectrum of Ti_4O_7 reference powder (Bowden, White, Brown, Ryan, & Gainsford, 1996); (C) SEM image of the surface of Ti_4O_7 electrode; (D) The result of mercury intrusion analysis on Ti_4O_7 electrode showing pore size distribution.

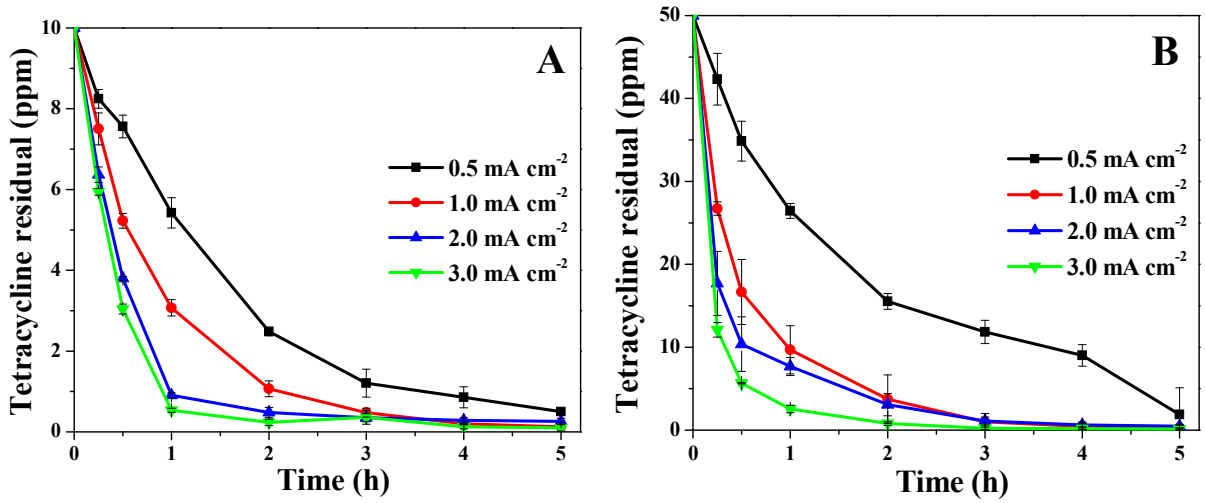

Figure 4.2. Removal of TC during electrochemical oxidation at Magnéli phase Ti_4O_7 anode under various current densities: (A) initial TC concentration at 10 mg L^{-1}, 100 mM Na_2SO_4; pH 6; (B) initial TC concentration at 50 mg L^{-1}, 100 mM Na_2SO_4; pH 6.

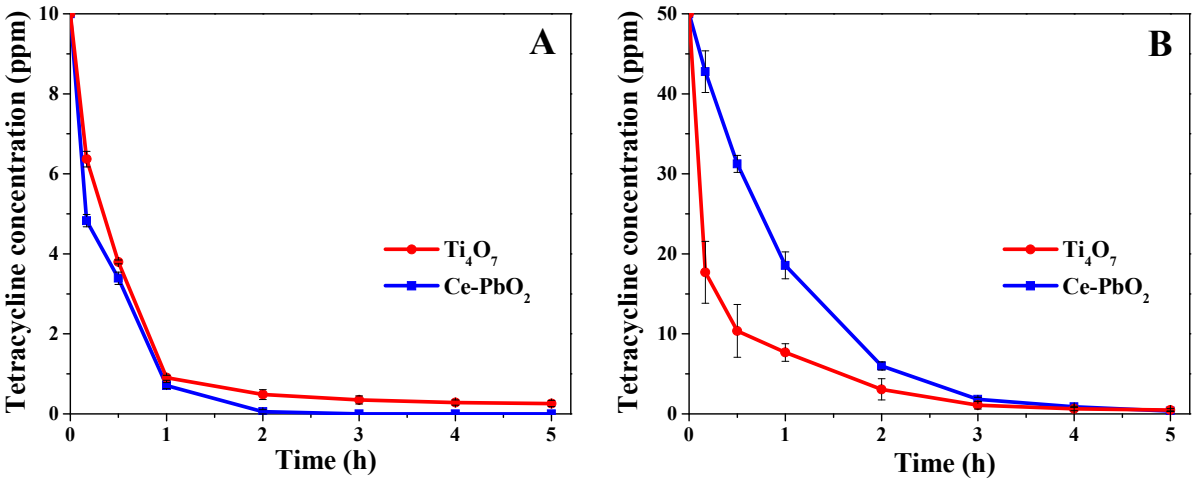

Figure 4.3. Removal of TC during electrochemical oxidation process at different electrodes at current density of 2 mA cm^{-2}: (A) initial TC concentration at 10 mg L^{-1}, 100 mM Na_2SO_4; pH 6; (B) initial TC concentration at 50 mg L^{-1}, 100 mM Na_2SO_4; pH 6.

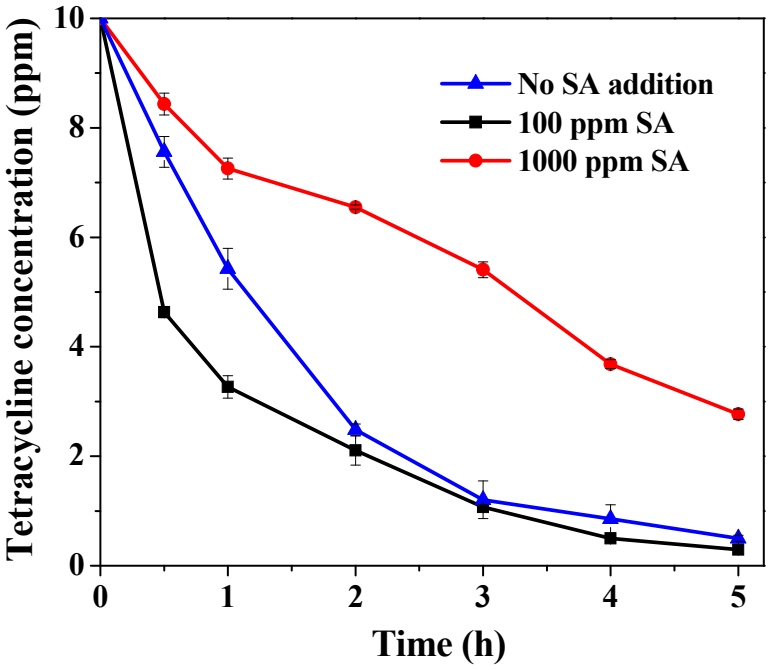

Figure 4.4. Concentration change of TC (10 mg L^{-1}) during electro-oxidation treatment with salicylic acid additions at various levels under current density of 0.5 mA cm^{-2}.

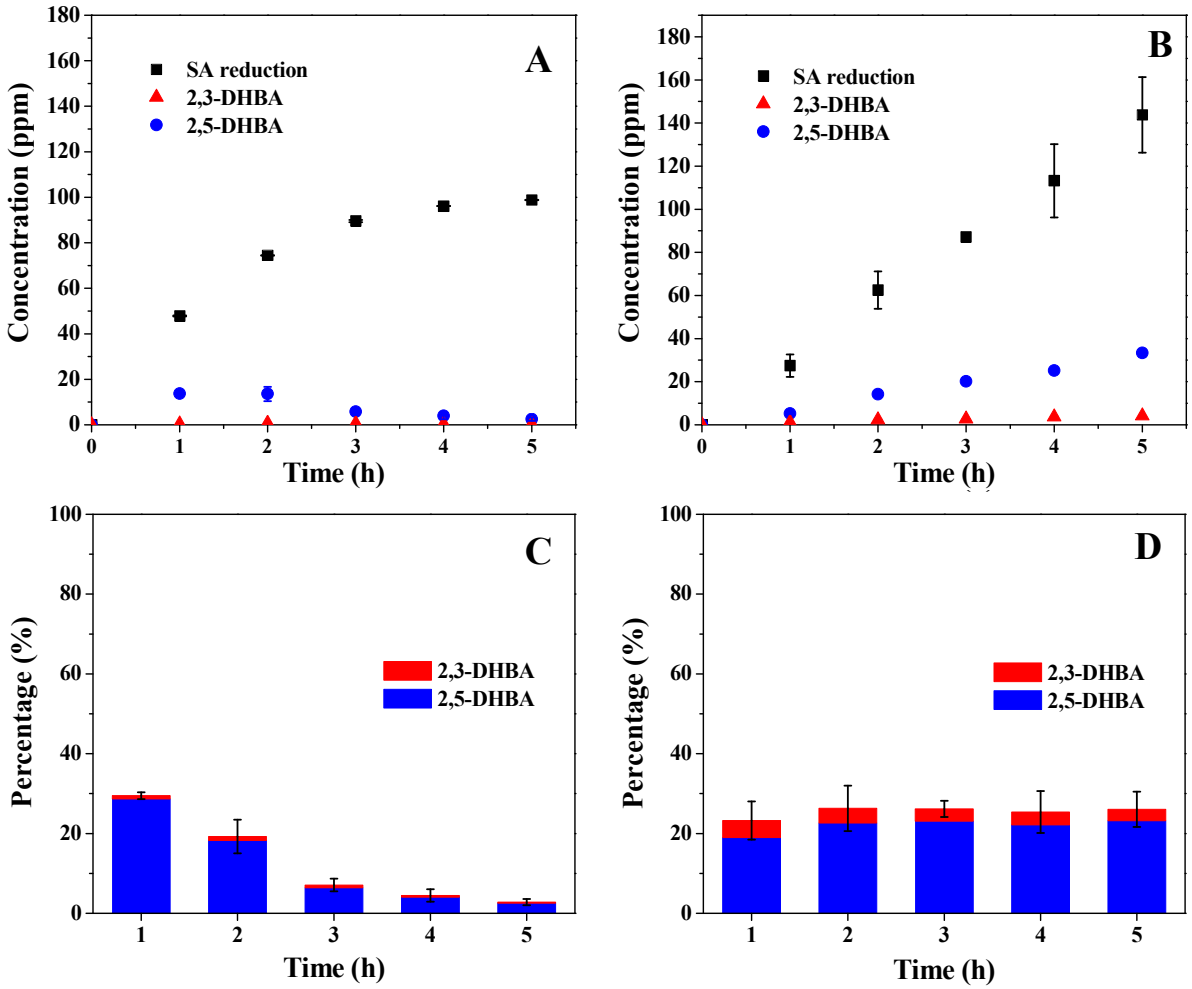

Figure 4.5. Concentration reduction of SA and concentration increase of 2,3-DHBA and 2,5-DHBA during electrochemical process with SA initial concentration at (A) 100 mg L^{-1} and (B) 1000 mg L^{-1}; Percentage of 2,3-DHBA and 2,5-DHBA generated on electrode with respect to the amount of SA reduction with SA initial concentration at (C) 100 mg L^{-1} and (D) 1000 mg L^{-1}.

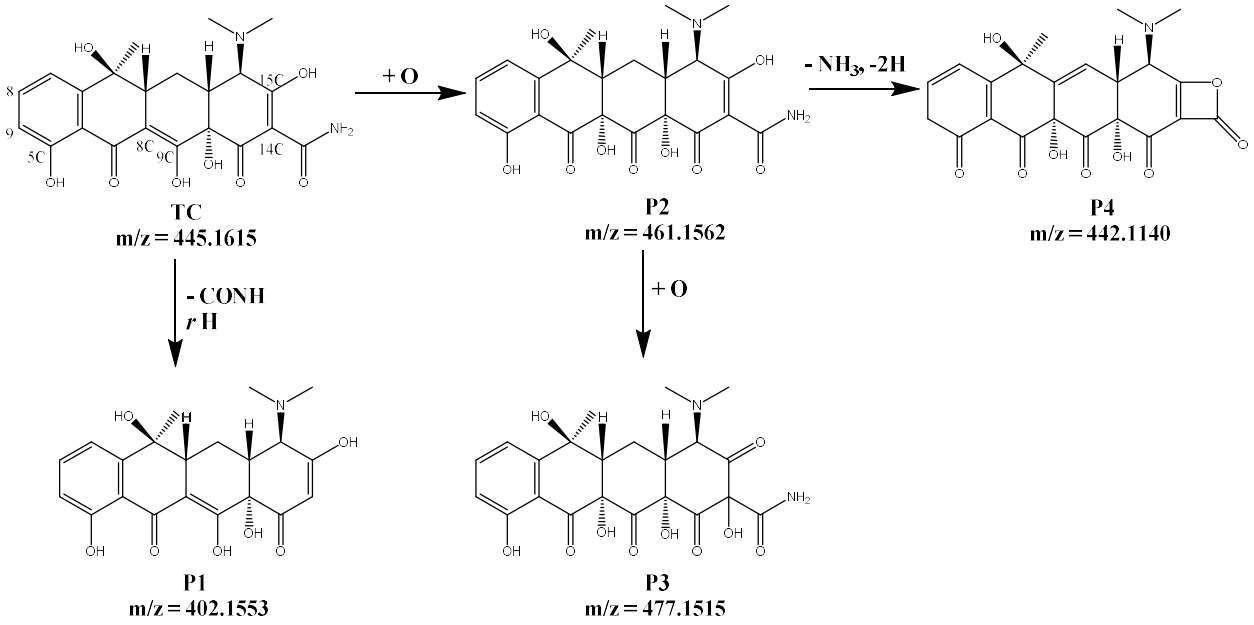

Figure 4.6. Proposed transformation pathways of TC in electrochemical oxidation treatment system.

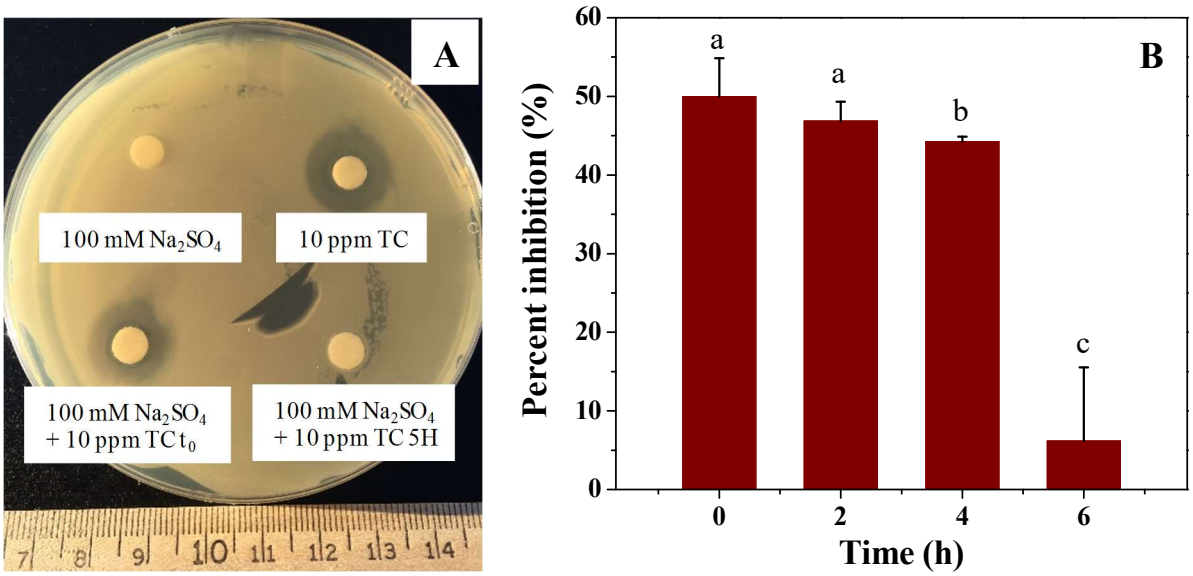

Figure 4.7. (A) results of agar diffusion test conducted on background electrolyte control, TC positive control, initial treatment solution and end-of-treatment solution using *E coli* as the test substance; (B) Percent inhibition of the specific growth rate of green algae *S. obliquus* by electrochemical treatment (TC initial concentration at 10 mg L^{-1}, current density at 0.5 mA cm^{-2}) solutions collected at varying time points. Means with different letters are significantly different ($p<0.05$).

CHARPTER 5

FILTRATION AND ELECTROCHEMICAL INACTIVATION OF E COLI USING A TI4O7 CERAMIC MEMBRANE[4]

[4] Liang, S., Lin, H., & Huang, Q. To be submitted to *Environmental Science and Technology*.

ABSTRACT

Attributed to simple equipment, fast radical generation capacity, and low formation rate of disinfection by-products, electrochemical process is considered as a promising point of use (POU) disinfection technology. In this study, a novel ceramic electrode, magneli phase Ti_4O_7 Ti_4O_7 electrode was tested in a dead-end filtration system to electrochemically inactivate a model pathogen *E coli* in water. The filtration system achieved greater than 5 log *E coli* removal at 10 mA/cm^{-2} applied current density, and the total removal rate remained above 99.5% under various current densities ranging from 0 to 10 mA/cm^{-2}. Protein concentrations in effluent as well as membrane pressure were monitored during the disinfection process, and they both showed positive correlations with current density. Flow cytometry results, TEM and SEM images of samples revealed that the main disinfection mechanisms involved were free radical inactivation, electric field disturbance, and physical separation. The effect of electroporation was considered minimal as no visible pores were found on cell membranes in SEM scanning photo.

Keywords: electrochemical, filtration, disinfection, E coli, mechanism

INTRODUCTION

According to a World Health Organization report (Organization, 2015), 663 million people still lack access to safe water in 2015, and most of them live in developing countries and rural areas. Waterborne pathogens can cause severe disease and death, thus remaining a primary threat to public health. Due to various limitations, the conventional disinfection methods, such as chlorination, ozonation, and UV irradiation, are implemented in centralized water treatment plants, but cannot meet dispersed disinfection needs. Additionally, ozonation and chlorination have the disadvantage of producing carcinogenic disinfection by-products (DBPs) (Y. Li et al., 2016; Rajab, Heim, Letzel, Drewes, & Helmreich, 2015; Schaefer, Andaya, & Urtiaga, 2015). Therefore, there

is a critical demand to develop point-of-use (POU) disinfection technologies that are effective in removing waterborne pathogens, inexpensive and easy to use.

Membrane filtration is the most commonly used POU water disinfection technology at present, but merely physically separate pathogens from water without killing them. Biofilms developed from live microorganisms can attach to the membrane surface, and block the passage of water, thus the filter needs to be replaced regularly to ensure disinfection efficiency (Brady-Estévez, Schnoor, Vecitis, Saleh, & Elimelech, 2010; Gkotsis, Banti, Peleka, Zouboulis, & Samaras, 2014). This adds up to the high maintenance cost, and thus makes membrane filtration less applicable in the long run. Photocatalysis based on semi-conductive metal oxides, such as titanium dioxides in particular, have been explored extensively for POU water disinfection use, because the reactive free radicals produced via photocatalysis can rapidly inactivate bacteria (Kikuchi, Sunada, Iyoda, Hashimoto, & Fujishima, 1997; Maness et al., 1999; Reed, 2004). Although many TiO_2-based photocatalytic reactors have been developed and proven effective in inactivating pathogens, the high cost of material fabrication and devices required for subsequent separation and collection of catalyst particles makes it hard to widely apply this technology in rural places (Belháčová, Krýsa, Geryk, & Jirkovský, 1999; Fernández-Ibáñez, Blanco, Malato, & De Las Nieves, 2003). Developing a technology that can simultaneously remove and inactivate pathogens is of important significance, and when it is coupled with membrane technology can reduce biological fouling and extend the service life of membrane filter.

Electrochemical inactivation of microbes has been long explored for POU water disinfection. It is particularly promising for dispersed disinfection uses at rural places because an electrochemical inactivation can be built in compacted mobile units, has high disinfection efficiency, requires low energy consumption, and can be potentially powered by solar energy.

Different electrode materials has been studied for electrochemical inactivation (Bruguera-Casamada, Sirés, Prieto, Brillas, & Araujo, 2016; Drees, Abbaszadegan, & Maier, 2003; Jeong, Kim, & Yoon, 2009; Y. Li et al., 2016; Rajab et al., 2015; Wen, Tan, Hu, Guo, & Hong, 2017). Over 5 log reduction of both gram-positive and gram-negative bacteria has been achieved in batch reactors using boron doped diamond (BDD) electrode at a current density of 33.3 mA/cm^{-2} in chloride-free solutions (Bruguera-Casamada et al., 2016). Similar disinfection efficiency was observed using mixed metal oxides (MMO) as anode, and the studies have proven the technology is effective in inactivating bacteria and virus in a short time at relatively low energy consumption (Särkkä, Vepsäläinen, Pulliainen, & Sillanpää, 2008). However, in most of those studies, disinfection relied on electrochemically generated chlorinated oxidative species, thus toxic disinfection by-products were inevitably formed (Schaefer, Andaya, & Urtiaga, 2015).

Reactive electrochemical membrane (REM) system has been developed in recent years, which improved disinfection efficiency and addressed the issue of DBP formation. A conductive porous material is used both as a membrane and an anode in the REM systems. A REM system using multiwalled carbon nanotubes (MWNT) as the filter has exhibited complete inactivation of both bacteria and virus by applying 2 to 3 V cell voltage (Rahaman, Vecitis, & Elimelech, 2012; C. D. Vecitis, Schnoor, Rahaman, Schiffman, & Elimelech, 2011). However, the key limitations of this particular REM application are the disputable toxicity of carbon nanotube and limited service life of the non-reusable filter. A commercially available porous sub-stoichiometric titanium oxides material has also be studied in REM setup as the electrochemical membrane for its disinfection efficiency using *Escherichia coli* (*E. coli*) as a model pathogen in chloride-free solutions (L. Guo, Ding, Rockne, Duran, & Chaplin, 2016). It is proposed that the disinfection effects resulted from electrostatic adsorption of bacteria on the electrode surface and the strong

acidic or alkaline conditions in the near-electrode microenvironment, while direct or indirect oxidation was not considered as a major cause. The sub-stoichiometric titanium oxide material is suitable for REM applications also because of its non-toxic nature and its physical, chemical, and electrochemical stabilities. It is however imperative to better understand the mechanism of disinfection and influential factors for the design and optimization of REM process based on sub-stoichiometric titanium oxide material.

The mechanisms that have been proposed to explain the electrochemical inactivation of bacteria with various electrodes under different conditions include (1) indirect oxidation; (2) direct oxidation; (3) permeabilization by transmembrane potential; and (4) electroporation (Drees et al., 2003; Jeong et al., 2009; Long, Ni, & Wang, 2015; Rajab et al., 2015). Direct oxidation has been proposed as the primary cause of bacteria inactivation in several studies, which occurs via the electrochemically generated reactive oxidizing species (Cl_2, HClO, ClO^-, OH•, H_2O_2, O_3), while, in chloride-free solutions, OH• is the major species responsible for bacteria inactivation (Jeong et al., 2009). A recent study indicates that reactive oxidants and electric field act synergistically in inactivating microorganisms (Bruguera-Casamada et al., 2016). Direct oxidation happens when membrane proteins and functional groups lose electrons on anode, causing lipid peroxidation and thus compromise of cell integrity (Long et al., 2015). Additionally, it was reported that transmembrane potential is induced when cells are exposed to external electric field (de Lannoy, Jassby, Gloe, Gordon, & Wiesner, 2013; Huo et al., 2016). In a pulsed electric field study, transmembrane potential above 1 V and longer pulse time led to irreversible membrane damage and cell death (Pillet, Formosa-Dague, Baaziz, Dague, & Rols, 2016). Electroporation is a process usually associated nanomaterials as electrodes, where a strong electric field (1-10 kV/cm) is formed at the tip of a wire- or rod-shaped nano particle, causing lethal damage to cells in touch

(Huo et al., 2016; C. Liu et al., 2013; Liu et al., 2014; Wen et al., 2017). An electrochemical disinfection process, depending on electrode type and treatment conditions, often involves two or more mechanisms acting simultaneously to inactivate pathogens. However, because limited electrode materials can produce large amount of OH• while sustain high voltages, most previous studies have focused on indirect oxidation in chloride-containing solution, although formation of DBPs is considered problematic (Cui, Quicksall, Blake, & Talley, 2013; X. Huang et al., 2016; Jeong et al., 2009; Rajab et al., 2015). Recent findings indicated that Magnéli phase Ti_4O_7 ceramic material enables REM with pathogen inactivation in chloride-free solutions, (L. Guo, Ding, et al., 2016), showing great promise for POU water disinfection. A comprehensive study is however needed to further elucidate the pathogen inactivation mechanisms involved in the process, and explore key factors governing the disinfection effectiveness.

The electrochemical inactivation of *Escherichia coli* in Na_2SO_4 solution was investigated using a REM system with Magnéli phase Ti_4O_7 ceramic membrane operated in dead-end filtration mode under different conditions to assess the disinfection effectiveness and governing factors. The electrode material was thoroughly characterized in respect to elemental composition, crystal morphology, porosity, permeability, oxygen evolution potential, and reusability. Additionally, the pathogen inactivation mechanisms of this novel electrode materials were explored by examining the change of *Escherichia coli* over the electrochemical treatment in cell integrity and viability, surface and morphology.

MATERIALS AND METHODS

Electrode fabrication and characterization

Magnéli phase Ti_4O_7 ceramic material was produced from Ti_4O_7 nano powder, which was generated by reducing TiO_2 powder at high temperature (950^oC) under hydrogen flow.

Subsequently, the Ti_4O_7 nano powder was mixed with binder (polyacrylamide/polyvinyl alcohol, 95/5, m/m) and 5% of water to form a slurry, which was spray-dried to small granulates before being pressed into a mold to form a compacted green body. The green body was then sintered under vacuum with temperature increasing from 85°C to 1250°C, to first release the binder and then develop a ceramic material. The physical and electrochemical properties of this electrode material made in house was characterized, and the results and methods used were described in Supporting Information.

Chemicals and strains

All chemicals used in this study were reagent-grade and obtained from Sigma-Aldrich (St. Louis, MO). All solutions were prepared with deionized water generated from Thermo Scientific Barnstead NANOpure water purification system (Waltham, MA) with a resistivity of 18 MΩ cm. *Escherichia coli* (ATCC 15597) was obtained from American Type Culture Collection (ATCC) (Manassas, VA).

Electrochemical inactivation in dead-end filtration

E coli (ATCC 15597) was used as the test strain for this study. An in-house made reactive electrochemical membrane (REM) device (**Figure 5.1**) was operated in dead-end filtration mode with solutions inoculated with the test strain to evaluate the electrochemical pathogen inactivation. The REM device consists of two Ti_4O_7 ceramic membrane disk (3 cm in diameter) as the anode and the cathode, respectively, separated by a rubber ring to form a interelectrode gap of 5 mm. All electrochemical experiments were conducted in 0.05 M Na_2SO_4 as supporting electrolyte, which is a common water composition and stable within the voltage range applied in this study. The electrolytic cell was powered by a controllable DC power source (Electro Industries Inc., Monticello, MN). Electrochemical filtrations were conducted by passing 150 mL of *E coli*

suspension (~10^6 CFU/mL) at the flow rate of 5 mL/min using a peristaltic pump through the REM device with the membranes supplied by direct electric current at different current density (0, 1, 5, or 10 mA/cm^2). The effluent samples were collected every five minutes and immediately cultured on agar plates to determine cell concentrations. In order to investigate the viability of cells on the membrane, both anode and cathode were extracted after each filtration process using 10 mL of 0.9% sterilized NaCl solution under continuous shaking at 120 rpm for one hour to extract bacteria from the membrane. The bacteria concentration in the effluent, membrane extract, and controls were measured using standard plate count method. To be specific, the samples were diluted with 0.9% saline to proper concentration prior to plating. Then, an aliquot (100 μL) of sample was spread over a LB agar plate and incubated at 37ºC for 24 h. After incubation, the number of colonies formed on the agar plate was determined to identify the cell concentration, which was expressed as colony forming unit per mL (CFU/mL).

The relationship between anode potential and cell voltage was determined using a CHI 660E (CH Instruments, Inc., Austin, TX) electrochemical workstation in a conventional three-electrode system consisting of the working electrode (Ti_4O_7 ceramic membrane disk, ø = 3 cm), the counter electrode (Ti_4O_7 ceramic membrane disk, ø = 3 cm) and the reference electrode (Ag/AgCl). The electrodes were placed in *E coli* solution (~10^6 CFU/mL) in 100 mM Na_2SO_4 background electrolyte during the test, with the anode and cathode placed 1 cm from each other in parallel, and the reference electrode 5 mm from the anode. The anode potential was recorded and plotted against the applied cell voltage.

Electrochemical inactivation in batch reactor

Batch reactor experiments were conducted in a one-compartment electrolytic cell (10 cm × 5 cm × 5 cm) with the same electrodes (two Ti_4O_7 ceramic membrane disks) and the same

interelectrode gap (5 mm) as in the filtration system. In each treatment, 150 mL of *E coli* suspension (~10^6 CFU/mL) in 0.05 M Na_2SO_4 background electrolyte was placed in the electrolytic cell with continuous stirring. A direct current was supplied at different current density (0, 1.0, 5.0 or 10.0 mA cm^{-2}) by a controllable DC power source (Electro Industries Inc., Monticello, MN). Triplicate samples were withdrawn from each reactor at time zero and after 30 minutes, and 100 µL of each sample was cultured on plate for cell density quantification during 2 h of electrolysis.

Cell characterization

The following cell characterizations were performed on selected treatment samples and corresponding control samples in order to explore possible pathogen inactivation mechanisms.

Protein leakage. Possible leakage of intracellular protein from *E Coli* cells was measured using Pierce™ bicinchoninic acid (BCA) protein assay kit (Thermo Scientific, Waltham, MA). The test was conducted by mixing 0.1 mL of sample with 2 mL BCA working reagent and then incubating the test tubes at 37°C for 30 minutes. The 562nm absorbance of color developed in each tube was measured using a Beckman Coulter DU 800 spectrophotometer (Brea, CA). A standard curve prepared with albumin standard solution was used to determine the protein concentration of each sample.

Flow cytometry. Flow cytometry analysis was performed on selected effluent samples using the Guava easyCyte™ Single Sample flow cytometer (EMD Millipore, Hayward, CA, USA). The LIVE/DEAD™ BacLight™ Bacterial viability kit (L34856, Invitrogen, Eugene OR, USA) containing the SYTO 9 and propidium iodide dyes were used for staining live and dead bacterial cells in both treatment and control samples. The untreated *E Coli* suspension (10^6 CFU/mL) served

as the control for detection of live cells and heat-killed cells were used as the control for detection of dead cells.

Cell morphology. Bacteria in effluent samples and on membrane electrodes were fixed in 2% glutaraldehyde to perverse the cell morphology. Transmission electron microscope (TEM) observations were made using a JEOL JEM 1011 (JEOL, Inc., Peabody, MA, USA) system at 80 kV. The morphologies of bacteria cells on membrane were also investigated using a FEI Teneo (FEI Co., Hillsboro, OR), a Field Emission Scanning Electron Microscope (FESEM), with an accelerating voltage at 5 kV.

RESULTS AND DISCUSSION

Characterization of Magnéli phase Ti_4O_7 membrane

The chemical composition of electrode material was assessed based on XRD spectra (**Figure S5.1-A**). The predominant phase of titanium suboxides in this electrode was Ti_4O_7, which exhibits the highest conductivity among all the phases, comparable to graphite (J. Smith et al., 1998). Thus, the high purity of Ti_4O_7 ensures superior electrochemical performance. The surface morphology of Ti_4O_7 ceramic membrane was shown in SEM image (**Figure 5.2-A**), suggesting interconnected pores of various diameters. The porous property of the electrode provides large surface area for ROS generation, and allows for size exclusion of contaminants and cells with different sizes. The results of mercury intrusion porosimetry indicated that the pores of a wide range of diameters co-exist in the Ti_4O_7 membrane (**Figure S5.1-B**). Macropores (> 50 nm) appear to dominate, favoring the permeability and mass transfer efficiency of the membrane. It was reported that macropores are beneficial in promoting the transfer of chemicals towards the electrode surface for reaction (Kong et al., 2002). Also, high percentage of macropores in Ti_4O_7 membrane contributes to high water flux (12895 LMH Bar^{-1}) rate (**Figure** 5.**2-B)**, about five times

higher than the general ultra filtration membranes used for drinking water filtration (Leiknes, Ødegaard, & Myklebust, 2004). Water permeability of a membrane material is directly related to its applicability in water treatment applications, and therefore the macroporouse nature of the Ti_4O_7 membrane makes it promising for point-of-use water treatment.

Electrochemical stability is one factor determining the service life of an electrode. For example, metal oxide electrodes are usually subjected to different levels of passivation caused by accumulation or precipitation of non-conductive chemical species on electrode surface (Rajeshwar, Ibanez, & Swain, 1994). In this study, the excellent electrochemical stability of Ti_4O_7 was demonstrated using continuous cyclic voltammetry scanning, and the electrochemical performance remained unchanged after 200 cycles of scanning.

Electrochemical inactivation of *E coli*

An REM system (**Figure 5.1**) equipped with two Ti_4O_7 membrane electrodes was operated in dead-end filtration mode to investigate the electrochemical inactivation of *E coli* under various current densities. Before regular tests, a preliminary study was conducted to assess the viability of *E coli* in both 0.05 M Na_2SO_4 and 0.15 M (0.9% w/w) NaCl solutions, which offers ionization strengths similar to natural fresh water (McCleskey, Nordstrom, & Ryan, 2011), and the cell concentration was found to be stable within 3.5 hrs of incubation (**Figure S5.3**). Therefore, saline water (0.9% w/w NaCl) was utilized as the diluent in plate counting procedure to maintain cell integrity and viability. To avoid the effects of reactive chlorine species, 0.05 M Na_2SO_4 was used as background electrolyte for all the experiments. Na_2SO_4 is in aquatic systems and inert during EC processes under our test conditions.

The change in cell concentrations in the effluent samples during 30 min of REM treatment at current densities ranging from 0–10 mA/cm^{-2} was monitored (**Figure 5.3**). As shown, the

concentrations of *E coli* were reduced by more than 2, 3, 5, and 6 log units when the filtration system reached steady state after 5 min at the current densities of 0, 1, 5, and 10 mA/cm^{-2}, respectively. When no electric power was applied to the device (0 mA/cm^{-2}), *E coli* cells were removed solely by physical separation through membrane sieving. The predominant pores in Ti_4O_7 ceramic membrane have diameters between 1 to 10 μm (**Figure S5.1-C**), thus some of them are capable of capturing *E coli* cells with a typical size of 0.5 μm in width and 2 μm in length. Similarly, 1 log *E coli* removal was observed in the permeate solution from a cross-flow filtration system with a tubular Ti_4O_7 electrode, presumably through bacteria adsorption and size exclusion (L. Guo, Ding, et al., 2016). Although the average pore size of the tubular electrode material in the earlier study was 1.7 μm, smaller than the average pore size (2.6 μm) of the Ti_4O_7 membrane electrodes in this study, the sieving effect was not as good as the 2-log reduction observed in this study. This might be due to the transmembrane pressure placed on bacteria cells during cross-flow filtration, which might force the cells to pass through membrane. Moreover, the interconnected pores of various diameters (**Figure 5.2-A**) led to greater tortuosity of the membranes in this study, and thus enhanced filtration efficiency. Increasing current density from 0 to 1 mA/cm^{-2} only enhanced the inactivation of bacteria by less than 1 log unit, which was most likely contributed by the electrostatic adsorption between the negatively charged bacteria and the anode surface with an opposite charge.

The pathogen inactivation effect was significantly enhanced when the current density was raised to 5 mA/cm^{-2} and 10 mA/cm^{-2}. As observed in previous studies, increase in applied current/potential was associated with greater pathogen inactivation efficiency in electrochemical disinfection systems regardless of the electrode types (L. Guo, Ding, et al., 2016; Pillet et al., 2016; Rahaman et al., 2012; Raut et al., 2014; Schmalz, Dittmar, Haaken, & Worch, 2009; C. D. Vecitis

et al., 2011). Increased charge on the positively charged anode surface would facilitate sorption of cells on the porous membrane, and it would also result in more efficient production of reactive oxygen species (ROS), including hydroxyl radicals. To verify this assumption, a three-electrode-system was employed to study the relationship between the anode potential and the applied cell voltage (**Figure S5.4**). The results indicated that when applied cell voltage was above 7 V, the anode potential became higher than the oxygen evolution potential (2.3 V) determined by linear voltammetry scanning (**Figure S5.2-A**). As known, strong oxidant hydroxyl radical (OH•) is mainly produced along with oxygen generation during water oxidation on non-active electrodes, such as Magnéli phase Ti_4O_7 electrode (Enache, Chiorcea-Paquim, Fatibello-Filho, & Oliveira-Brett, 2009; Marselli et al., 2003). As shown in **Table 5.1**, the cell voltages applied to the REM system for disinfection experiments were 6.4 V, 7.6 V and 9.5 V at current density of 1 mA/cm^{-2}, 5 mA/cm^{-2} and 10 mA/cm^{-2} respectively. According to **Figure S5.4**, these cell voltages would correspond to the potentials around 2.15 V, 2.52 V, and 3.43 V, respectively on the anode among which the latter conditions (5 mA/cm^{-2} and 10 mA/cm^{-2}) were way above the oxygen evolution potential, and thus would effectively generate hydroxyl radicals and other ROS but not for the first condition (1 mA/cm^{-2}). Although hydroxyl radical is the most powerful that can be disinfectant electrochemically generated, non-active anode can also produce weaker ROS, such as H_2O_2, O_3, and •O (Sultana, Babauta, & Beyenal, 2015). For example, generation of a significant amount of H_2O_2 during electrooxidation (EO) treatment of aqueous samples using a mixed metal oxide (MMO) anode was believed to be the primary cause of the inactivation of *E coli*. (Cui et al., 2013). All those ROS species are helpful for pathogen inactivation because of their ability to alter membrane permeability and cause cell rupture.

No significant variation in pH (~6.5) was observed in effluent samples collected during the REM treatment at various conditions (data not shown). This indicated that, in this undivided electrolytic reactor setup, the hydrogen ion formed on the anode from water hydrolysis was counterbalanced by the hydroxyl ion produced on cathode. Thus, change in acidity or alkalinity, observed in the earlier study with an divided electrolytic cell setup (L. Guo, Ding, et al., 2016), was unlikely a factor responsible for inactivation of bacteria in this study. It is worth noting that earlier studies have shown that *E coli* cells did not undergo any kind of inactivation within 60 minutes at acidified conditions (pH ~ 3) (Bruguera-Casamada et al., 2016; Geveke & Kozempel, 2003). Indeed, *E coli* can tolerate a rather wide range of pH 3.7 ~ 8.0 (Presser, Ratkowsky, & Ross, 1997).

The pressure of the peristatic pump for solution delivery during the course of REM treatment was monitored, and the result was shown in **Figure S5.5**. As indicated, the initial pressures for the treatments at 5 mA/cm^{-2} and 10 mA/cm^{-2} are higher than those at 0 mA/cm^{-2} and 1 mA/cm^{-2}, and reached plateau much faster. This is probably due to the gas generation on the electrodes at high current densities as mentioned above. The trend of the increasing pressure at 0 mA/cm^{-2} over time indicates the accumulation of bacteria mass on the membranes. It is therefore critical to investigate the quantity and viability of cells on membrane to evaluate the efficiency of the REM system to inactivate *E coli*. The membrane electrodes were extracted in 10 mL 0.9% NaCl for one hour to remove the bacteria after each operation, and the concentration of *E coli* in extract were determined (**Figure S5.6**). In general, the concentrations of the viable cells in the extracts lower at greater as the applied current density increased, although those of 1 and 5 mA/cm^{-2} treatment were similar. In **Table 5.1**, we listed the total number of live cells detected on membrane as well as in effluent, and they were expressed as percentage comparing to the number

of cells delivered to the filtration device within the total 30 minutes of test. The total inactivation rates were thus calculated as 99.640%, 99.895%, 99.981%, and 99.998% for 0, 1, 5, and 10 mA/cm^{-2} treatment, respectively. The mechanisms that may have caused such significant disinfection effect had been explored and elucidated below.

For a comparison, the electrochemical inactivation of *E coli* was also evaluated in a batch reactor setup using the same Ti_4O_7 ceramic electrodes used in the REM study. To this end, the two electrodes were placed in parallel at 5-mm distance (as in the REM unit) in 150 mL of 0.05 M Na_2SO_4 solution spiked with *E coli* for 30 minutes, and was supplied with same series of current densities applied in the REM study. No apparent reduction in cell density was found in the batch reactor at zero current density (**Figure 5.4**), unlike the REM treatment, where the cell concentration was reduced by more than 2 log comparing to original solution. This result suggested that the physical adsorption of *E coli* cells on the electrode was negligible, and that they were held on the membrane electrodes primarily by the sieving effect during filtration in REM treatment. No significant bacteria inactivation was found at 1 mA/cm^{-2} in the batch reactor either, which indicated that the transmembrane potential formed under this condition was not strong enough to cause lethal damage to the cells. Increasing current density to 5 and 10 mA/cm^{-2} resulted in significant inactivation of *E coli* at 1.4 and 2.1 log reduction, respectively, but much lower than the log reduction (3.4 log and 4.5 log) achieved in REM treatment at the same current density. The greater disinfection effect in the REM process in comparison to the batch reactor operation may result from the convection-facilitated mass transfer during filtration in REM (C. D. Vecitis et al., 2011; Zaky & Chaplin, 2014), where the cells were forced passing through the interconnected pores in the electrodes, thus increasing the chance of getting in contact with ROS generated also on the electrode surface. In addition, the portion of bacteria retained on membrane due to sieving effect

was exposed to electric field for a longer time, and the longer exposure time to external electric field would cause more severe and lethal damages to the cells (C. D. Vecitis et al., 2011; Zeng et al., 2010). Such significant bacteria inactivation, in particular at 10 mA/cm^{-2} current density, was probably achieved by the synergetic actions of physical filtration, reactive oxygen species, transmembrane potential and electroporation. Related information will be discussed in more detail below.

Possible disinfection mechanisms during REM treatment

During the REM treatment experiments, the protein concentration in the effluent was monitored as an indicator of membrane permeability alteration to assess protein leakage. As shown in **Figure 5.5**, the protein level remained stable at zero-current control. Interestingly, increasing current density to 1 mA/cm^{-2} led to significantly higher concentration of protein in the effluent solutions, while the bacteria inactivation effect was not so pronounced. This suggests that the electric fields applied at relatively low voltages might temporarily injure the bacteria cells, causing intracellular protein leakage, but not necessarily kill them (Huo et al., 2016). Those injured but viable cells were still able to grow on culture media and potentially recover from the nonfatal damage (A. R. Smith et al., 2013). As for the treatments at 5 and 10 mA/cm^{-2}, the protein concentrations increased rapidly within the initial ten minutes, and then became stabilized. The increase in protein concentration was likely due to the increasing numbers of cell retained and subsequently inactivated on the membrane after being exposed to electric potential and ROS for a longer period of time. This was also evidenced by the similar pattern in pressure change (**Figure S5.5**) predominately caused by bacterial mass accumulation on the membrane.

Flow cytometry was employed in this study to assess the viability of cells during REM treatment in an attempt to assist in disinfection mechanism interpretation. Flow cytometry

measures the light scattering of a laser beam by stained cells, which is dependent on the viability of the cells. When the measurement results of control samples prepared with live or dead cells were plotted according to their fluorescence features, two regions (also called gates) were defined, which can serve as the frame of reference to differentiate the viable cells from inactivated ones. **Figure 5.6 s**hows the flow cytometry results of the effluent samples collected during different treatments, indicating the compositions of live and dead cells in each solution. Comparing to the live cell control, the percentage of dead cells increased dramatically at 1 mA/cm^{-2} current density treatment, and it further increased when the current density raised to 5 mA/cm^{-2}. This trend agreed well with the conclusion reached by the plate counting that the higher current density caused more severe damage and death to the cells. However, it is important to note that, for both 1 and 5 mA/cm^{-2} treatment, the percentage of "live" cells identified by flow cytometer was much higher than the results determined using the plate counting method as shown in **Figure 5.2**. This difference was most likely because some cells are viable but not culturable (VBNC), i.e., they were detectable by flow cytometry as they still maintain the cell integrity, but have lost their ability to grow into a visible colony on agar plates due to serious injury. Apart from serious injury, pathogens may also enter into the VBNC state as a survival strategy when exposed to extreme conditions (Ding et al., 2017; Fakruddin, Mannan, & Andrews, 2013). Those VBNC pathogens can bring potential health risk once they recover with reproducibility. Therefore, it is critical to differentiate VBNC cells from dead cells, while conducting disinfection study and evaluating disinfection efficiency. As implemented in this study, coupling flow cytometry and differential staining technique with direct microscopic enumeration can be an effective tool for the detection of VBNC cells (L. Li, Mendis, Trigui, Oliver, & Faucher, 2014).

Surprisingly, the density of cells (represented by dots in Figure 6) were much lower in 10 mA/cm^{-2} treatment than the other treatments, indicating that the treated effluent contained much less stainable cells. Bacterial cells only become non-detectable by flow cytometry when the membrane structure was completely altered or the whole cell was broken down into small species or debris (Tung et al., 2007). Therefore, it is possible that the high current density and high voltage might be vital to ensure complete destruction of bacteria cells and eliminate the possibility of pathogen recovery and disease spreading. The result of flow cytometry not only confirmed the increasing disinfection efficiency with higher current densities, but also offered more information on the viability of cells resulting from REM treatment.

TEM was performed to investigate the *E coli* cells in the effluents to provide information on the cell morphology before and after REM treatments (**Figure 5.7**). For the zero-current control, the cells remained in their original rod shape with smooth membrane and intact cytoplasm (**Figure 5.7A**). Some changes in cell morphology occurred when voltage was added to the electrolytic cell: for 1 mA/cm^{-2} treatment (**Figure 5.7B**), cell membrane became rougher; in 5 mA/cm^{-2} sample, some cells showed signs of cytoplasm leakage, although the cell membrane remained intact (**Figure 5.7C**); when the applied current density was increased to 10 mA/cm^{-2}, cell membrane started to undergo dissociation and break into pieces (**Figure 5.7D**). It was obvious that higher current density caused more severe damages to the cells, leading to alteration of cell shape, leakage of cytoplasm, and, more seriously, membrane dissociation. The mechanisms of cell inactivation by reactive oxidative species (ROSs) have been described previously (Caselli et al., 1998; Cho, Kim, Kim, Yoon, & Kim, 2010; Nimse & Pal, 2015), including ROSs diffuse toward the outer layer of cell and penetrate through membrane, reach and subsequently react with cytoplasmic proteins and unsaturated lipids. As a result, affected cells may undergo lysis, and release

cytoplasmic components into the surrounding environment, causing elevated protein concentration in solution. Meanwhile, ROSs can infiltrate through the membrane with altered permeability, and bond to the enzymes and DNA molecules (Hunt & Mariñas, 1999).

The results of SEM characterization of the treatment samples were highly consistent with the observations made with the TEM images, showing cell shrinkage at moderate electrical strength (1 and 5 mA/cm^{-2}) (**Figure S5.7-B and S5.7-C**) while cells remaining intact at zero current control (**Figure S5.7-A**). At 10 mA/cm^{-2} treatment, cell membrane appeared to be rough with visible damages on the surface (**Figure S5.7-D**). Another possible mechanism of electrochemical pathogen inactivation is electroporation or electro-permeabilization reported in several previous studies (Wen et al. 2017, Huo et al. 2016, Liu et al. 2014, Liu et al. 2013). Although electroporation was considered effective in inactivating bacteria in seconds, it is unlikely a significant contributor in the present study where low electric field strength (<10V) was applied, since electroporation is usually associated high-voltage discharge (thousands of volts) that could be generated through point discharge on nano-scale materials. It has been reported that irreversible pores formed in cell membranes when resulting transmembrane potential is between 0.2 and 1V, for which the external electric fields were in the kV cm^{-1} range (Garcia, Ge, Moran, & Buie, 2016; Machado, Pereira, Martins, Teixeira, & Vicente, 2010). It is shown in results of SEM characterization (**Figure S5.7**) that no pores were evident on the cell membranes, suggesting the minimal effects of electroporation.

Another important observation was that large clusters of cell debris were found when examining the 5 mA/cm^{-2} and 10 mA/cm^{-2} samples under SEM at lower magnifications (**Figure 5.7E and 5.7F**). This result again suggested substantial intracellular material leakage out of the cells after electrolysis at high current densities, and afterwards those cellular components bond

together and formed aggregates of cell debris. Similar results were previously reported by Bruguera-Casamada et al. (2016), who observed cell debris clusters in all the test strains (*Escherichia coli*, *Pseudomonas aeruginosa*, *Bacillus atrophaeus*, *Staphylococcus aureus*, and *Enterococcus hirae*) upon electrochemical disinfection treatment at a current density of 33.3 mA/cm^{-2} in a batch reactor setup with BDD anode in 7 mM Na_2SO_4 solution.

CONCLUSIONS

Electrochemical treatment process is effective in inactivating *E Coli* bacteria, reaching > 5 log removal in solution at 10 mA/cm^{-2} applied current density. Comparing to batch reactor, the filtration operation significantly enhanced the treatment efficiency to 3 orders of magnitude. This design is beneficial because by passing the solution through the interconnected pores in a 3D electrode, the mass transfer of bacteria towards electrode surface was largely promoted, leading to better contact between cells and oxidizing agents generated on electrode. For future study, such a ceramic electrode can be modified into a tubular reactor with greater water flux to achieve higher efficiency.

Flow cytometry, TEM and SEM served as powerful tools to help understand the dominant disinfection mechanisms involved. It is important to differentiate VBNC bacteria from live and dead bacteria because the results of plate culture can be biased. In this study, VBNC bacteria is still detectable by flow cytometry in the effluent samples under highest current density, while no colony was observed through direct plating. The dramatically increased disinfection efficiency observed when anode potential was above oxygen evolution potential suggested the significant role of oxidizing agents generated at along with water hydrolysis. Moreover, the positive correlation between inactivation rate and current density/anode potential also indicated the contribution of electric field. Several drawbacks of the system need to be addressed in the

subsequent research, such as the accumulation of membrane pressure and viable cells retained on the membrane by physical separation. Extending the retention time of cells on electrode and periodical back wash after certain time of operation to clean the electrode will be worth trying to solve the issues.

SUPPORTING INFORMATION AVAILABLE

Results of XRD, SEM, mercury intrusion analysis, and transmembrane pressure test of electrode; linear scan voltammetry plots; viability of *E Coli* in electrolyte; the relationship between cell voltage and anode potential; membrane pressure; the number of bacteria extracted from electrodes; SEM images of effluent samples.

ACKNOWLEDGEMENTS

The study was supported in part by U.S. Department of Defense SERDP ER 2717. We thank the Georgia Electron Microscopy facility at the University of Georgia for performing the TEM and SEM analysis for our samples.

LITERATURE CITED

Ai, S., Wang, Q., Li, H., & Jin, L. (2005). Study on production of free hydroxyl radical and its reaction with salicylic acid at lead dioxide electrode. *Journal of Electroanalytical Chemistry, 578*(2), 223-229.

Alfaro, M. A. Q., Ferro, S., Martínez-Huitle, C. A., & Vong, Y. M. (2006). Boron doped diamond electrode for the wastewater treatment. *Journal of the Brazilian Chemical Society, 17*(2), 227-236.

Balouiri, M., Sadiki, M., & Ibnsouda, S. K. (2016). Methods for in vitro evaluating antimicrobial activity: A review. *Journal of Pharmaceutical Analysis, 6*(2), 71-79.

Barhoumi, N., Labiadh, L., Oturan, M. A., Oturan, N., Gadri, A., Ammar, S., & Brillas, E. (2015). Electrochemical mineralization of the antibiotic levofloxacin by electro-Fenton-pyrite process. *Chemosphere, 141*, 250-257.

Bejan, D., Guinea, E., & Bunce, N. J. (2012). On the nature of the hydroxyl radicals produced at boron-doped diamond and Ebonex® anodes. *Electrochimica Acta, 69*, 275-281.

Bowden, M., White, G., Brown, I., Ryan, M., & Gainsford, G. (1996). Improved powder diffraction patterns for the titanium suboxides Ti n O 2n− 1 (4≤ n≤ 9). *Powder Diffraction, 11*(01), 60-68.

Brodersen, D. E., Clemons, W. M., Carter, A. P., Morgan-Warren, R. J., Wimberly, B. T., & Ramakrishnan, V. (2000). The structural basis for the action of the antibiotics tetracycline, pactamycin, and hygromycin B on the 30S ribosomal subunit. *Cell, 103*(7), 1143-1154.

Chaplin, B. P. (2014). Critical review of electrochemical advanced oxidation processes for water treatment applications. *Environmental Science: Processes & Impacts, 16*(6), 1182-1203.

Chen, G., Betterton, E., & Arnold, R. (1999). Electrolytic oxidation of trichloroethylene using a

ceramic anode. *Journal of Applied Electrochemistry, 29*(8), 961-970.

Clarke, R., & Harnsberger, S. (1988). New electrically conductive ceramic--a fundamental advance in electrode technology. *American Laboratory, 20*(6), 8.

Dalmázio, I., Almeida, M. O., Augusti, R., & Alves, T. M. (2007). Monitoring the degradation of tetracycline by ozone in aqueous medium via atmospheric pressure ionization mass spectrometry. *Journal of the American Society for Mass Spectrometry, 18*(4), 679-687.

Ferreira, M., Varela, H., Torresi, R. M., & Tremiliosi-Filho, G. (2006). Electrode passivation caused by polymerization of different phenolic compounds. *Electrochimica Acta, 52*(2), 434-442.

Graves, J., Pletcher, D., Clarke, R., & Walsh, F. (1991). The electrochemistry of Magnéli phase titanium oxide ceramic electrodes Part I. The deposition and properties of metal coatings. *Journal of Applied Electrochemistry, 21*(10), 848-857.

Gruber, M., Wiesner, G., Burger, R., & Lindner, R. (2006). The salicylate trapping method: Is oxidation of salicylic acid solution oxygen and time dependent and metal catalysed? *Journal of Chromatography B, 831*(1), 320-323.

Guinea, E., Arias, C., Cabot, P. L., Garrido, J. A., Rodríguez, R. M., Centellas, F., & Brillas, E. (2008). Mineralization of salicylic acid in acidic aqueous medium by electrochemical advanced oxidation processes using platinum and boron-doped diamond as anode and cathodically generated hydrogen peroxide. *Water Research, 42*(1), 499-511.

Guo, L., Jing, Y., & Chaplin, B. P. (2016). Development and characterization of ultrafiltration TiO2 Magnéli phase reactive electrochemical membranes. *Environmental Science and Technology, 50*(3), 1428-1436.

Halling-Sørensen, B., Sengeløv, G., & Tjørnelund, J. (2002). Toxicity of tetracyclines and

tetracycline degradation products to environmentally relevant bacteria, including selected tetracycline-resistant bacteria. *Archives of Environmental Contamination and Toxicology, 42*(3), 263-271.

Janssen, L., & Koene, L. (2002). The role of electrochemistry and electrochemical technology in environmental protection. *Chemical Engineering Journal (Lausanne), 85*(2), 137-146.

Janzen, E. G., Radicals, S. F., & Traps, D. (2012). A critical review of spin trapping. *Free radicals in biology, 4*, 116-154.

Jen, J.-F., Leu, M.-F., & Yang, T. C. (1998). Determination of hydroxyl radicals in an advanced oxidation process with salicylic acid trapping and liquid chromatography. *Journal of Chromatography A, 796*(2), 283-288.

Jiao, S., Zheng, S., Yin, D., Wang, L., & Chen, L. (2008). Aqueous photolysis of tetracycline and toxicity of photolytic products to luminescent bacteria. *Chemosphere, 73*(3), 377-382.

Kapałka, A., Fóti, G., & Comninellis, C. (2008). Kinetic modelling of the electrochemical mineralization of organic pollutants for wastewater treatment. *Journal of Applied Electrochemistry, 38*(1), 7-16.

Kapałka, A., Fóti, G., & Comninellis, C. (2009). The importance of electrode material in environmental electrochemistry: formation and reactivity of free hydroxyl radicals on boron-doped diamond electrodes. *Electrochimica Acta, 54*(7), 2018-2023.

Khan, M. H., Bae, H., & Jung, J.-Y. (2010). Tetracycline degradation by ozonation in the aqueous phase: proposed degradation intermediates and pathway. *Journal of Hazardous Materials, 181*(1), 659-665.

Kong, C. S., Kim, D.-Y., Lee, H.-K., Shul, Y.-G., & Lee, T.-H. (2002). Influence of pore-size distribution of diffusion layer on mass-transport problems of proton exchange membrane

fuel cells. *Journal of Power Sources, 108*(1), 185-191.

Li, C. W., Ciston, J., & Kanan, M. W. (2014). Electroreduction of carbon monoxide to liquid fuel on oxide-derived nanocrystalline copper. *Nature, 508*(7497), 504-507.

Lin, H., Niu, J., Xu, J., Huang, H., Li, D., Yue, Z., & Feng, C. (2013). Highly efficient and mild electrochemical mineralization of long-chain perfluorocarboxylic acids (C9–C10) by Ti/SnO2–Sb–Ce, Ti/SnO2–Sb/Ce–PbO2, and Ti/BDD electrodes. *Environmental Science and Technology, 47*(22), 13039-13046.

Marselli, B., Garcia-Gomez, J., Michaud, P.-A., Rodrigo, M., & Comninellis, C. (2003). Electrogeneration of hydroxyl radicals on boron-doped diamond electrodes. *Journal of the Electrochemical Society, 150*(3), D79-D83.

Martínez-Huitle, C. A., & Andrade, L. S. (2011). Electrocatalysis in wastewater treatment: recent mechanism advances. *Quimica Nova, 34*(5), 850-858.

McLafferty, F. W., & Tureček, F. (1993). *Interpretation of mass spectra*: University science books.

Miller-Folk, R. R., Noftle, R. E., & Pletcher, D. (1989). Electron transfer reactions at Ebonex ceramic electrodes. *Journal of electroanalytical chemistry and interfacial electrochemistry, 274*(1-2), 257-261.

Nanayakkara, K. N., Zheng, Y.-M., Alam, A. K., Zou, S., & Chen, J. P. (2011). Electrochemical disinfection for ballast water management: technology development and risk assessment. *Marine Pollution Bulletin, 63*(5), 119-123.

Niu, J., Lin, H., Xu, J., Wu, H., & Li, Y. (2012). Electrochemical mineralization of perfluorocarboxylic acids (PFCAs) by Ce-doped modified porous nanocrystalline PbO2 film electrode. *Environmental Science and Technology, 46*(18), 10191-10198.

Peralta, E., Roa, G., Hernandez-Servin, J., Romero, R., Balderas, P., & Natividad, R. (2014).

Hydroxyl radicals quantification by UV spectrophotometry. *Electrochimica Acta, 129*, 137-141.

Radjenovic, J., & Sedlak, D. L. (2015). Challenges and opportunities for electrochemical processes as next-generation technologies for the treatment of contaminated water. *Environmental Science and Technology, 49*(19), 11292-11302.

Raut, A. S., Cunningham, G. B., Parker, C. B., Klem, E. J., Stoner, B. R., Deshusses, M. A., & Glass, J. T. (2014). Disinfection of E. coli contaminated urine using boron-doped diamond electrodes. *Journal of the Electrochemical Society, 161*(12), G81-G85.

Smith, J., Walsh, F., & Clarke, R. (1998). Electrodes based on Magnéli phase titanium oxides: the properties and applications of Ebonex® materials. *Journal of Applied Electrochemistry, 28*(10), 1021-1033.

Tomita, M., Okuyama, T., Watanabe, S., & Watanabe, H. (1994). Quantitation of the hydroxyl radical adducts of salicylic acid by micellar electrokinetic capillary chromatography: oxidizing species formed by a Fenton reaction. *Archives of Toxicology, 68*(7), 428.

Tsolaki, E., Pitta, P., & Diamadopoulos, E. (2010). Electrochemical disinfection of simulated ballast water using Artemia salina as indicator. *Chemical Engineering Journal (Lausanne), 156*(2), 305-312.

Walsh, F., & Wills, R. (2010). The continuing development of Magnéli phase titanium sub-oxides and Ebonex® electrodes. *Electrochimica Acta, 55*(22), 6342-6351.

Wang, Y., Zhang, H., Zhang, J., Lu, C., Huang, Q., Wu, J., & Liu, F. (2011). Degradation of tetracycline in aqueous media by ozonation in an internal loop-lift reactor. *Journal of Hazardous Materials, 192*(1), 35-43.

Wollenberger, L., Halling-Sørensen, B., & Kusk, K. O. (2000). Acute and chronic toxicity of

veterinary antibiotics to Daphnia magna. *Chemosphere, 40*(7), 723-730.

Wu, D., Liu, M., Dong, D., & Zhou, X. (2007). Effects of some factors during electrochemical degradation of phenol by hydroxyl radicals. *Microchemical Journal, 85*(2), 250-256.

Wu, W., Huang, Z.-H., & Lim, T.-T. (2016). A comparative study on electrochemical oxidation of bisphenol A by boron-doped diamond anode and modified SnO2-Sb anodes: Influencing parameters and reaction pathways. *Journal of Environmental Chemical Engineering, 4*(3), 2807-2815. doi: http://dx.doi.org/10.1016/j.jece.2016.05.034

Xu, L., & Scantlebury, J. (2003). Electrochemical Surface Characterization of IrO2 Ta2 O 5 Coated Titanium Electrodes in Na2 SO 4 Solution. *Journal of the Electrochemical Society, 150*(6), B288-B293.

Yang, W., Tang, Z., Zhou, F., Zhang, W., & Song, L. (2013). Toxicity studies of tetracycline on Microcystis aeruginosa and Selenastrum capricornutum. *Environmental Toxicology and Pharmacology, 35*(2), 320-324.

Zaky, A. M., & Chaplin, B. P. (2013). Porous substoichiometric TiO2 anodes as reactive electrochemical membranes for water treatment. *Environmental Science and Technology, 47*(12), 6554-6563.

Zaky, A. M., & Chaplin, B. P. (2014). Mechanism of p-substituted phenol oxidation at a Ti4O7 reactive electrochemical membrane. *Environmental Science and Technology, 48*(10), 5857-5867.

Zhu, L., Santiago-Schübel, B., Xiao, H., Hollert, H., & Kueppers, S. (2016). Electrochemical oxidation of fluoroquinolone antibiotics: Mechanism, residual antibacterial activity and toxicity change. *Water Research*.

Table 5.1. Summary of current density, applied voltage, live cells in effluent, live cells retained on membrane, and total inactivation rate.

Current density (mA/cm^2)	Applied voltage (V)	Live cells in effluent (%)	Live cells on membrane (%)	Total inactivation rate (%)	Total log reduction	Energy consumption (kWh/m^3)
0	0.0	0.303	0.057	99.640	2.43	0.00
1	6.4	0.096	0.010	99.895	2.98	0.21
5	7.6	0.001	0.018	99.981	3.72	1.26
10	9.5	0.000	0.000	99.998	4.69	3.18

Note: All percentage values were compared to the number of cells pumped into filtration system from feed tank during 30 minutes' treatment.

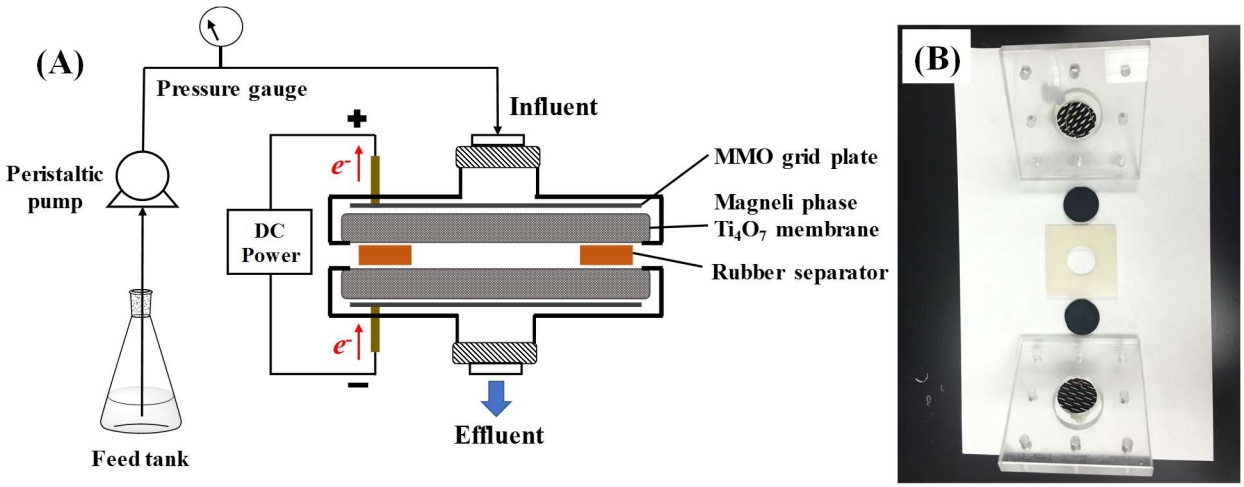

Figure 5.1. (A) Electrochemical Magnéli phase Ti_4O_7 ceramic membrane filtration system design and setup; (B) Picture of the real filtration device. The diameter of Magnéli phase Ti_4O_7 ceramic membrane disk electrodes is 3 cm.

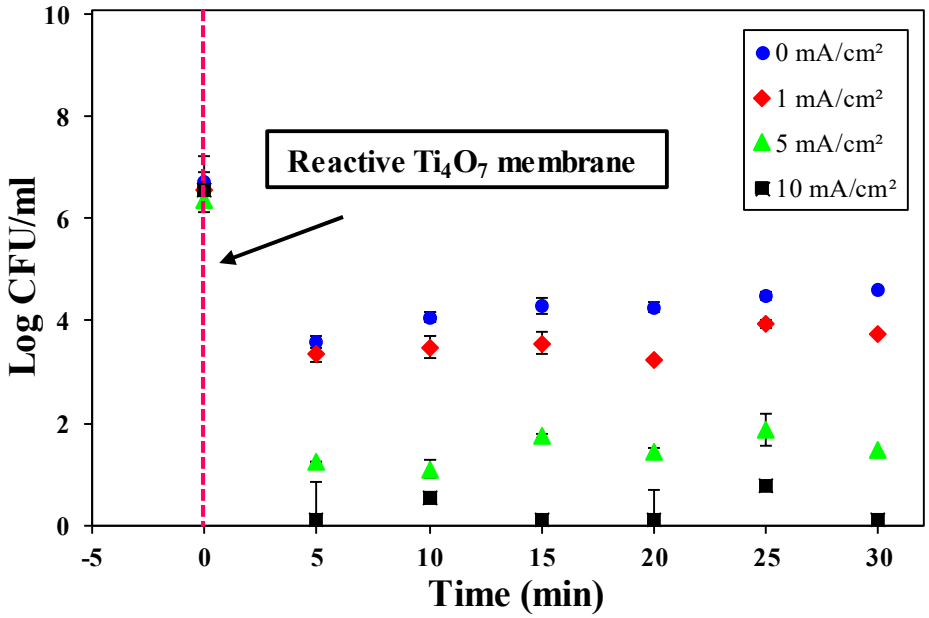

Figure 5.2. Inactivation kinetics of *E coli* using Magnéli phase Ti_4O_7 membrane filtration system in dependence on the current densities.

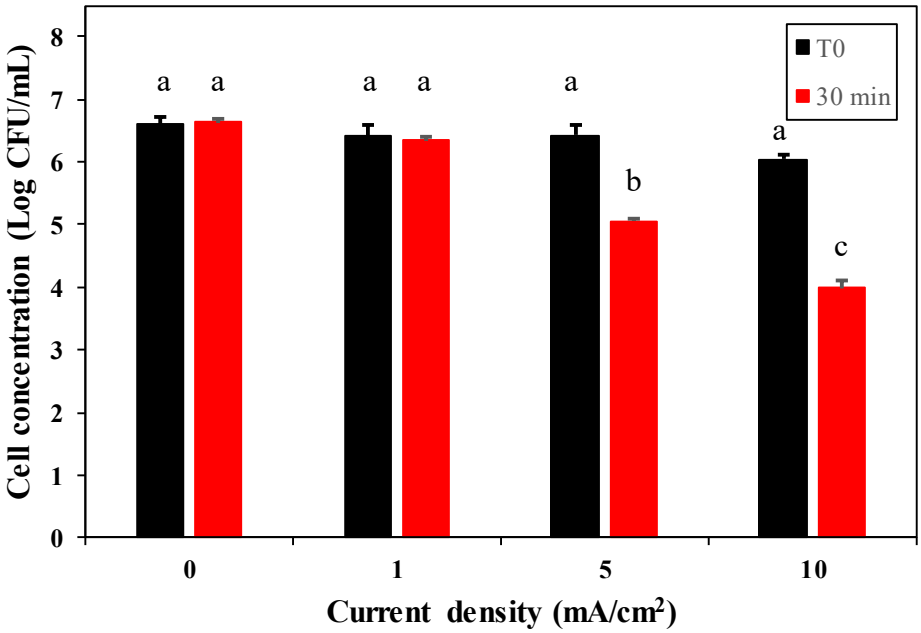

Figure 5.3. Inactivation kinetics of *E coli* using Magnéli phase Ti_4O_7 membrane in batch reactor. Means with different letters are significantly different ($p<0.05$).

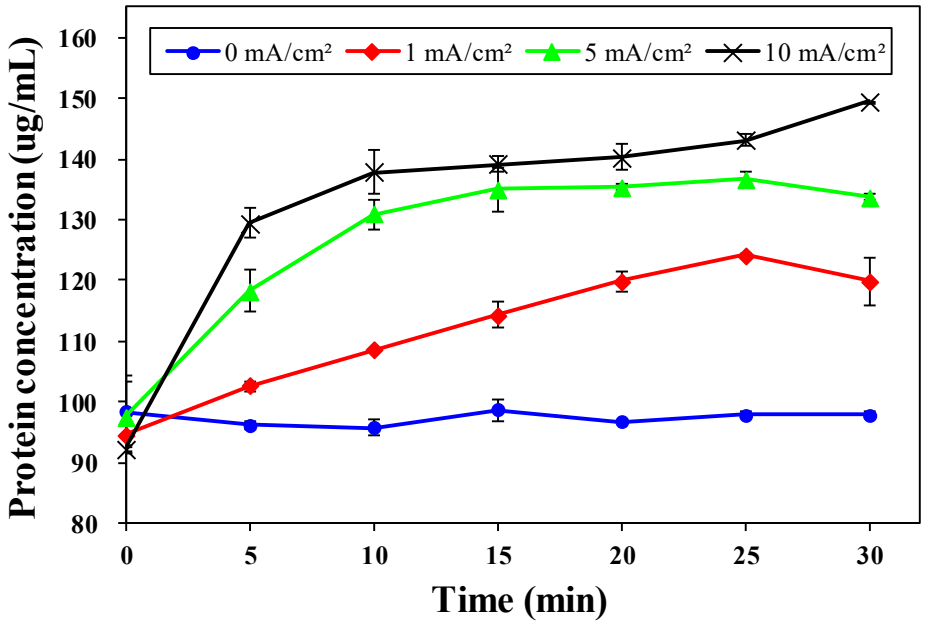

Figure 5.4. Leakage of proteins change with electrochemical disinfection treatments at different current densities.

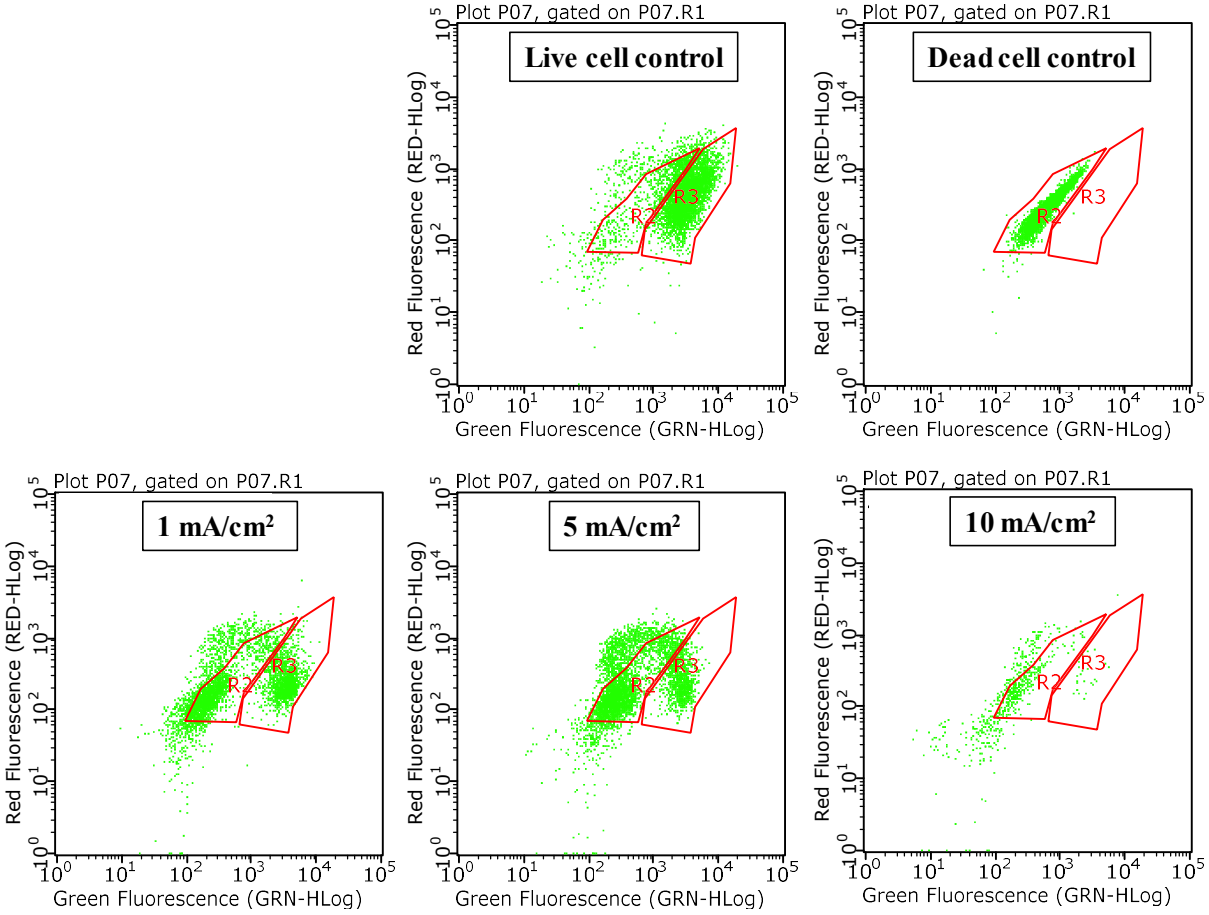

Figure 5.5. Flow cytometry analysis of effluent samples collected during electrochemical disinfection process.

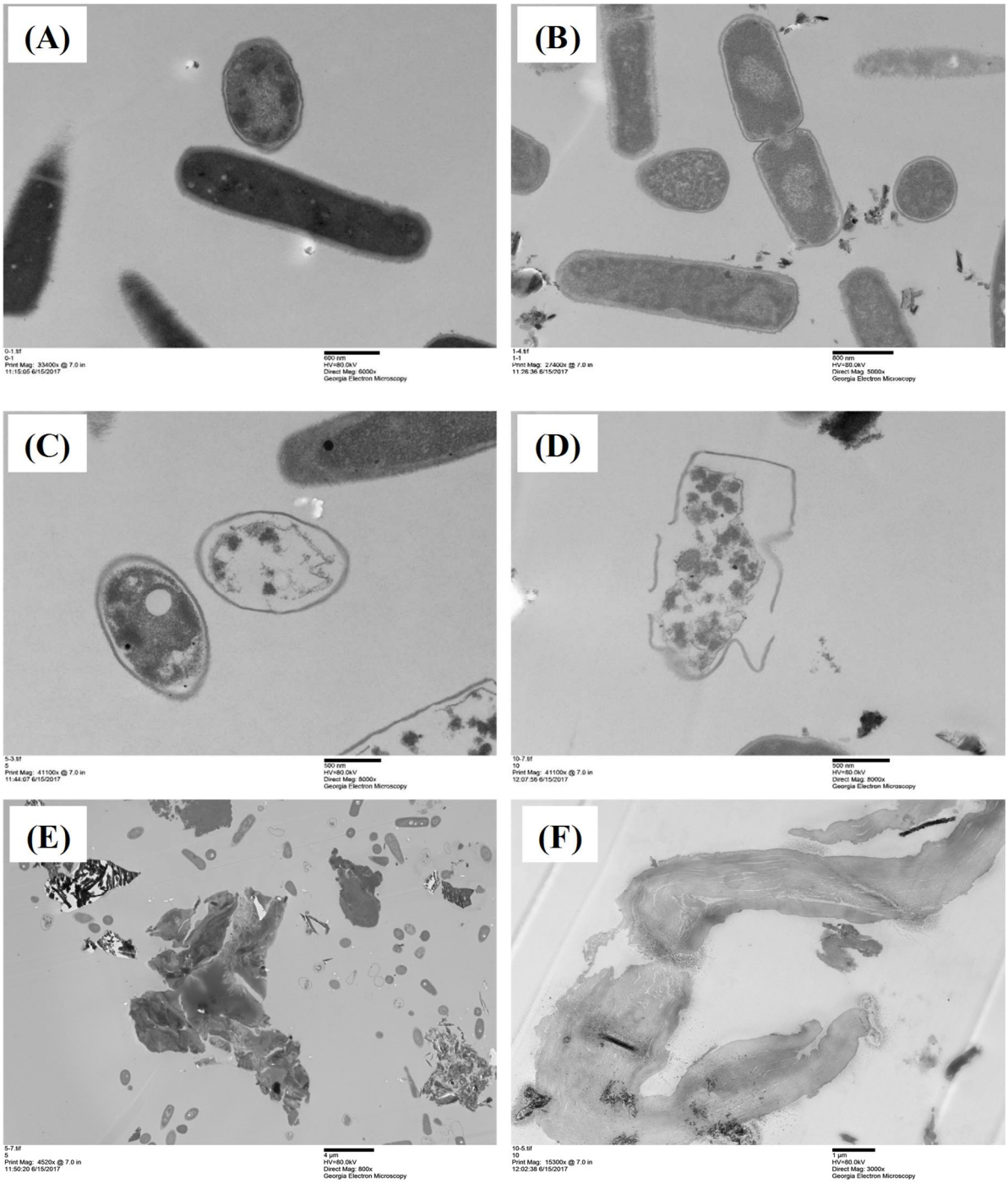

Figure 5.6. TEM images of effluent samples collected during electrochemical disinfection process. (A) No current control; (B) 1 mA/cm^2 applied current density; (C) 5 mA/cm^2 applied current density; (D) 10 mA/cm^2 applied current density; (E) Cell debris observed in 5 mA/cm^2 treatment sample; (E) Cell debris observed at 10 mA/cm^2 treatment sample.

CHAPTER 6

CONCLUSIONS

This dissertation is focused on research and development of innovative technologies to treat the emerging contaminants in the environment, depending on two types of catalytic oxidation processes, enzymatic oxidation reaction and electrochemical oxidation process. The enzymatic oxidation studied here, ECOHR, is a mild, environmentally benign and energy effective process, which is derived from a natural humification reaction, and can be applied for *in situ* remediation, while electrochemical oxidation process based on Ti_4O_7 anode exhibits high efficiency with some energy input, and can be used for *ex situ* treatment of highly concentrated waste liquids.

The study described in Chapter 2 explored the water extract of a natural organic matter, soybean meal, to provide mediators that facilitated the laccase-catalyzed ECOHR leading to degradation of sulfadimethoxine. With the assistance of state-of-art high resolution mass spectrometry, three natural phenolic compounds were identified as the key mediators in soybean meal extract. Their mediating efficiency were further confirmed by individual degradation tests. This finding is important because it provides fundamental knowledge to guide possible use of ECOHRs in remediation practices with soybean meal or other similar natural materials included in amendments to provide mediators.

The study of Chapter 3 deals with extremely persistent contaminants of emerging concern, perfluorinated compounds, which have been widely detected in groundwater, especially in military sites. Although adsorption on GAC is the predominant technology used in full-scale

remediation project, and has been proven successful in multiple sites, the requirement of frequent change-out has always been a concern. This research aimed to solve this problem by coupling GAC with destructive enzymatic oxidation process. The experiments in this study have used real groundwater from contaminated sites and the granular activated carbon from a commercial supplier with numerous successful *in situ* applications. In batch reactor, PFOA reached 30% removal after 60 days of incubation even for treatments without metal ion additions. The same trends were observed in micro-column study, where the concentration of PFOA in effluent was only 60% of the influent for GAC+enzyme treatment, while PFOA reached complete breakthrough in the control column. However, the effect was insignificant when groundwater was used in the test, which was most likely because of the extremely low concentration of PFOA and PFOS in groundwater.

The efficiency of electrochemical oxidation in degrading emerging contaminates was also investigated using a novel electrode material Magneli phase Ti_4O_7. This novel ceramic electrode exhibits high conductivity, stability in extreme chemical conditions and high oxygen evolution potential. During electrochemical oxidation in batch reactor, more than 95% removal of tetracycline concentration was achieved within 6 hrs with the antibiotic effect of the solution completely eliminated at the end of the treatment. Several oxidation products of tetracycline were identified based on the data of high resolution mass spectrometry. EO was demonstrated as a powerful and cost-efficient treatment technology when Magneli phase Ti_4O_7 was used as anode.

Electrochemical inactivation of *E Coli* was tested using Magneli phase Ti_4O_7 as the anode in a reactive electrochemical membrane (REM) system operated in dead-end filtration mode. The system achieved 5-log removal of *E Coli* in solution, and the efficiency increased

with the increasing current densities. The bacteria activity was assessed using plate counting method, and more information was obtained from flow cytometry, SEM and TEM characterization. The additional information showed some cells may remain alive, even though they might have lost growing capability. Considering the possible pathogenic effect of live but non-culturable bacteria, it is recommended to evaluate a disinfection technology using more complete set of data instead of merely plate count results. In addition, our results suggested that flow through operation largely enhanced the EO reaction efficiency, but further improvement is needed to address pressure accumulation caused by membrane fouling.

Development of treatment technologies for emerging contaminants is a research field with increasing interests and focus. ECOHR is a process proven to degrade antibiotics and PFASs in our studies, and it is laccase-catalyzed process that can be enhanced by addition of natural mediators. Electrochemical oxidation appeared to be a technology applicable *ex situ* in various forms, which is also effective in inactivating pathogens, although it is more energy intensive. Enzymatic oxidation and electrochemical oxidation are both sustainable and non-selective destructive technologies that are worth exploring in future studies, and being tested in environmental remediation practices, which hold great promise to provide alternative tools in dealing with emerging contaminants.

APPENDIX A

SUPPORTING INFORMATION:

DEGRADATION OF SULFADIMETHOXINE CATALYZED BY LACCASE WITH SOYBEAN MEAL EXTRACT AS NATURAL MEDIATOR: MECHANISM AND REACTION PATHWAY

Figure S2.1. Degradation of sulfadimethoxine (SDM) in laccase-mediator systems at 25°C with multiple SBE additions. Reaction conditions were the same as Figure 1B. The SBE addition was made at 72 h and 90 h by amending 1 mL of SBE solution and the SMD residual (%) was calculated by the total amount of remaining SDM to that of the initial amount.

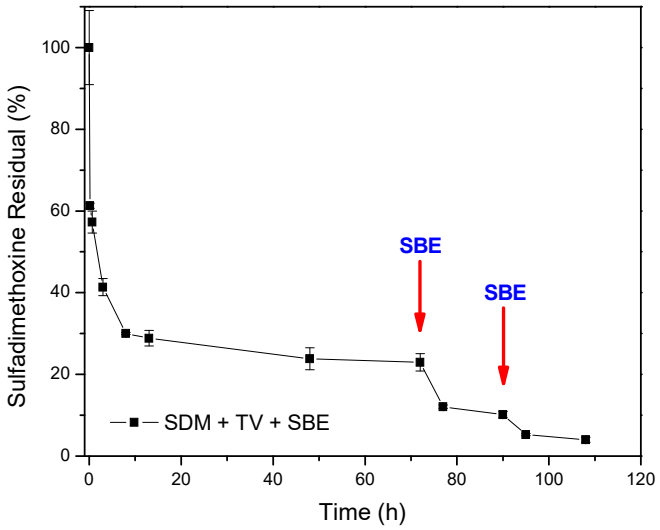

Figure S2.2. The high resolution MS-MS spectra of DMPO-mediator coupling products and proposed structures of their fragment ions.

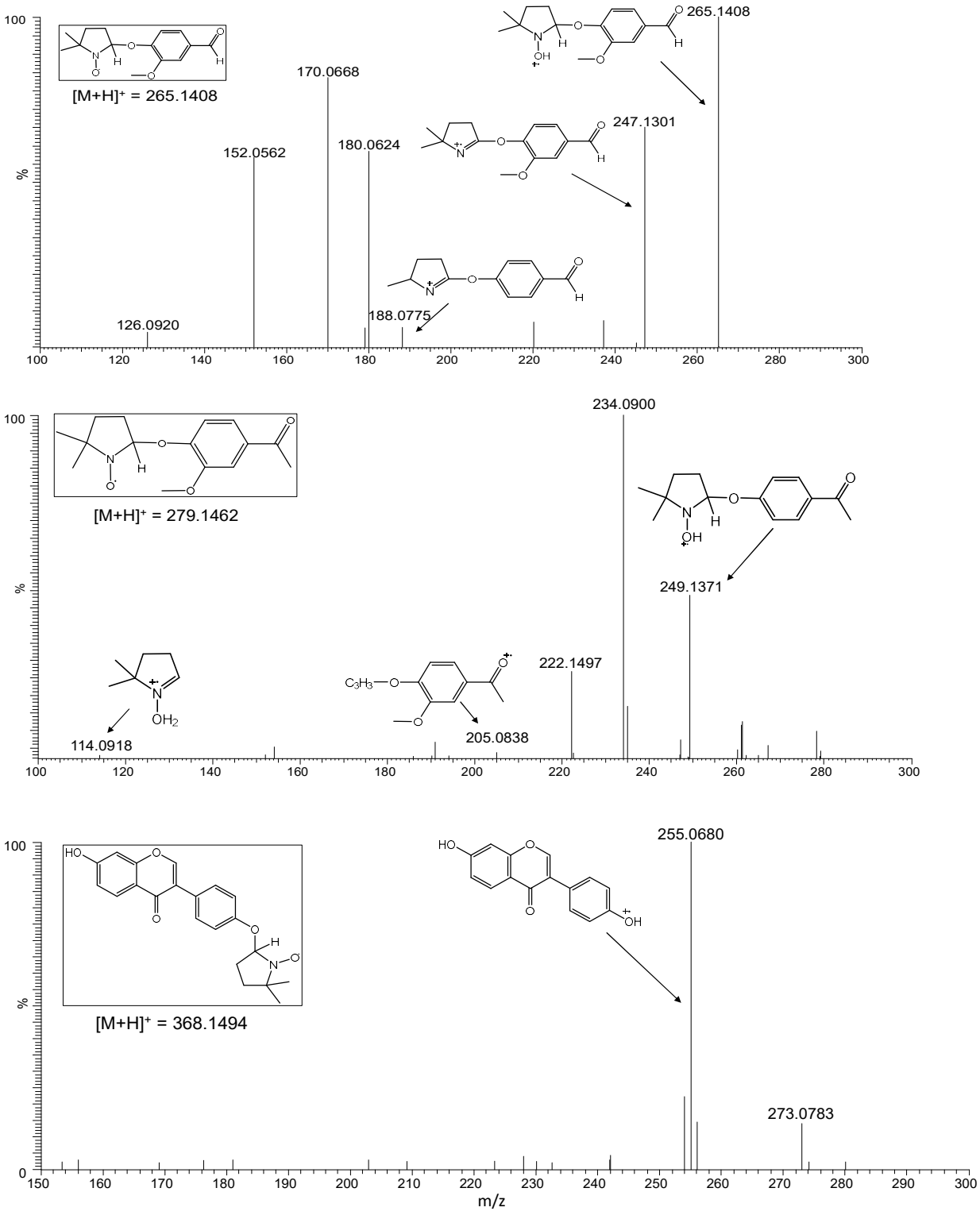

Figure S2.3. The high resolution MS-MS spectra of sulfadimethoxine degradation products and proposed structures of their fragment ions.

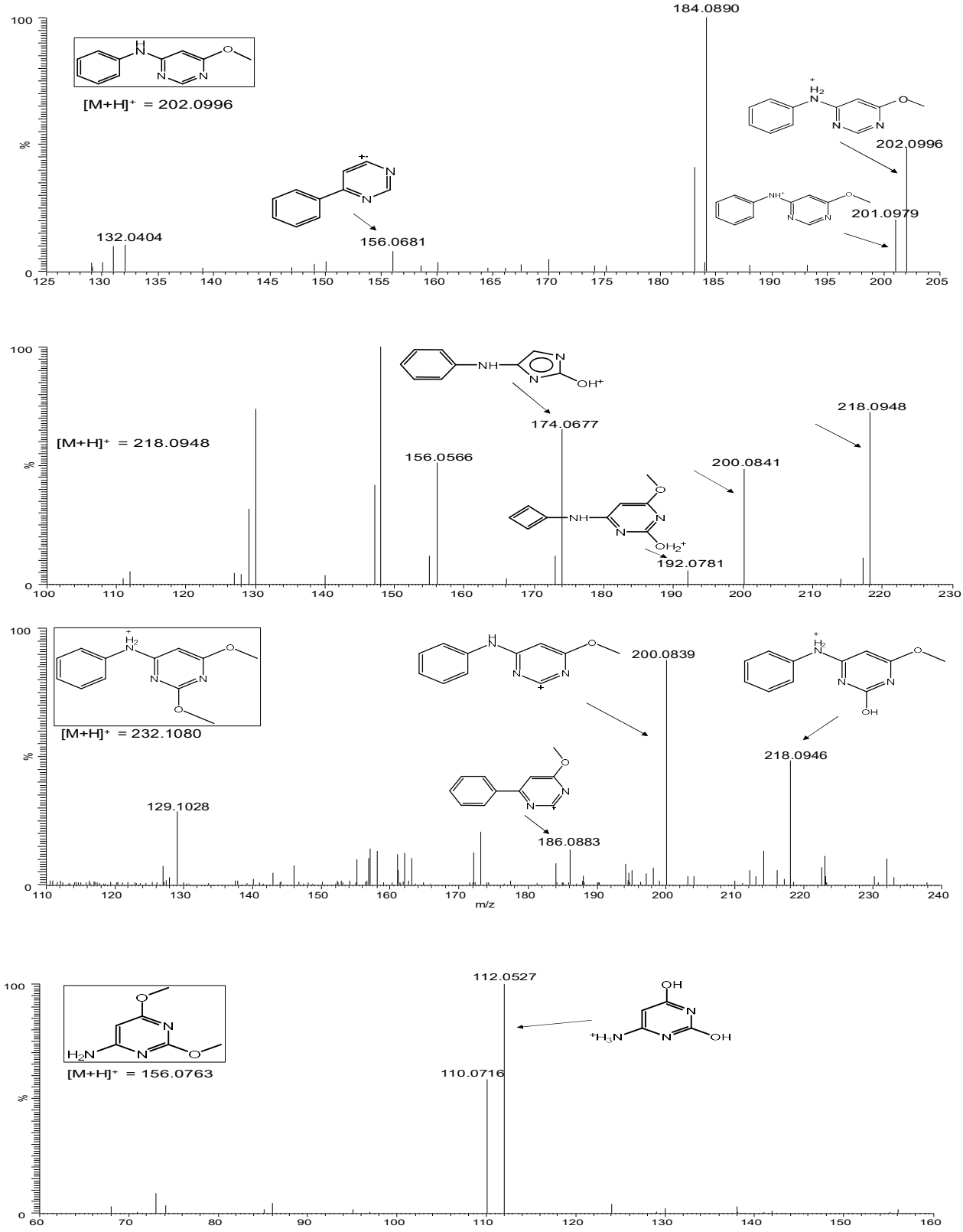

Table S2.1. Laccase activities in each treatment solution after 9 h of reaction.

Inital SDM Concentraion	Initial Enzyme Acivity	Treatment	Enzyme Acitivity ($U\ ml^{-1}$)
$1\ mg\ L^{-1}$	$0.5\ U\ ml^{-1}$	SDM + TV + SBE	0.1210
		SDM + TV + HBT	0.2058
		SDM + TV + ABTS	0.2293
		SDM + TV + COU	0.1927
$10\ mg\ L^{-1}$	$5\ U\ ml^{-1}$	SDM + TV + SBE	1.5831
		SDM + TV + HBT	3.1040
		SDM + TV + ABTS	3.9403
		SDM + TV + COU	3.5634

Table S2.2. Total phenolic contents of soybean meal extract (SBE), p-Coumaric acid (COU), 1-Hydroxybenzotriazole (HBT), and 2,2´-azinobis(3-ethylbenzthiazoline-6-sulfonate) (ABTS).

Mediator Solution	Total Phenolic Content (mg GAE L^{-1})
SBE	91.0
10 mg L^{-1} COU	7.19
10 mg L^{-1} HBT	0.07
10 mg L^{-1} ABTS	4.12

Table S2.3. Total organic carbon and metal content in soil and soybean meal extract solution.

Extract Solution	Total Organic Carbon (mg L^{-1})	Na (mg L^{-1})	Mg (mg L^{-1})	Al (mg L^{-1})	Ca (mg L^{-1})	Fe (mg L^{-1})	Cu (mg L^{-1})
Soil	172.9	4.05	3.74	1.89	9.47	3.93	<0.008
Soybean meal	1865.0	<1.00	78.33	<0.080	78.67	<0.6	0.0411
Mushroom Compost	269.9	36.18	13.49	1.83	9.49	1.14	1.4704

APPENDIX B

SUPPORTING INFORMATION:

COUPLING GRANULAR ACTIVATED CARBON WITH LACCASE CATALYZED HUMIFICATION REACTION FOR SEPARATION AND DESTRUCTION OF PFAS

MATERIALS AND METHODS

Sorption isotherm

Langmuir equation is expressed as:

$q_e = q_m C_e/(K + C_e)$

Where K_l is Langmuir affinity coefficient($mg \cdot L^{-1}$) ; and q_m is sorption capacity, $mg \cdot g^{-1}$; q_e is equilibrium sorption amount, $\mu mol \cdot g^{-1}$; C_e is equilibrium solution phase concentration, $\mu mol \cdot L^{-1}$. The curve fitting of sorption isotherms was accomplished by Origin Pro 9.0 software.

Table S3.1. The treatment conditions in batch reactor using spiked PFOA solution.

Treatment	PFOA ($\mu mol\ L^{-1}$)	PS ($Unit\ mL^{-1}$)	HBT ($\mu mol\ L^{-1}$)	Fe^{3+} ($\mu mol\ L^{-1}$)
PFOA	1	0	0	0
PFOA+PS+HBT	1	4	40	0
PFOA+PS+HBT+Fe	1	4	40	10

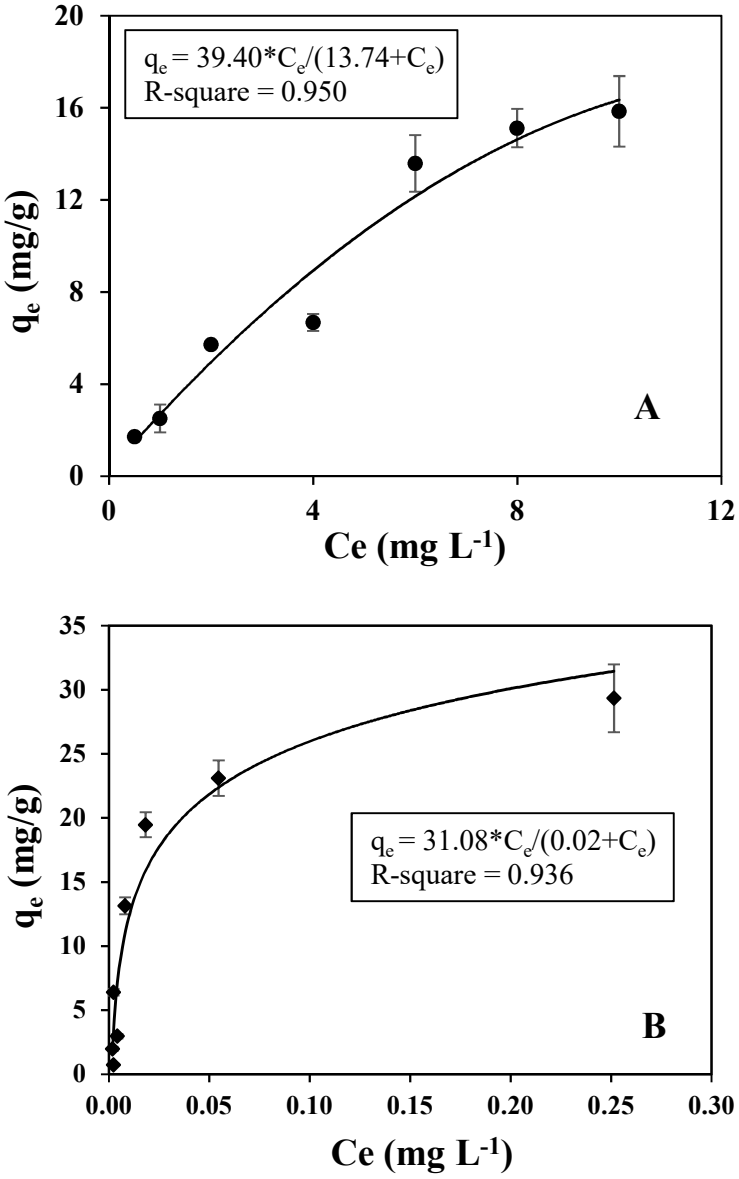

Figure S3.1. The sorption isotherm of PFOA on Sigma Aldrich GAC (A) and CalgonCarbon GAC (B).

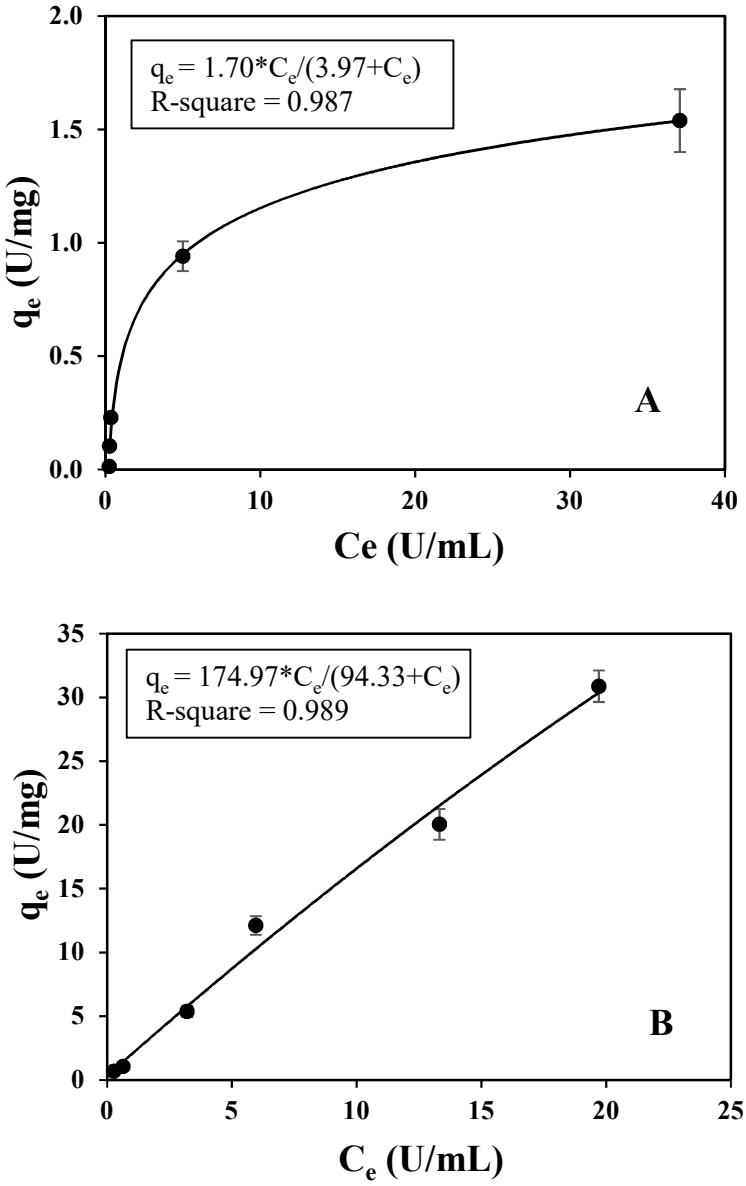

Figure S3.2. The sorption isotherm of PS laccase on SigmaAldrich GAC (A) and CalgonCarbon GAC (B).

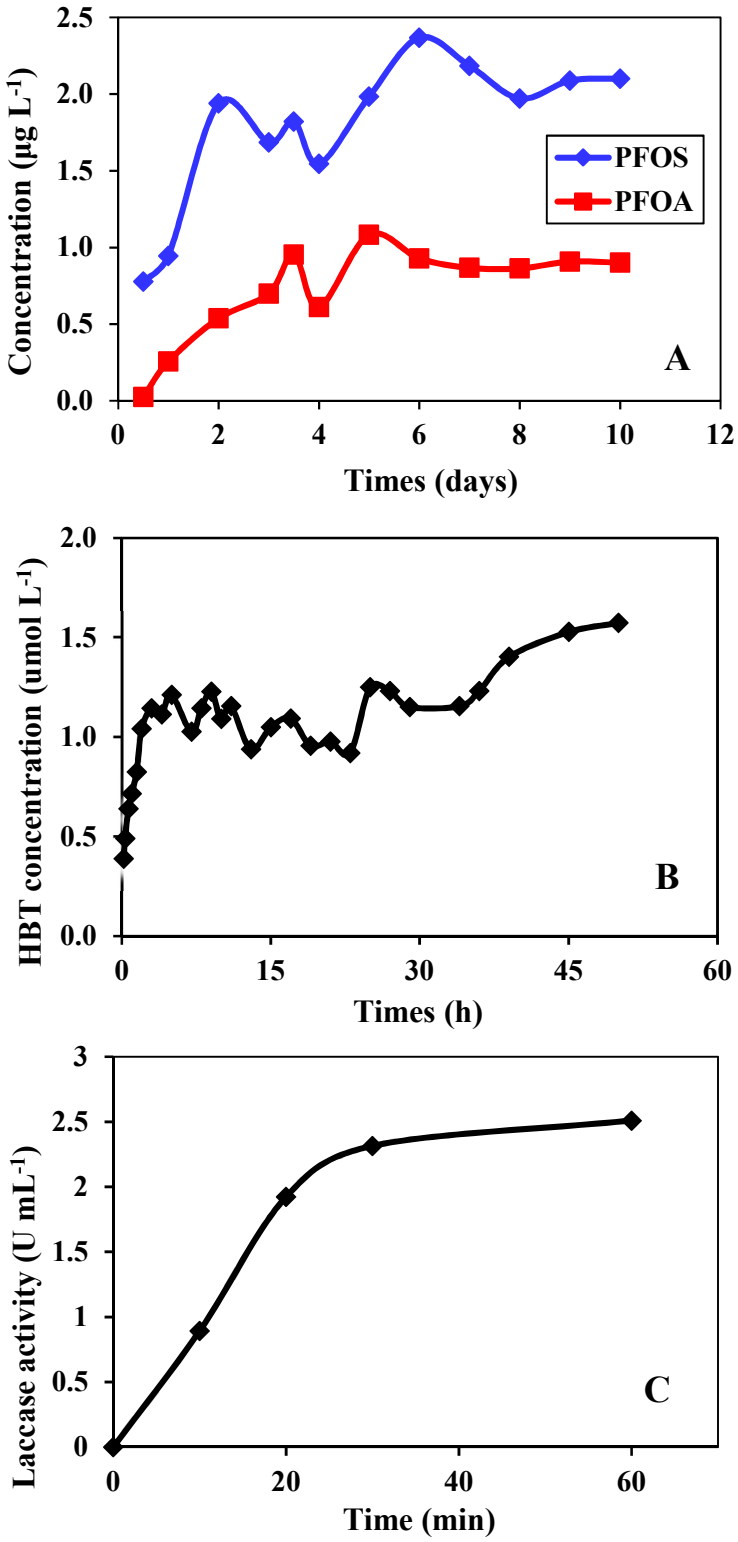

Figure S3.3. The breakthrough curves of PFOA (0.87 µg L^{-1}) and PFOS (3.92 µg L^{-1}) (A), HBT (B) (2 µmol L^{-1}), and PS laccase (2 Unit/mL) (C) on CalgonCarbon GAC (0.1 g) columns.

APPENDIX C

SUPPORTING INFORMATION:

ELECTRO-OXIDATION OF TETRACYCLINE BY A MAGNELI PHASE TI4O7 POROUS ANODE: KINETICS, PRODUCTS, AND TOXICITY

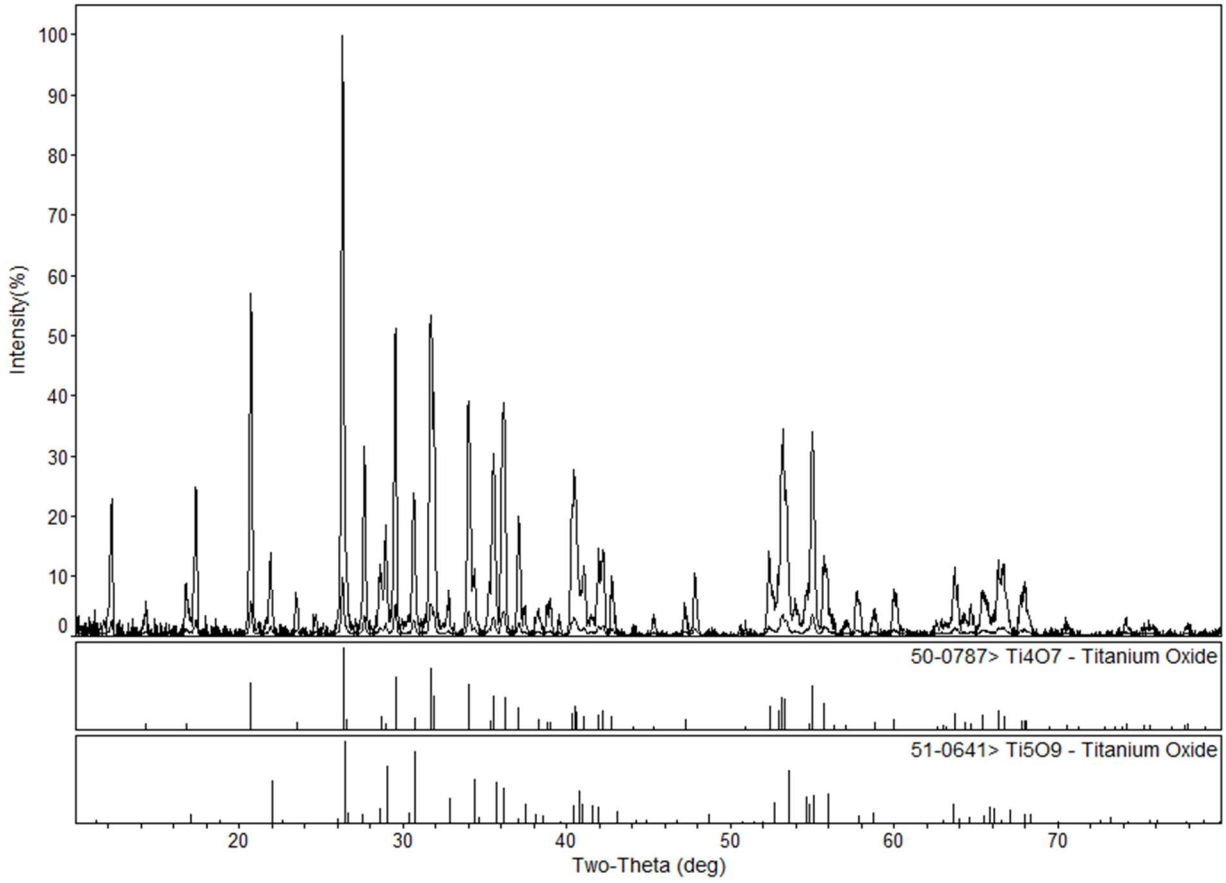

Figure S4.1. Figure S-1. X-ray diffraction pattern of electrode material along with the top matching reference plots. Quantitative analysis using Reference Intensity Ratio (RIR) method (ref) indicated that the material contains 77% of Ti_4O_7 phase and 23% of Ti_5O_9.

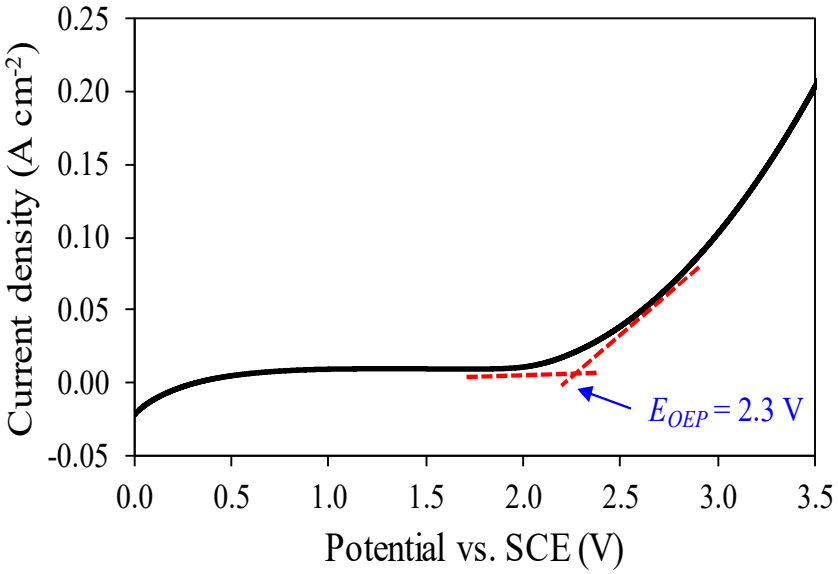

Figure S4.2. Linear scan voltammetry (LSV) plot of Magnéli phase Ti_4O_7 as anode at a scan rate of 100 mV s^{-1}.

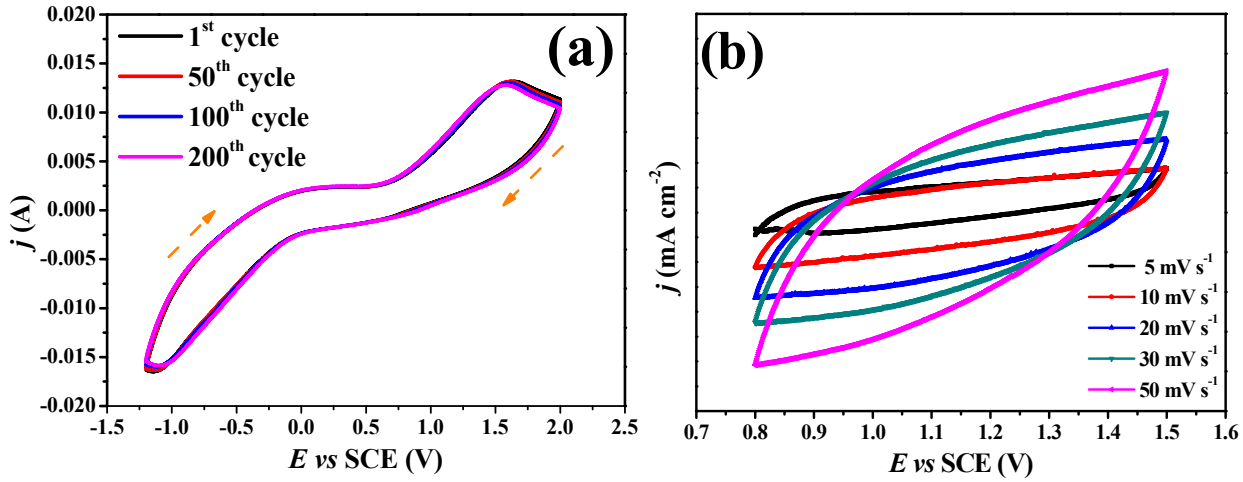

Figure S4.3. (a) Cyclic voltammetry curves of porous Ti_4O_7 ceramic electrode in 10 mM $K_4Fe(CN)_6$ + 0.1 M KNO_3 solution; (b) Cyclic voltammograms of porous Ti_4O_7 ceramic electrode in 0.25 M Na_2SO_4 solution at different scan rate.

Figure S4.4. The electrical resistance of Ti_4O_7 ceramic electrode (Left) and graphite plate (Right) measured by multimeter.

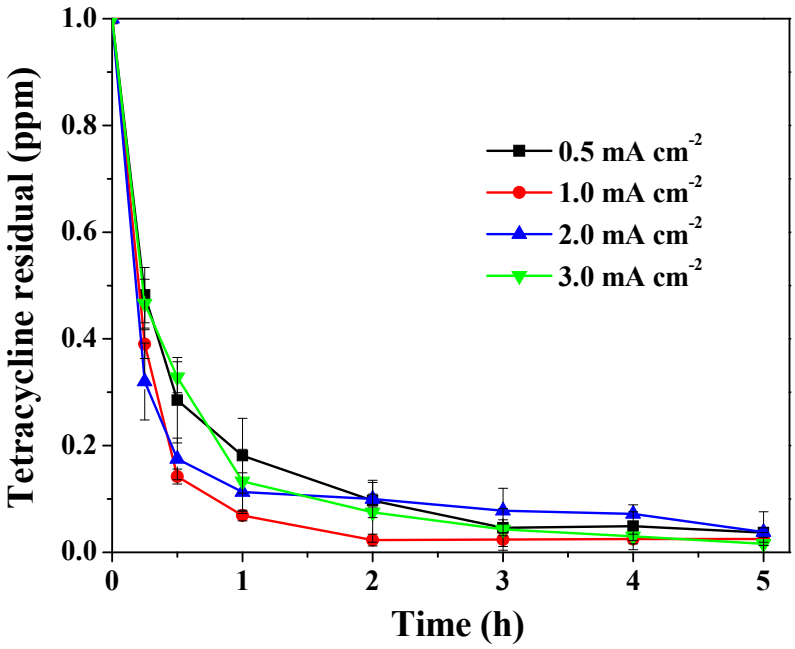

Figure S4.5. Removal of TC at 1 mg L^{-1} initial concentration during electrochemical oxidation at Magnéli phase Ti_4O_7 anode under various current densities.

Text S4.1. Kinetic modeling.

The mechanisms of electrochemical oxidation of tetracycline are proposed as the following steps. First, the negatively charged tetracycline (pK_{a2} = 7.68) molecule migrates to the positively charged anode surface due to electrostatic attraction, and undergoes single electron transfer, becoming short-lived cation radical (G. Chen et al., 1999; G. Chen, Betterton, Arnold, & Ela, 2003). This step is expressed by Butler-Volmer equation:

$$\frac{dm_c}{dt} = Ak_a C_s \exp(\frac{n_0 \alpha F E_a}{RT}) \quad (3)$$

Where: dm_c/dt is the conversion rate of tetracycline (mmol s^{-1}); A is the geometry electrode surface area (cm^2); C_s is the concentration of tetracycline at anode surface (M); k_a is the rate constant for electron transfer from tetracycline to electrode (cm s^{-1}); n_0 is the number of electron transferred and assumed to be 1; α is the anode transfer coefficient; F is the Faraday constant (96500 C mol^{-1}); E_a is the anode potential (V); R is the gas constant (8.314 J mol^{-1} K^{-1}); and T is the absolute temperature (K).

Meanwhile, tetracycline molecules continuously diffuse to the electrode surface due to the concentration difference in bulk solution and at the anode surface. This process is considered to be the rate-limiting step of electrochemical reaction of tetracycline unless the concentration of contaminate is high enough. The mass transfer rate can be expressed as:

$$\frac{dm}{dt} = Ak_m(C_b - C_s) \quad (4)$$

Where dm/dt is the mass transfer rate of tetracycline (mmol s^{-1}); A is the geometry electrode surface area (cm^2); k_m is the mass transfer rate constant (cm s^{-1}); C_b is the concentration of tetracycline in bulk solution (M); C_s is the concentration of tetracycline at anode surface (M).

Under steady-state condition, the mass transfer rate is assumed to be equal to the rate of tetracycline being converted. Cs can thus be solved by combining equation (3) and (4), which can then be substituted into equation 4 to yield:

$$\frac{dm}{dt} = AC_b \left[\frac{1}{k_m} + \frac{1}{k_a}\exp\left(-\frac{\alpha F E_a}{RT}\right)\right]^{-1} \quad (5)$$

Integrating equation (5) over time will result in:

$$\frac{m_t - m_0}{A\int_0^t C_b\, dt} = \left[\frac{1}{k_m} + \frac{1}{k_a}\exp(-\frac{\alpha F E_a}{RT})\right]^{-1} \quad (6)$$

In equation 6, m_t and m_0 are the total amount of tetracycline (mmol) at time t and 0, respectively. Therefore, $\frac{m_0 - m_t}{A\int_0^t C_b dt}$ represents the surface-area normalized observed rate constant (k_{ob}), which can thus be defined in equation 7:

$$k_{ob} = \left[\frac{1}{k_m} + \frac{1}{k_a}\exp(-\frac{\alpha F E_a}{RT})\right]^{-1} \quad (7)$$

Using the time-course TC degradation data, m_0 - m_t was plotted against $A\int_0^t C_b\, dt$ to yield linear regression lines whose slopes are the k_{ob} values for different anode potential (E_a) (Figure S3-A). The k_{ob} values thus obtained were then fitted to equation 7, with the parameters k_m, k_a, and α that characterize the kinetic behavior of tetracycline reaction (Figure S3-B). The mass transfer rate constant (k_m) of this reaction system was determined to be 1.27×10^{-3} cm s^{-1}.

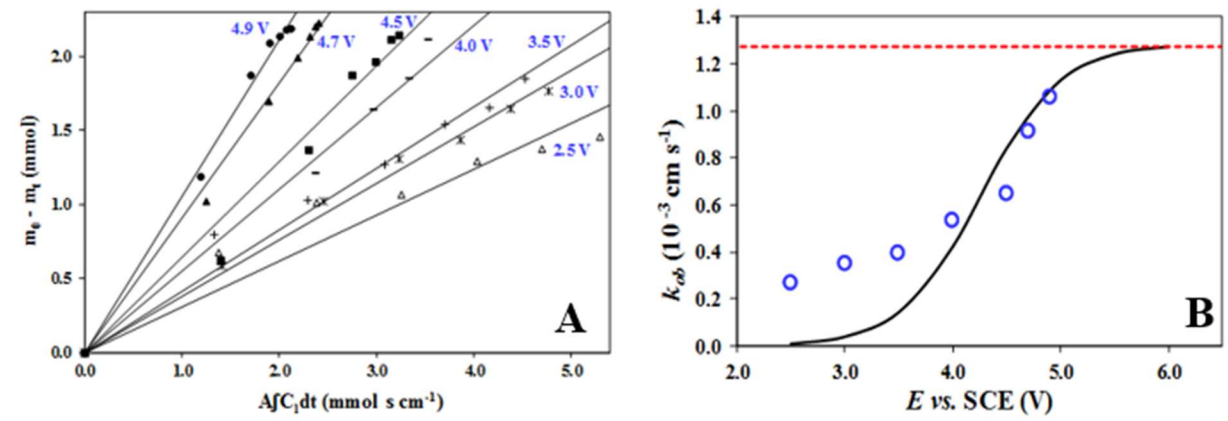

Figure S4.6. (A) Mass of TC removed in electrolytic cell as a function of $A\int_0^t C_b\,dt$ for 10 mg L^{-1} initial TC concentration at various anode potentials (E); (B) Voltage-dependent surface area-normalized rate constant (k_{ob}) for TC oxidation at Magnéli phase Ti_4O_7 anode. Black line was the simulation curve obtained by nonlinear regression. Red dot line indicated the estimated value of mass transfer rate (k_m).

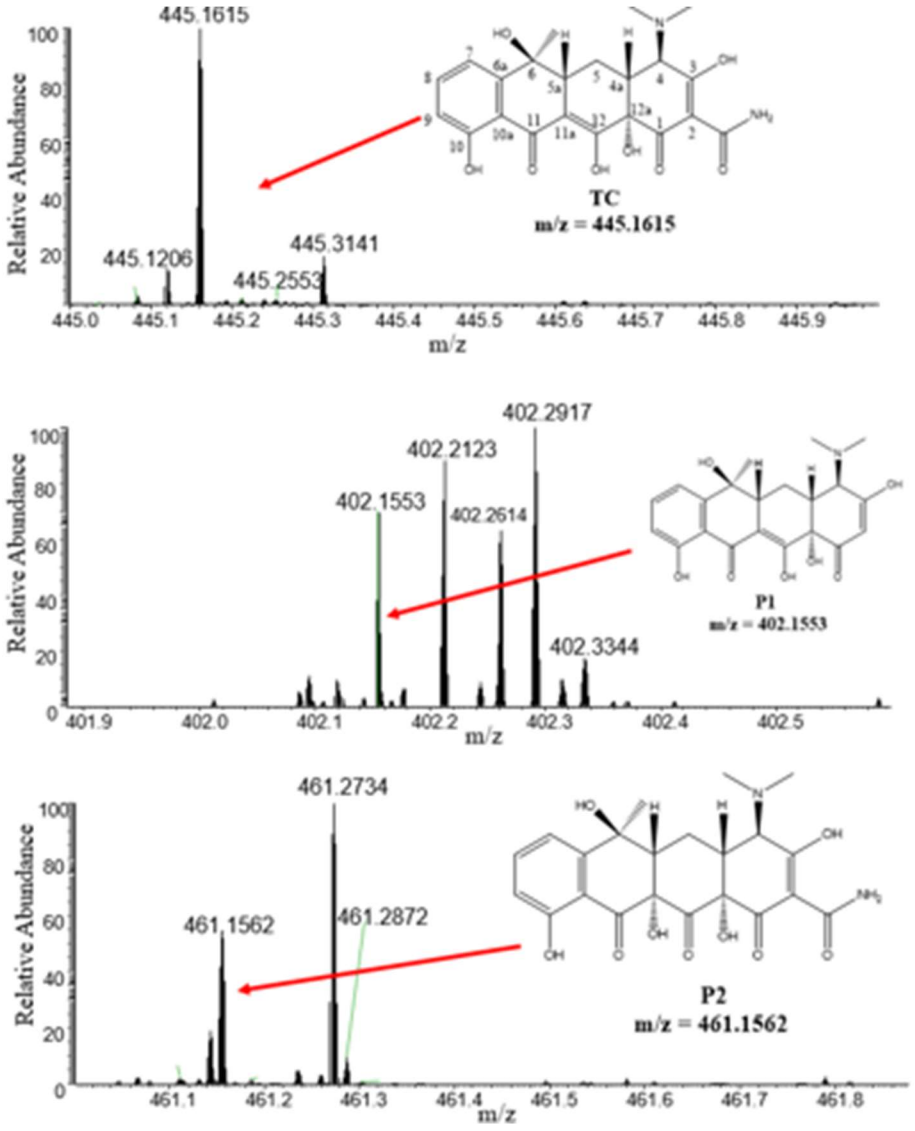

Figure S4.7. The parent ion (TC) and transformation products (P1 and P2) identified by HRMS.

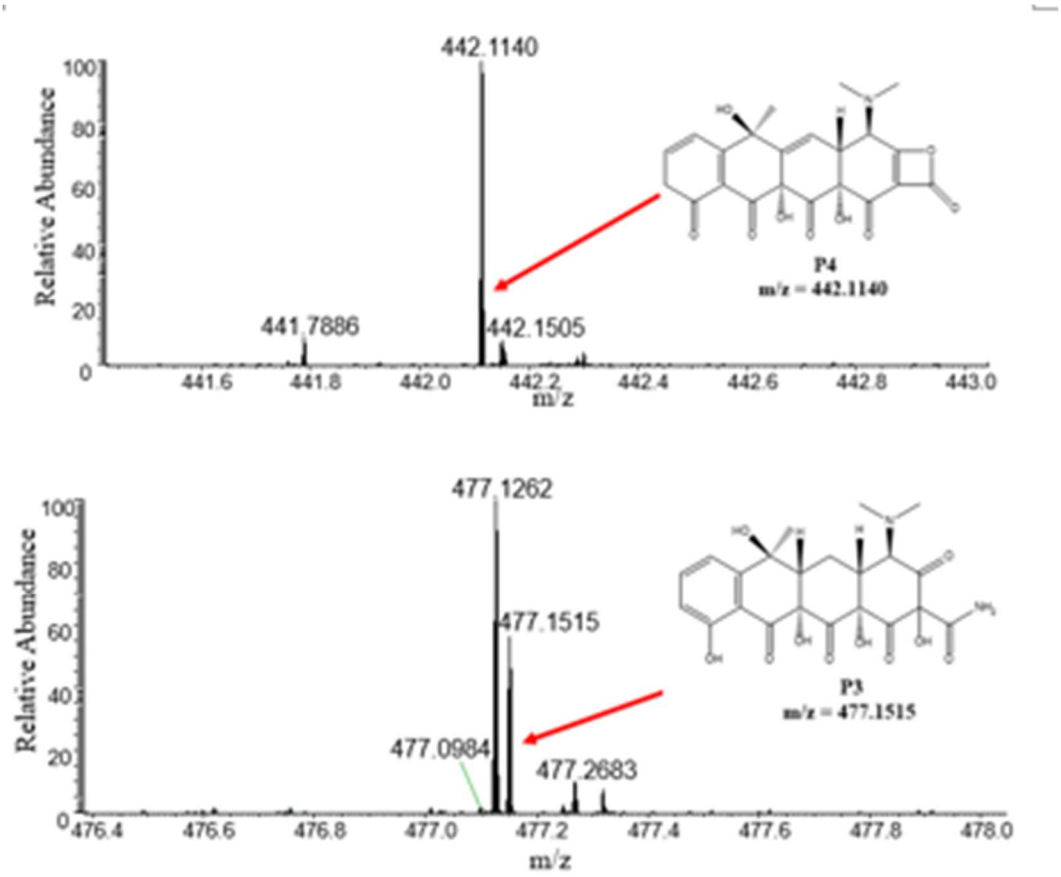

Figure S4.8. The transformation products (P3 and P4) identified by HRMS.

Text S4.2. Molecular density functional theory.

The optimized geometry and atom charges of tetracycline were calculated by density functional theory (DFT) (Kohn & Sham, 1965; Parr, 1980; Politzer & Seminario, 1995) at B3LYP[4,5]/6-311++G(d,p) (Becke, 1993; C. Lee, Yang, & Parr, 1988) level of theory using Gaussian 09 software package (Frisch et al., 2004). Vibrational analysis indicates all structures are stable and correspond to the minimum point on the potential energy surface.

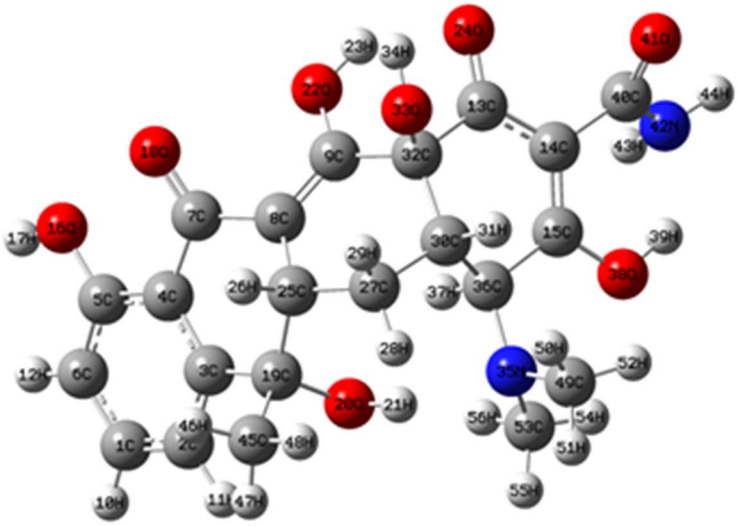

Figure S4.9. The optimized geometry of tetracycline molecule.

Table S4.1. Atomic charges of tetracycline calculated at B3LYP/6-311++G(d,p) level.

Atoms	Atomic Charges	Atoms	Atomic Charges
1C	-0.351	20O	0.009
2C	-0.064	22O	-0.122
3C	0.082	24O	-0.233
4C	0.280	25C	-0.514
5C	0.172	27C	-0.187
6C	-0.119	30C	0.379
7C	-0.467	32C	-0.378
8C	0.412	33O	-0.088
9C	-0.182	36C	-0.558
13C	-0.087	38O	-0.169
14C	0.130	40C	-0.259
15C	-0.416	41O	-0.235
16O	-0.152	45C	-0.855
18O	-0.170	49C	-0.323
19C	-0.317	53C	-0.243

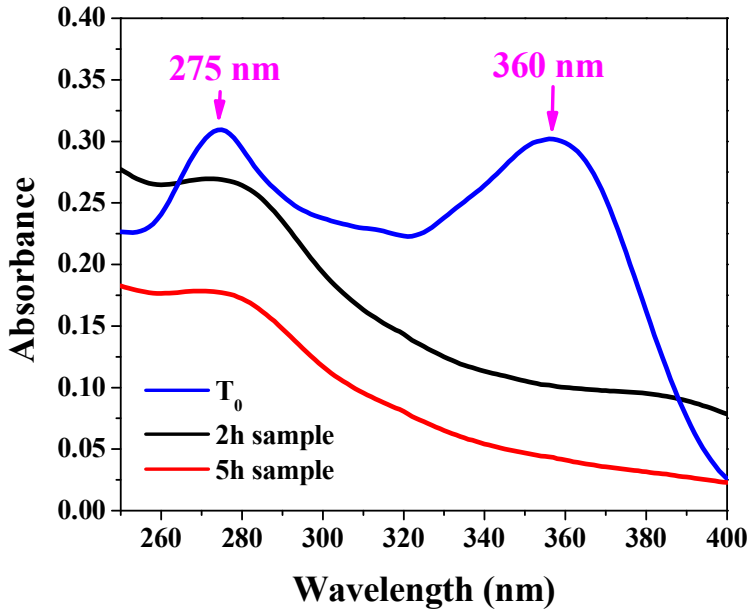

Figure S4.10. UV absorption spectrum of treatment solution collected at different sampling points during electrochemical oxidation.

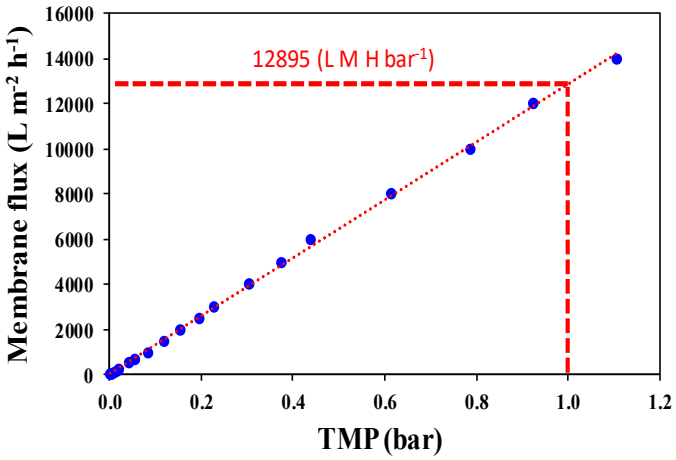

Figure S4.11. Plot of pure water flux as a function of trans membrane pressure through the Magnéli phase Ti_4O_7 electrode.

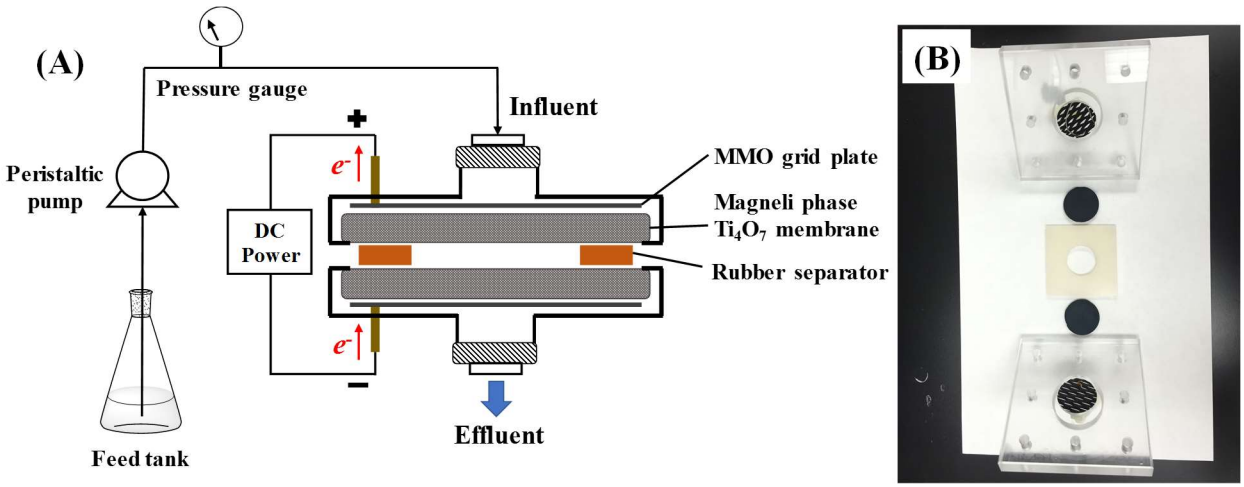

Figure S4.12. (A) The design and setup of a Reactive Electrochemical Membrane system with the Magnéli phase Ti_4O_7 ceramic electrode; (B) A picture of the devices used in the REM system. The Magnéli phase Ti_4O_7 ceramic electrodes are disks in shape with 3-cm diameter and 3-mm thickness.

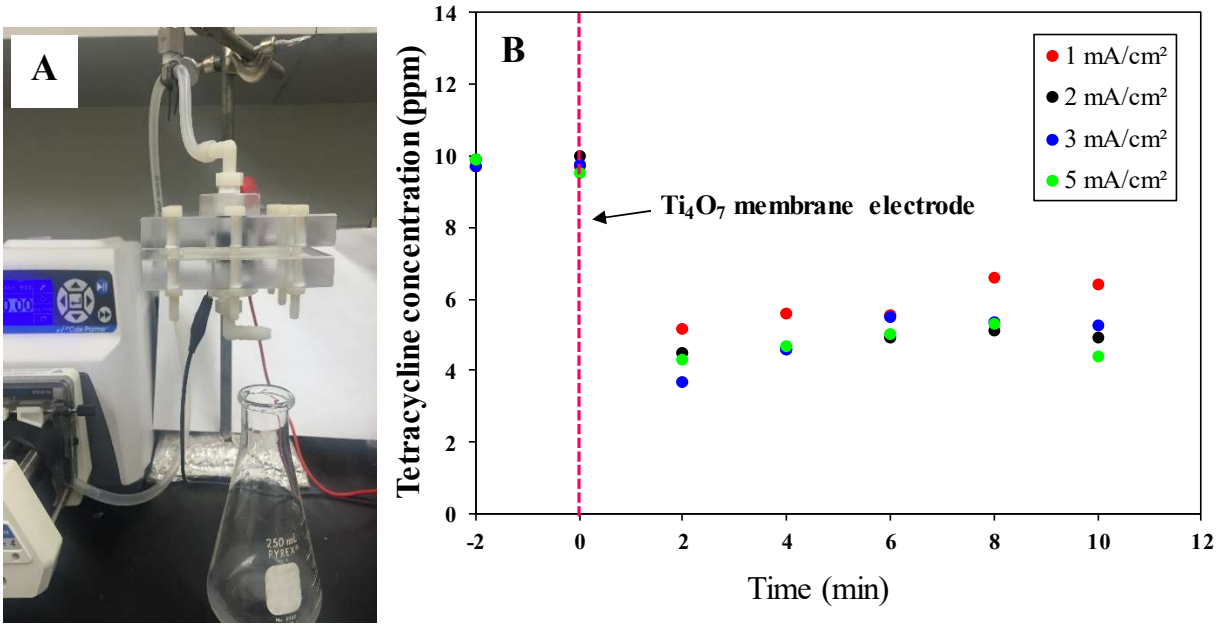

Figure S4.13. (A) A picture of the REM system in operation; (B) The change of tetracycline concentration after being filtered through the Ti_4O_7 ceramic electrode in the REM operation at a flow rate of 10 mL/min and under different applied current densities.

APPENDIX D

SUPPORTING INFORMATION FOR:

FILTRATION AND ELECTROCHEMICAL INACTIVATION OF E COLI USING A TI4O7 CERAMIC MEMBRANE

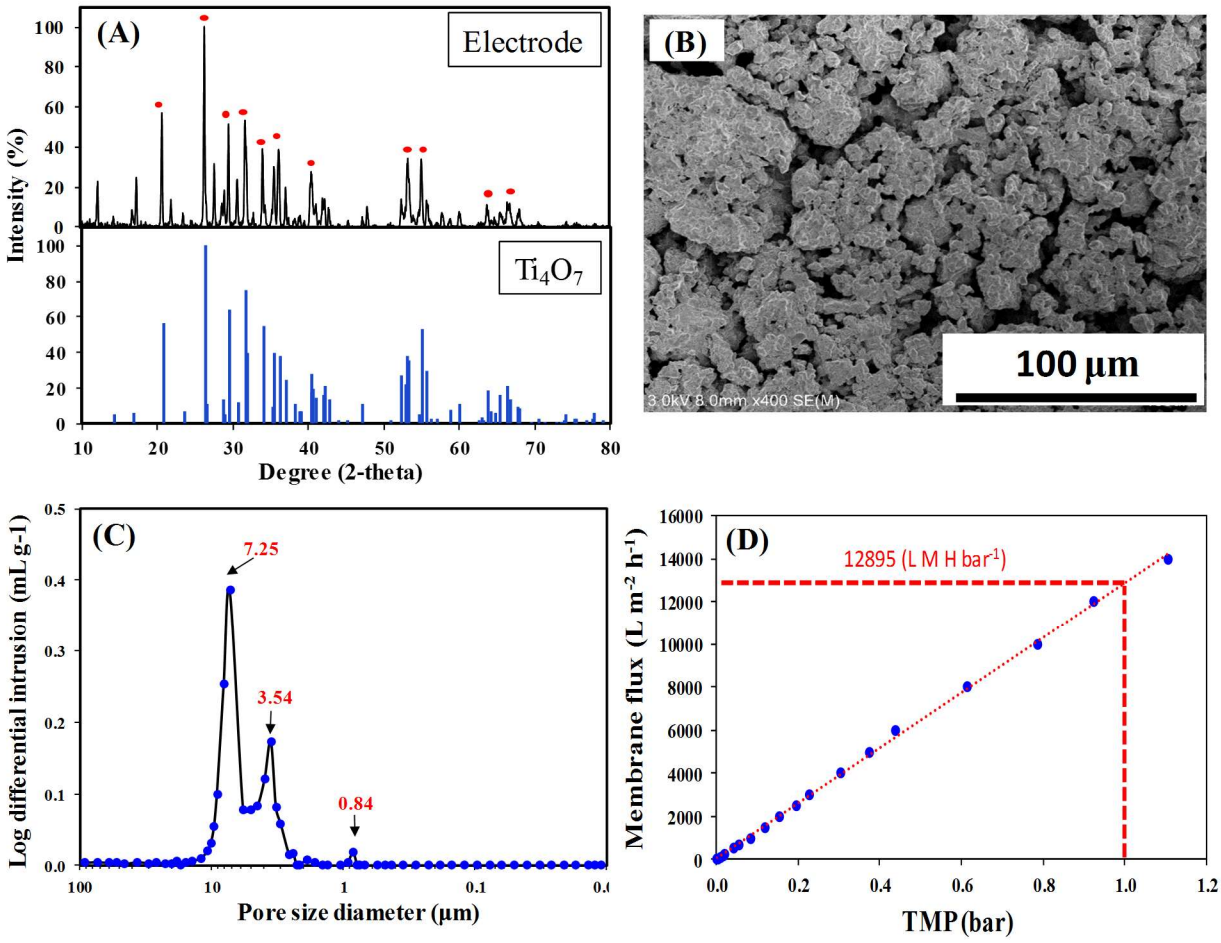

Figure S5.1. (A) XRD data of Magnéli phase Ti_4O_7 electrode material and reference Ti_4O_7 powder (PDF# 900-050-0787); (B) SEM image of the surface of Ti_4O_7 electrode; (C) The result of mercury intrusion analysis on Ti_4O_7 electrode showing pore size distribution; (D) Pure water flux as a function of trans-membrane pressure through the Magnéli phase Ti4O7 electrode.

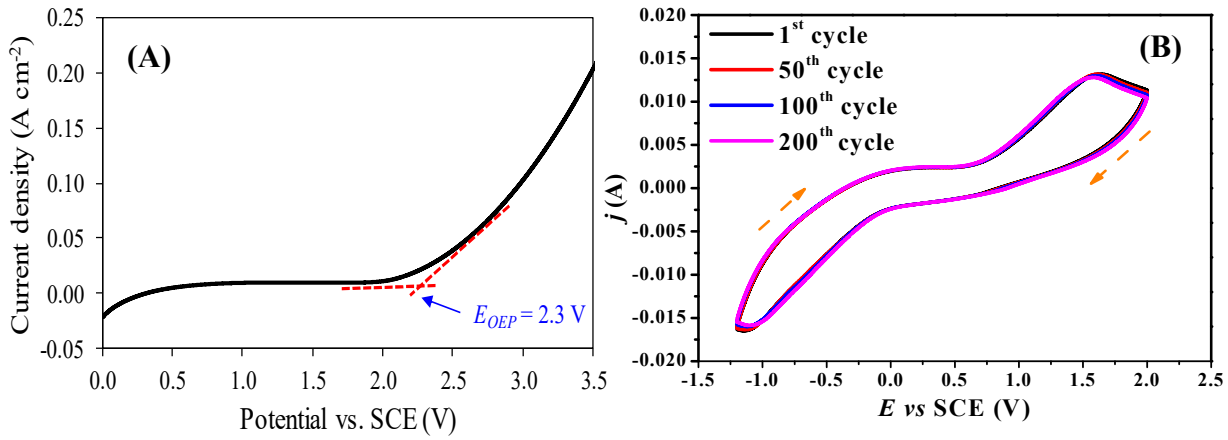

Figure S5.2. (A) Linear scan voltammetry (LSV) plot of Magnéli phase Ti_4O_7 as anode at a scan rate of 100 mV s^{-1}; (B) Cyclic voltammetry curves of porous Ti_4O_7 ceramic electrode in 10 mM $K_4Fe(CN)_6$ + 0.1 M KNO_3 solution.

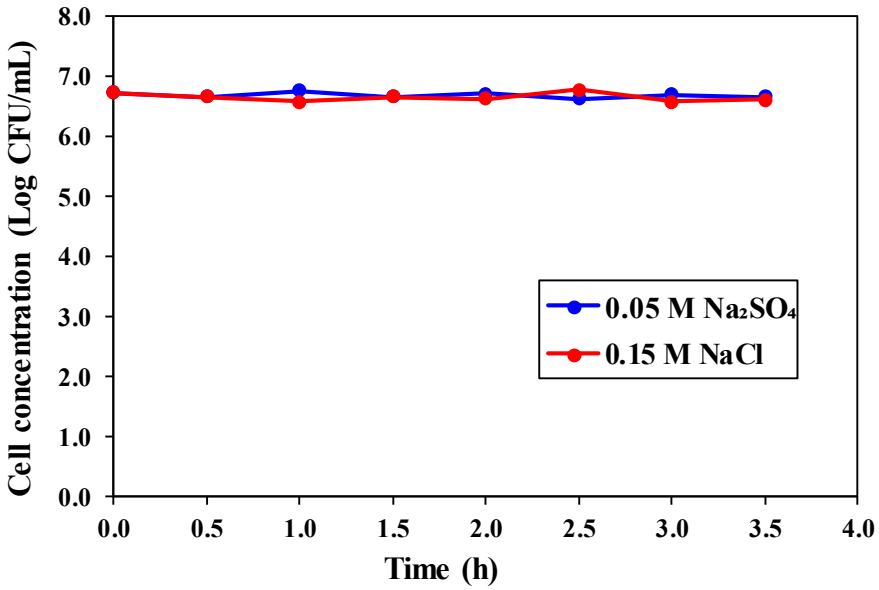

Figure S5.3. The viability of *E Coli* in 0.05 M Na_2SO_4 or 0.15 M NaCl solution during 3.5 hrs incubation at room temperature.

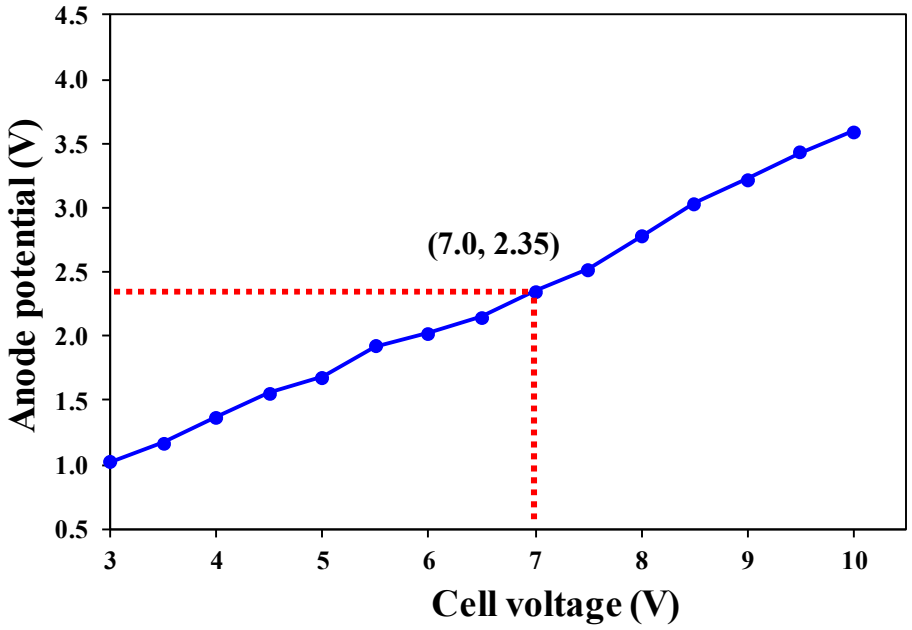

Figure S5.4. The relationship between anode potential and cell voltage in one-compartment reactor using Magnéli phase Ti_4O_7 as anode.

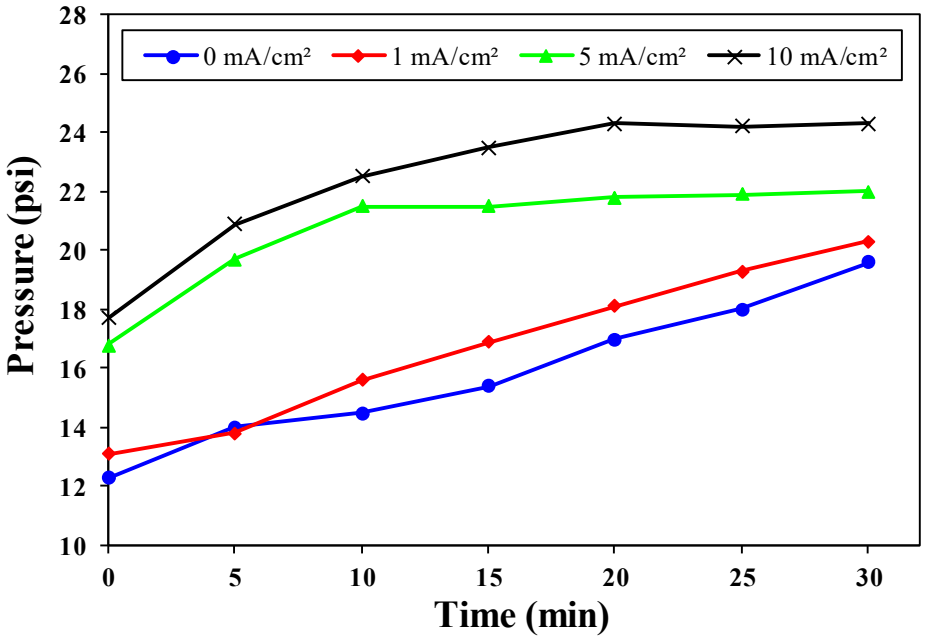

Figure S5.5. The inlet pressure as a function of electrochemical disinfection time under various current densities.

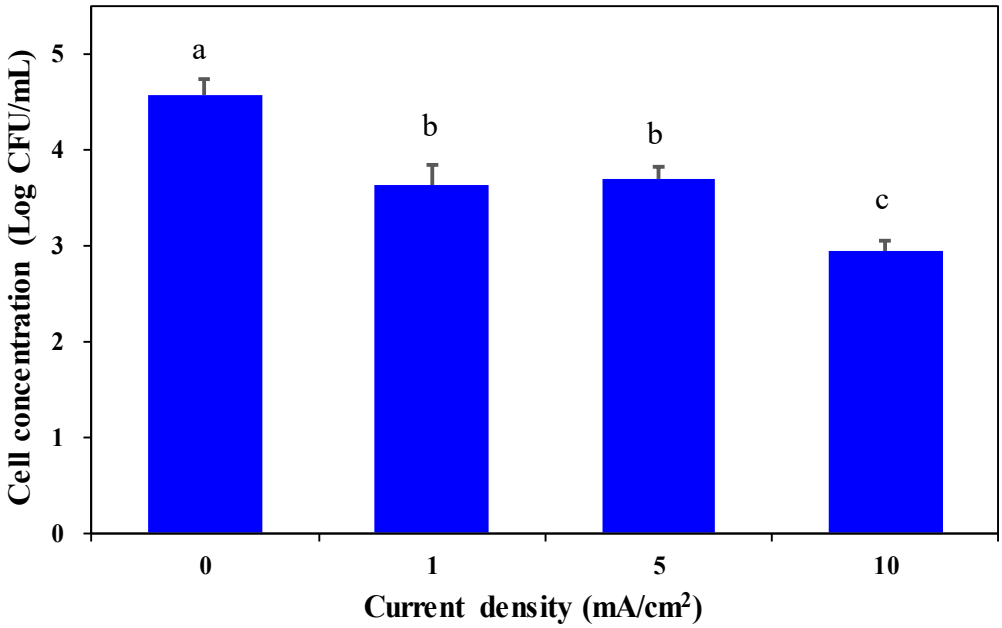

Figure S5.6. The concentration of bacteria extracted from the membrane electrode used in disinfection study at different current densities. Means with different letters are significantly different ($p<0.05$).

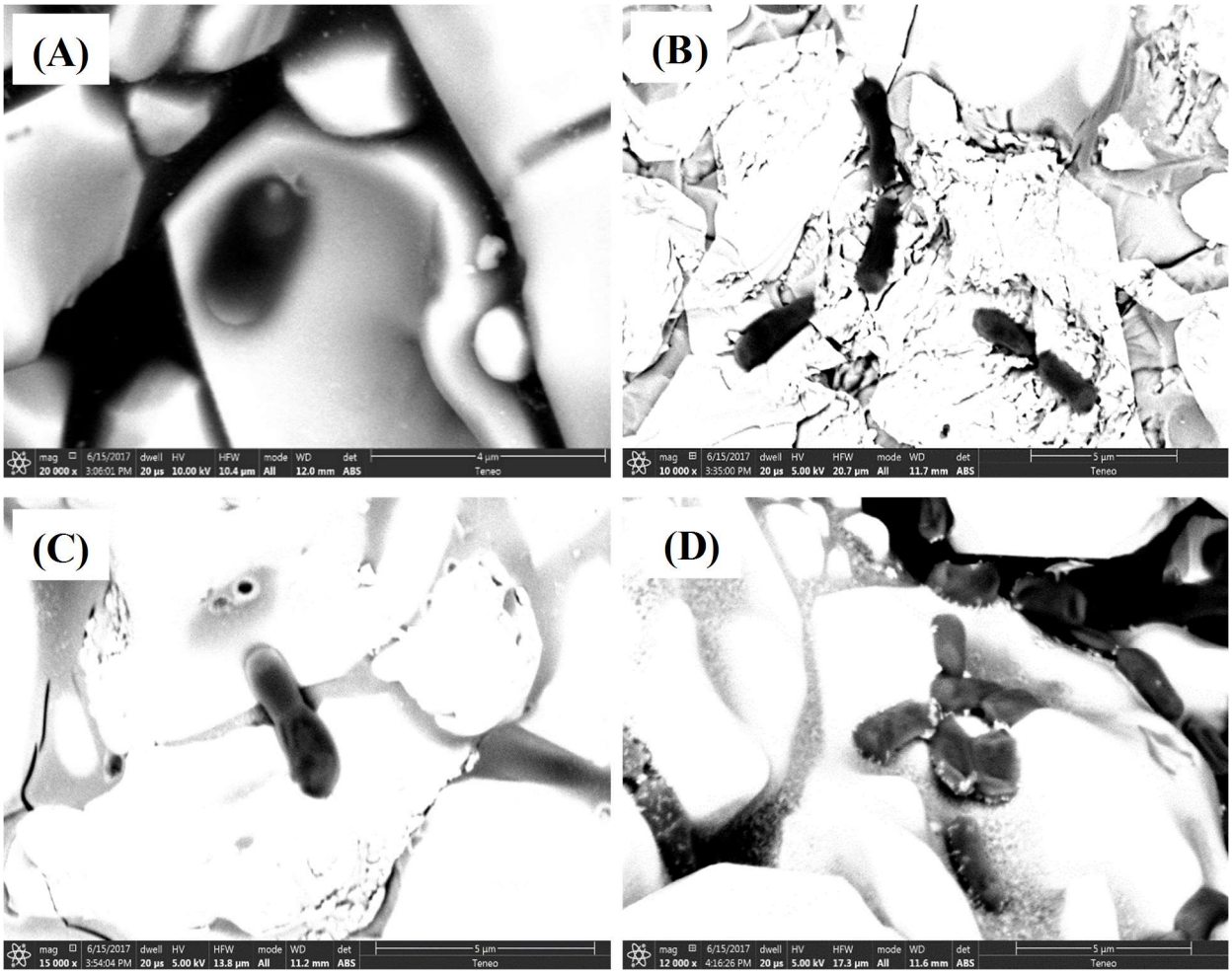

Figure S5.7. SEM images of effluent samples collected during electrochemical disinfection process. (A) No current control; (B) 1 mA/cm^2 applied current density; (C) 5 mA/cm^2 applied current density; (D) 10 mA/cm^2 applied current density.